

### Authors' response to Hess-2018-395-RC1

(Hess-2018-395, by Bing-Qi Zhu et al., words in blue color)

*Author's response: The author's response should be structured in a clear and easy-to-follow sequence: (1) comments from referees/public, (2) author's response, and (3) author's changes in manuscript. Regarding author's changes, a marked-up manuscript version (track changes in Word, latexdiff in LaTeX) converted into a \*.pdf including the author's response must be submitted.*

(1) Hess-2018-395-RC1

Interactive comment on "Direct or indirect recharge on groundwater in the middle-latitude desert of Otindag, China?" by Bing-Qi Zhu et al.

Anonymous Referee #1.

Received and published: 20 November 2018

The objective of this manuscript is the understanding of groundwater recharge under arid conditions. The authors provide a detailed discussion on the different assumptions they made to explain this recharge. However, this discussion is mainly based on geochemical data including isotopes. To my knowledge, the developed methodology is not new, or, in other words, the authors did not sufficiently highlight the originality of the methodology. Furthermore, the discussion lacks of hydrological considerations. For example, the measured concentrations are the result of the mixing of water moving in the aquifer and the water coming from the recharge. The resulting concentration depends on the different water fluxes which have to be estimated for proper interpretations. Moreover, the travel time in the unsaturated zone has to be discussed in detail. It can be of several decades under these climatic conditions for a groundwater depth up to 60m. For these reasons, the paper should not be accepted for HESS.

Authors response and Author's changes in manuscript:

We thank the anonymous Referee #1 very much for his/her help in reviewing and commenting on our manuscript. According to above comments, we have revised the original manuscript. First of all, we think that we need to explain to the reviewer #1 here about the question on the research method of this study: (1) Up to now, no any geoscientist has done any research work on groundwater recharge and its sources in the Otindag Desert before, and our research work is the first and pioneering one; (2) because no any study work has been done for groundwater research in this extensive area before, therefore, our study have no any existing information and data of predecessors (especially hydrogeological and hydrological data) to refer to, so we use the traditional methods to carry out preliminary research; However, both the collection of samples, the acquisition of analytical data and the research results based on these methods are the first achievements in this blank area, which are very valuable and also pioneering.

Secondly, as to the hydrological problems raised by the reviewer #1, we have actually considered them in the initial sage of this research work. We would like to make the following explanations: (1) About surface water, almost all of these rivers observed in the field are intermittent in space and in time and there is no any hydrological data available for these rivers to be used or referenced by us, so there is no hydrological data for discussion in this study; However, in order to remedy this problem, we are currently conducting field monitoring work in order to obtain these hydrological data; at present, however, we have no systematic data obtained and we can only carry out systematic discussions after obtaining the data in the late years; (2) about groundwater, being similar to surface water, there is no previous hydrological data available for reference in the study area; in order to obtain dynamic hydrological data of groundwater in the study area, at present we are also conducting real-time monitoring of groundwater level in the field. Due to the reason that currently there is no systematic data to discuss, we can only carry out systematic discussions after the data are obtained in the late years. In this study we believe that although the lack of hydrological data is regrettable, it will not conceal the correctness and validity of our discussions using geochemical and isotope geochemical data to explore the recharge sources of groundwater in the Otindag Desert.

Thirdly, about the questions of the mixing process, dissolution process, chemical concentrations

of groundwater and their water flux, saturation and unsaturation of groundwater proposed by the reviewer, we believe that they are essentially related to the water-rock interaction between groundwater and surrounding rocks, i.e., the speciation modeling and hydrogeological modeling. Therefore, in view of the above problems, we have added new discussions about the processes of water-rock interaction, mechanism of groundwater recharge and related hydrogeological modeling for groundwater in the study area in the discussion part of the revised manuscript. The detailed contents of these revision are also shown here as follows:

#### 4. 6. Speciation modeling and hydrogeological conceptual model

Speciation modeling. Selected results of speciation modeling are provided in Table 6. All samples are undersaturated with respect to calcite, aragonite, dolomite, halite and gypsum. The values of  $\log PCO_2$ , ranging between -4.77 and -1.45 in the samples from the sedimentary sandy aquifer, indicating that groundwater in the study area is not at equilibrium with atmospheric  $PCO_2$ .

Based on the above analyses, a conceptual model of groundwater recharge was suggested to facilitate understanding of the hydrogeological conditions in the study area. Local and regional modern precipitation is a negligible source. Quaternary unconsolidated sediments with large exposed area form the main aquifer in the study area. Groundwater is recharged by cold water from remote mountain areas, and it flows from east to west along the Solonker Suture Zone. Evaporation is a minor process during groundwater hydrogeochemical evolution. Mineral dissolution may contribute to groundwater salinization, because saturation indices of all minerals are less than zero, indicating that these minerals still can dissolve into groundwater. These clues mean that the origin of groundwater in the desert is mainly controlled by geological structures and processes. The tectonic settings are more important than climatic and topographical settings to explain the origin of groundwater in the desert.

In a view of orogenic belt of the global middle-latitude regions, various groundwater and hydrogeological case studies have established a link between geological perspectives and origin of groundwater flows. Tague and Grant (2004) identify, for instance, the dominant control of a young volcanic geological unit on the groundwater regime of the studied region in Oregon, this geological formation having an exceptionally high permeability. Pfister et al. (2017) show that bedrock permeability significantly influences the ratio between average summer and winter run-off of 16 investigated catchments in Luxembourg. For a selection of Swiss catchments, Naef et al. (2015) associate lower groundwater flow with slowly draining porous bedrock and low streamflow during dry periods for catchments dominated by Moraine deposits. Kaser and Hunkeler (2016) have shown that alluvial aquifers, even if they represent only a small portion of the catchment surface, can contribute significantly to the catchment groundwater outflow especially during low-flow periods. Alluvial aquifers can thus also be relevant for total catchment groundwater storage. Chen and Wang (2009) proposed that earthquake is a possible mechanism for groundwater releasing in the Qilian Mountains and discharging it in the Hexi Corridor. Carlier et al. (2018) statistically analyzed 22 catchments of the Swiss Plateau and Prealpes to establish relationships between streamflow indicators and various geological and hydrogeological properties of the bedrock and Quaternary deposits, along with meteorological, soil, land use, and topographical characteristics. The study shows that the geological characteristics dominate catchment response during high and low groundwater flow conditions.

These studies focused the influence of base/surrounding rock, topography, recharge source and permeability on groundwater flow in orogeny area. According to the hydrologically active bedrock hypothesis (Uchida et al. 2008) the bedrock is an active reservoir that significantly contributes to baseflow (Tague and Grant 2004; Andermann et al. 2012; Welch and Allen 2012; Birkel et al. 2014). The hydraulic conductivity of the bedrock controls storage processes (Hale et al. 2016; Pfister et al. 2017). Most importantly, the ratio of the hydraulic conductivity to recharge rates has been shown to be relevant for water table elevation (Gleeson and Manning 2008). Haitjema and Mitchell-Bruker (2005) propose a criterion based on the Dupuit-Forchheimer approximation combining this ratio with geometrical aquifer properties and topographical characteristics to determine whether the water table is controlled by the topography or the recharge. From the above review it can be seen that various studies have used spatially distributed, synthetic groundwater models to identify and explore how topography, recharge

and/or bedrock permeability influence groundwater fluxes and flow patterns (e.g., Gleeson and Manning 2008; Welch et al. 2012; Welch and Allen 2012; Welch and Allen 2014).

These studies highlight the complex interplay of topography and hydrogeology on groundwater flow. They, however, mainly focus on the geology of the bedrock, no studies mentioned the important role of tectonic structure on the groundwater flow. Thus, based on this study in the Otindag Desert, we proposed a simple conceptual model of multiprocesses that constrain the mechanism of groundwater recharge in the desert, namely mountain water (M) – tectonic fault hydrology (T) – unconfined vadose zone with underlying buried fault (V) – groundwater formation and recharge (G), i.e. the MTVG mechanism. Although the model is still conceptual but not practical at present, it provides a new perspective into the origin and evolution of groundwater resources in the middle-latitude deserts of the arid Asia.

Thank the reviewers and the editor of HESS again for your help in dealing with our manuscript.

We look forward to hearing from you at your earliest convenience.

Best regards,

B.Q. Zhu

25 Jan 2019

**Comments from previous Referee #1**  
(hess-2018-71)

Interactive comment on “Direct or indirect recharge on groundwater in the middle-latitude desert of Otindag, China?” by Bing-Qi Zhu and Xiao-Zong Ren, Anonymous Referee #1, Received and published: 22 May 2018.

The manuscript describes interesting results about the recharge mechanisms of arid zones in China, especially considering the importance of the topic. Despite the multidisciplinary approach, which is very useful in groundwater recharge studies, there are many weak points which have to be improved for a publication in HESS. The main points are listed below: 1) The datasets belong to sampling campaigns carried out in different moments (years) and seasons and for this reason in my opinion cannot be discussed together, without a clear distinction between the different phases. 2) A reconstruction of the piezometric morphology as well as a stratigraphy of the considered study areas should be reported. This could help also the discussion of the groundwater preferential pathways. 3) The organization of the paper is still at a draft level, since there is not a clear distinction between the results and discussion paragraphs. Many paragraphs need to be summarized and better explained. 4) The number of figures should be reduced (probably putting together some and deleting others). 5) The English is very poor and there are many typo errors. The reported delta notation is wrong. Due to the consideration of these main points the manuscript can be accepted only if major revision will be reported.

Interactive comment on Hydrol. Earth Syst. Sci. Discuss., <https://doi.org/10.5194/hess-2018-71>, 2018.

**The authors' responses to the comments from Referee #1**

Dear Dr/Professor Referee #1:

On behalf of my co-authors, we thank you very much for giving us an opportunity to revise our manuscript. We appreciate you very much for your positive and constructive comments and suggestions on our manuscript (hess-2018-71). We have studied your comments carefully and have made revision which marked in red in the revised manuscript. We tried our best to revise our manuscript according to the comments point by point. Attached please find the revised version, which we would like to submit for your kind consideration. Thank you and best regards.

1) The datasets belong to sampling campaigns carried out in different moments (years) and seasons and for this reason in my opinion cannot be discussed together, without a clear distinction between the different phases.

Our response: AGREE AND NO CHANGES MADE.

Firstly, we thank you very much for this comment from you and we truly agree this point that water samples collected in different moments (years) and seasons cannot be discussed together without a clear distinction between the different water phases. In fact, although we stated in the manuscript that our fieldwork had taken place during the summer season of 2011 and the spring season of 2012, we collected the natural water samples at the same time for the same phases in the study area. For example, (1) all the groundwater samples discussed in this paper were collected during the 2011 summer in five days in the Otindag Desert. For other natural water samples discussed in this study, the detailed sampling methods are as follow: (2) all the spring water samples and (3) the precipitation water sample (p1) discussed in this paper were also collected during the 2011 summer in five days in the study area, and (4) all the river water samples and (5) lake water samples were collected during the spring season of 2012 in three days in the study area. This is to say that the water samples within the same phase are discussed together in the paper.

2) A reconstruction of the piezometric morphology as well as a stratigraphy of the considered study areas should be reported. This could help also the discussion of the groundwater preferential pathways.

Our response: AGREE AND CHANGES MADE.

We thank you very much for this comment. And yes, according to this comment, we revised the manuscript and focused on reporting the geological (tectonic, lithological, sedimentological and structural), geomorphological, hydrogeological and stratigraphical settings of the study area. Please see the section 2 “Regional setting” of the revised manuscript in its pages 3-5 lines 103-189.

3) The organization of the paper is still at a draft level, since there is not a clear distinction between the results and discussion paragraphs. Many paragraphs need to be summarized and better explained.

Our response: AGREE AND CHANGES MADE.

We thank you very much for this comment. And yes, we have revised the manuscript accordingly. The structure and content of the paper has been thoroughly reorganized in the revised manuscript, especially for the results and discussion sections, to make the content and context of the paper being more logic, coherent and readable. And yes, almost all of the paragraphs in the paper are newly summarized and explained. The detailed changes can be easily observed in the revised manuscript by reading one of the two resubmitted MS-Word files with the “changes marked” version (in contrast, another version is “clear copy”).

4) The number of figures should be reduced (probably putting together some and deleting others).

Our response: AGREE AND CHANGES MADE.

We thank you very much for this comment. And yes, we have revised the manuscript accordingly. We reduced the number of figures in the revised manuscript by putting some figures together and deleting several figures. At last the revised manuscript has 11 figures compared with the original manuscript that including 15 figures. For example, the Figs. 5, 11, 13, 14a in the original manuscript are deleted in the revised manuscript, and the Figs. 7 and 8, the Figs. 10, 12 and 14a are combined, respectively. In addition, two newly-built figures are added into the revised manuscript according to the second comment from you (the detailed content of this comment can be seen above). The specific changes and the final results of these figures can be seen in the newly submitted revised manuscript.

5) The English is very poor and there are many typo errors. The reported delta notation is wrong.

Our response: AGREE AND CHANGES MADE.

We thank you very much for this comment. We are very sorry for our poor and incorrect English writing in the original manuscript. For the shortcomings of the English presentation and the grammatical edit in the first paper, we have checked and revised the whole manuscript carefully to avoid language errors, and finally we have got the help of a native English speaking professional to check and improve the English quality of the revised manuscript. We believe that the language is now acceptable for the publishing purpose.

In addition, the wrong use of the delta notation in the original manuscript, such as  $\delta^2\text{H}$ , has been corrected as “ $\delta\text{D}$ ” in the revised manuscript.

6) Due to the consideration of these main points the manuscript can be accepted only if major revision will be reported.

Our response: AGREE AND CHANGES MADE.

Special thanks to you for your good comments. We have tried our best to improve the manuscript and made specific changes in the revised manuscript according to the comments from you one by one. These changes will not influence the content and framework of the paper. And here we did not list the changes but marked in red in the revised paper. We hope that the correction will meet with approval. Once again, thank you very much for your comments and suggestions.

**Comments from previous Referee #2**  
(hess-2018-71)

Interactive comment on “Direct or indirect recharge on groundwater in the middle-latitude desert of Otindag, China?” by Bing-Qi Zhu and Xiao-Zong Ren, Anonymous Referee #2, Received and published: 6 June 2018.

Groundwater availability in arid and semi-arid regions is one of the key issues in hydrogeology and is becoming even more important because of the expected climate changes. Within this context, the contribution by Zhu and Ren provides an interesting analysis on the possible recharge supporting the availability of significant groundwater resources in the Otindag desert, north-eastern China. The analyses have been carried out using hydrogeochemical tracers and isotopic measurements on water samples collected from groundwater, surficial (river, lake, and spring) waters, and precipitation water, as well as in-situ records of temperature, pH, conductivity, and TDS concentration. The various steps implemented by the authors to reject possible hypotheses on the groundwater origin (e.g., water flowing from another nearby arid area, precipitation, paleo-water resources) are presented in detail and discussed. Zhu and Ren concludes that, based on the available evidences, the groundwater resources in this region are recharged by the leakage through the bed on incise rivers bounding the desert to the east and conveying downward the waters originated from the precipitation on Daxinganling Ranges. Hence, an “indirect” recharge is the main mechanism supporting the water availability in the study arid lands.

Two are the main weaknesses of this ms: 1) the chemical/isotopic investigations seem not supported by a (at least minimum) knowledge of the hydrogeological setting. This is likely one of the reasons why the analyses carried out by the authors are mainly able to exclude recharge mechanisms, but not definitely explain from where this water is originated. The last part of Section 5.5 provides a list of speculative mechanisms (lines 614-652): how the Xilamulun river can recharge the Dali lake when Fig. 15 shows that the bed of the former is less elevated than that of the latter? What support the “speculation” about the “flash floods” in the southern portion of the desert? How you only “theoretically estimate” the isotopic firm of the precipitation on the Yinshan Ranges? 2) the contribution is over-long. The introduction addresses the topic with a too-wide perspective, concepts are repeated, with verbose descriptions. There are also too many figures that can be fruitfully combined. The English form must be improved too. Moreover, the location of the study area is unclear: Fig 1a is obscure, the various portions of the desert are not provided in the maps shown in Figs. 1b and 2, a large part of the toponymy cited in the text is not added to the maps. Because of this, the ms need a major revision.

Interactive comment on Hydrol. Earth Syst. Sci. Discuss., <https://doi.org/10.5194/hess-2018-71>, 2018.

**The authors’ responses to the comments from Referee #2**

Dear Dr/Professor Referee #2:

On behalf of my co-authors, we thank you very much for giving us an opportunity to revise our manuscript. We appreciate you very much for your positive and constructive comments and suggestions on our manuscript (hess-2018-71). We have read your comments carefully and have made revision which marked in red in the revised manuscript. We tried our best to revise our manuscript according to your comments and suggestions one by one. Attached please find the revised version, which we would like to submit for your kind consideration. Thank you and best regards.

1) The chemical/isotopic investigations seem not supported by a (at least minimum) knowledge of the hydrogeological setting. This is likely one of the reasons why the analyses carried out by the authors are mainly able to exclude recharge mechanisms, but not definitely explain from where this water is originated. The last part of Section 5.5 provides a list of speculative mechanisms (lines 614-652): how the Xilamulun river can recharge the Dali lake when Fig. 15



shows that the bed of the former is less elevated than that of the latter? What support the “speculation” about the “flash floods” in the southern portion of the desert? How you only “theoretically estimate” the isotopic firm of the precipitation on the Yinshan Ranges?

Our response: AGREE AND CHANGES MADE.

We thank you very much for this comment. Yes, any chemical and isotopic investigations need to be supported by knowledge of the regional- and local-scale hydrogeological settings. According to this comment, we have added the specific information about the hydrogeological, geological (tectonic, lithological, sedimentological and structural), geomorphological, stratigraphical settings of the study area in the revised manuscript. Detailed changes and the added information can be seen from the section “2. Regional settings” and the section “4.5 remote water recharge on groundwater in the Otindag: mountains waters” in the revised manuscript (pages 3-5 lines 103-189 and pages 12-13 lines 442-484). Besides, two newly-built figures about the geological and hydrogeological maps of the study area are also provided as auxiliary instructions to illustrate the hydrogeological characteristics of the Otindag Desert in the revised manuscript. These figures are Figs. 2 and 3 in the revised manuscript. With the help of these newly-added materials we believe that we can definitely and logically explain from where the groundwater in the Otindag is originated.

About the Fig. 15 in the original manuscript (at present it is Fig. 11 in the revised manuscript) and the question “how the Xilamulun river can recharge the Dali lake when Fig. 15 shows that the bed of the former is less elevated than that of the latter?”, our explanation is that: actually, the elevation of the Xilamulun river channel is not lower than the Dali lake. The recent elevation of the Dali Lake is 1,226 m above sea level (Xiao et al., 2008, J Paleolimnol, 40, 519-528). The elevations of the river samples collected from the Xilamulun River in this study ranges between 1360 and 1374 m (Table 1). The real elevation data (measured by handheld GPS in the field) for the river samples I1, I2, I3, I4, I5, I6 in this study are 1368 m, 1368m, 1365 m, 1366 m, 1360 m and 1374 m (Table 1), respectively. Thus, the elevation of the Xilamulun river channel is about 140 m higher than that of the Dali Lake. In Fig. 15 (Fig. 11 in the revised manuscript), it shows the variation of the topographical elevation along the section S1 (see Fig. 1b) from the upstream of the Dali Lake to the location site of the spring water samples s2. It does not show the elevations of the river samples from the Xilamulun River. Strictly speaking, however, this sketch map (Fig. 15) is likely to cause misunderstanding if we think about the river water but not the spring water. So we specially stated that “Note that no river water samples are shown in this figure” in the figure caption of Fig. 11 in the revised manuscript.

About the question “What support the “speculation” about the “flash floods” in the southern portion of the desert?”, we have added specific information about the hydrological settings of the flash floods derived from the Yinshan Piedmont in the section “2. Regional settings” in the revised manuscript (see page 5 lines 158-189).

About the question “How you only “theoretically estimate” the isotopic firm of the precipitation on the Yinshan Ranges?”, we use the words “theoretically estimate” because we have not obtained the precipitation water samples from the Yinshan Mountains in this study. Thus the isotopic firm of the precipitation on the Yinshan Ranges is calculated based on the altitude effect of mountain temperature on stable isotopes fractionation in the original manuscript. It is thus a theoretical estimation. In order to avoid ambiguity, we deleted the discussion of this “theoretically estimation” in the revised manuscript.

2) The contribution is over-long. The introduction addresses the topic with a too-wide perspective, concepts are repeated, with verbose descriptions. There are also too many figures that can be fruitfully combined. The English form must be improved too.

Our response: AGREE AND CHANGES MADE.

We thank you very much for this comment. Yes, according to the comment that “the contribution is over-long”, we have rewritten the manuscript and made an intensive compression on the length of the paper. At present the number of text words in the revised manuscript has been greatly decreased compared with the original manuscript.

According to the comment that “The introduction addresses the topic with a too-wide

perspective, concepts are repeated, with verbose descriptions”, we have rewritten the introduction section of the manuscript to make the topic being specific and not being too broad in its perspective. We tried our best to avoid repeat and verbose descriptions in the revised manuscript whatever on the concept or the context of this section. The detailed changes can be seen in pages 1-3 lines 32-101 in the revised manuscript.

According to the comment that “There are also too many figures that can be fruitfully combined”, we reduced the number of figures in the revised manuscript by putting some figures together and deleting several figures. At last the revised manuscript has 11 figures compared with the original manuscript that including 15 figures. For example, the Figs. 5, 11, 13, 14a in the original manuscript are deleted in the revised manuscript, and the Figs. 7 and 8, the Figs. 10, 12 and 14a are combined, respectively. In addition, two newly-built figures are added into the revised manuscript according to the first comment from you (the detailed content of this comment can be seen above). The specific changes and the final results of these figures can be seen in the newly submitted revised manuscript.

About the comment that “The English form must be improved too”, we are very sorry for our poor and incorrect English writing in the original manuscript. For the shortcomings of the English presentation and the grammatical edit in the first paper, we have checked and revised the whole manuscript carefully to avoid language errors, and finally we have got the help of a native English speaking professional to check and improve the English quality of the revised manuscript. We believe that the language is now acceptable for the publishing purpose.

Moreover, the location of the study area is unclear: Fig 1a is obscure, the various portions of the desert are not provided in the maps shown in Figs. 1b and 2, a large part of the toponymy cited in the text is not added to the maps.

Our response: AGREE AND CHANGES MADE.

We thank you very much for this comment. According to this comment, we have revised the Fig. 1a and 1b and Fig. 2 (now it is Fig. 4 in the revised manuscript) to make them clear and make sure that the various portions of the Otindag Desert are provided in the corresponding maps. We tried our best to add each of the toponymy cited in the text to be included in these maps. The specific changes and the final results of these figures can be seen in the newly submitted revised manuscript (Figs. 1-4).

Finally, we want to say that special thanks to you for your good comments. We have tried our best to improve the manuscript and made specific changes in the revised manuscript according to the comments from you one by one. These changes will not influence the content and framework of the paper. And here we did not list the changes but marked in red in the revised paper. We hope that the correction will meet with approval. Once again, thank you very much for your comments and suggestions.



**Potential source of groundwater Direct or indirect recharge on groundwater in the middle-latitude desert of Otindag, China?**

Bing-Qi Zhu<sup>1\*</sup>, Xiao-Zong Ren<sup>2</sup>, Patrick Rioual<sup>3</sup>

<sup>1</sup>KLWCRES, IGSNRR, CAS, Beijing, China

<sup>2</sup>SGS, TYN, Jinzhong, China

<sup>3</sup>KLCGE, IGGCAS, Beijing, China

Correspondence to: Bing-Qi Zhu (zhubingqi@sina.com)

**Abstract.** The Otindag Desert in the middle-latitude desert zone of northern Hemisphere (NH) is essential to livestock-economy and ecoenvironment of northern China. Many areas in this zone are unexpectedly rich with groundwater resources although they have been under arid or hyper-arid climate ~~for a long time~~. Widespread fresh groundwater deep to 60 m was found at the eastern part of the Otindag Desert. The occurrence of this massive fresh groundwater raises doubts on the long-lasting hypothesis in academic circles that regional atmospheric precipitation or palaeowater, ~~namely the direct recharge~~, is the source of water in the middle-latitude desert aquifers of northern China. Understanding of the recharge sources of this fresh groundwater is important in evaluating the feasibility of groundwater exploitation and utilization. In this study we conducted hydrogeochemical and isotopical analyses to assess possible origin and recharge of these groundwaters. The analytical results indicate that the fresh groundwater is neither originated from regional atmospheric precipitation derived from the Asian Summer Monsoon system, nor from palaeowater that formed during the last glacial period. These findings suggest that the groundwater in this desert is possible to originate from remote mountain areas via the faults of the Solonker Suture zone, ~~including the Daxing'anlin and Yinshan Mountains~~. In addition, it is concluded that the hydrogeological linkage between desert aquifers and mountain systems through the suture zone is crucial to the hydrological functioning of the Otindag aquifer. This suggests that the modern indirect recharge mechanism, instead of the direct recharge and the palaeo-water recharge, is the most significant for groundwater recharge in the Otindag Desert. This study provides a new perspective into the origin and evolution of groundwater resources in the middle-latitude desert zone of HA.

**Keywords:** fresh groundwater recharge; atmospheric precipitation; direct recharge; indirect recharge; palaeowater recharge; fault hydrology; middle-latitude desert; Otindag Desert.

## 1. Introduction

The deficit of rainfall occurs globally in semi-arid to arid regions. It is usually made up by extracting groundwater to supply the needs of a growing population and a higher standard of living. Many areas in the middle-latitude desert zone of northern China such as the Badanjilin Desert, the Mu US sandy Land and the Hobq Desert (Chen et al., 2012a; Chen et al., 2012b), are unexpectedly rich with large groundwater resources although they have been under arid or hyper-arid climate for

a long time (Sun et al., 2010). How these groundwaters originated and how they are recharged in these deserts are thus fundamental scientific questions. Until now, however, no consensus has been achieved in academic circles.

The Otindag Desert is one of the largest sandy lands located at the monsoon margin of northern China and is the geographical centre of the northeastern Asian Continent (Fig. 1), which can be regarded as a significant repository of information relating to the groundwater recharge in the arid Inner Asia. At present, the eastern Otindag is also a typical case for its unexpected groundwater resources, because there is abundant groundwater in this desert land and even rivers originate there due to the spillover of spring water, such as the tributaries of Xilamulun River in its north and the Shandian River in its south (Fig. 1). Climatically, the monsoon margin of northern China refers to a strip along the present East Asian Summer Monsoon (EASM) limits and is considered to be sensitive to climate change (Wang and Feng, 2013). Geologically, the Otindag Desert lies in a tectonic depression of the central Solonker suture zone with a few faults stretching east and west (Fig. 2), with its northern margin along a fault marked by a series of lake basins. Thus, the large-scale hydrogeological conditions of the Otindag Desert belong to a fault zone under the influence of the EASM climate.

Until now, however, whether the climate or other factors affected the groundwater recharge in the Otindag is still not known. Little data about the groundwater and its origin is available in the literature, and knowledge and reliable data on various hydrogeological characteristics of the desert such as the catchment extent, input/output, the hysteretic hydraulic functions, the transient hydraulic conditions, in-homogeneities, and on transfer functions to overcome scale problems are also missing. Under such conditions, conventional methods such as water balance and hydraulic methods sometimes fail in determining groundwater recharge, particularly in extreme environments (arid, semi-arid, or cold) (Drever, 1997). Because pristine aquatic conditions may significantly differ from managed conditions in arid environment, and thus groundwater recharge is not a fixed number, but may vary with the boundary conditions of the recharge system (Seiler and Gat, 2007).

Groundwater recharge can be broadly classified into two categories: the direct recharge by native water resources and the indirect recharge by external water resources (Herczeg and Leaney, 2011). Water infiltration of atmospheric precipitation through the unsaturated zone to the groundwater is hydrologically defined as the direct recharge, and the indirect recharge is defined as recharge from mappable features such as rivers, canals, lakes and originates from remote areas (Scanlon et al., 2006; Healy, 2010). It is well known that groundwater recharge can be influenced by environmental factors, including climate change, underlying soil and geology, land cover and the growth in human population that affects withdrawal and economic development (Zhu et al., 2015, 2017). Among these environmental factors, climate and land cover largely determine precipitation and evapotranspiration, whereas the underlying soil and geology dictate whether a water surplus (precipitation minus evapotranspiration) can be transmitted and stored in the subsurface (Doll, 2008, 2009; Giordano, 2009).

For some earth scientists, the direct recharge is thought to be very important for groundwaters in the wide desert lands of north China due to the lack of surface runoffs (Yang et al., 2010; Yang and Williams, 2003; Zhao et al., 2017). They argued

that although the amount of atmospheric precipitation is small, the vast catchment area in the desert region could concentrate the rainfall into large inland basins, creating an aquifer with large storage capacity and great thickness. However, some hydrologists estimated by the chloride mass balance method that the direct recharge was 1.4 mm/year, which represents approximately only 1.7% of the mean annual precipitation in a cold large desert (Badanjilin) in northern China (Gates et al., 2008). A similar estimation of 1 mm/year was given for Gobi deserts from the Hexi Corridor to the Inner Mongolia Plateau in northwestern China (Ma et al., 2008). Consequently, they thought that heavy potential evaporation and little precipitation make it difficult for direct recharge to meet the supply of groundwater in these desert areas. Thus, the indirect recharge is considered to be an important mechanism for groundwater recharge in these desert areas. For example, Zhao et al. (2012) suggested that little precipitation had recharged into groundwaters in the Badain Jaran Desert. Chen et al. (2004) argued that the groundwaters in the Badanjilin Desert were recharged by palaeo-glacial melt water through faults and deep carbonate layers far away from the local desert. Many studies also suggested that palaeowaters stored in an aquifer during wetter climate periods could recharge to groundwater under certain conditions in arid lands (Edmunds et al., 2006; Ma and Edmunds, 2006). Other kinds of indirect recharge, such as mountain front recharge from adjacent mountain blocks, are also proposed to offer an important inflow to aquifers within arid to semiarid catchments (Blasch and Bryson, 2007).

In this paper, we focus to answer the question that whether groundwater recharge in Otindag is mainly direct or indirect, using hydrochemical and isotopic indicators as tracers to offer a valuable support for identifying the contributions of precipitation recharge on groundwater, since these indicators reflect the composition of water molecules and are sensitive to physical processes such as mixing and evaporation (Sultan et al., 2000; Guendouz et al., 2003; Petrides et al., 2006; Scanlon et al., 2006; Zhu et al., 2007, 2008; Jobbágy et al., 2011). The detailed objectives are: (1) to recognize the major sources of groundwater in the area, and (2) to identify the key mechanism of groundwater recharge in the desert.

## 2. Regional settings

**Geographical location.** The Otindag Desert lies between latitudes 42° and 44°N and longitudes 112° and 118° E (Fig. 1). It is an east part of the great middle-latitude desert zone between northwestern and northeastern China which extends from the Taklamakan Desert in northwestern China to the Kelqin Desert in northeastern China, near the west coast of the Pacific Ocean. The desert has an area of approximately 21,400 square kilometers located in the eastern Inner Mongolia and at the monsoon margin of northern China (Fig. 1). It is the fourth largest sandy lands in China (Yang et al., 2012) and is bordered by a flat steppe terrain of Dali Basin to the north, the Yinshan Mountains and mountainous loess landscape to the south, and the the Greater Khingan (Daxing'Anling) Mountains to the east (Fig. 1). The Otindag Desert is essential to livestock-economy and ecoenvironment of northern China. Settlements in this desert are constrained to oases to frequent springs, groundwater with high level and areas where cultivation and irrigation are feasible. Some herdsmen live a precarious life by grazing livestock in the desert.

**Topography and geomorphology.** The relief in the Otindag Desert is varied with

a combination of extensive dune fields and rugged piedmonts and mountains along the eastern and southern rims. In the east, the Daxing'Anling Mountains has an average elevation ranging from 1,100 to 1,400 m and extend from the Heilong River Valley into the upper reach valleys of the Xilumulun River from northeast to southwest, with a gradual increase in height northwards from about 180 m near Huma to Huanggangliang, where the highest mountaintop reach 2,029 m. In the south and southeast, the Yinshan Mountains decline gradually near Duolun and Zhenglanqi, and in some areas leave wide alluvial plains. The terrain of the Otindag Desert is less rough and elevations decrease from ca. 1300 m in the southeast to ca. 1000 m in the northwest. Over the greater part of this desert the ground cover consists of fixed and semi-fixed sandy dunes, with a few mobile dunes in area of little vegetation. The dominated dune types are represented from parabolic to barchans, linear and grid-formed types, ranging from a few meters to over 40 m in height (Zhu et al., 1980; Yang et al., 2008).

Climate, vegetation and soil. The climate of the Otindag Desert was not uniform in geological period, with much sand movement, occasional rainy years, and several wetter intervals during the Holocene (Yang et al., 2015; Tian et al., 2017). At present the whole desert belongs to the arid and semi-arid temperate zone, with a mean annual temperature of 2 °C in the north and 4°C in the south (Liu and Yang, 2013). At the regional scale, the climate of the desert is typically controlled by the East Asian Monsoon system, characterized by a warm summer, with precipitation transported by the EASM, and by a cold and dry winter under the influence of the East Asian Winter Monsoon (EAWM). The rainfall in the desert exhibits a wide variation in space and time. Influence of the EASM changes from southeast to northwest in the desert, varying with the distance increase from the Pacific Ocean and leading to the mean annual rainfall decreasing from ~450 mm in the southeast to ~150 mm in the northwest (Yang et al., 2013). The spatial inequality of rainfall makes a great impact on the availability of near-surface moisture, consequently on the distribution of vegetation, soil and the animal husbandry potential of local communities. The major soil type is the grey desert soil in the west and changes to the sierozems and chernozem or chestnut soil in the east. Through the desert, vegetation is sparse in the west and relatively abundant in the east. The native vegetation is scrub woodland in the east and is steppe in the west, showing a natural characteristic of the temperate desert or semi-desert. It is greatly affected by temperature, rainfall and elevation in the growing season due to the scarcity of surface runoff.

Geology. The Otindag Desert is located in a tectonic depression of the Solonker Suture Zone (Jian et al., 2010) bounded by the Northern Early to Mid-Paleozoic Orogen Zone and the Hatug Uul Block to the north, the Southern Early to Mid-Paleozoic Orogen Zone and the North China Craton system to the south (Fig. 2). A few faults such as the Xar Moron Fault and Chifeng-Bayan Obo Fault stretch east and west, with its northern margin along the Solonker Suture Zone marked by a series of lake basins (Figs. 1 and 2). The tectonostratigraphic units and overall structural trends are mainly oriented NE–SW (Fig. 2), which may be interpreted as resulting from overall compressive stresses oriented principally in the NW–SE quadrants during orogenesis (Jian et al., 2010; Zhang et al., 2015). Diverse rock types from unlithified and lithified clastic sediments through to carbonate, crystalline, and volcanic rocks are distributed in and around the Otindag Desert (Zhang et al., 2015)

(Figs. 2 and 3). Tertiary and Quaternary sandstones and mudstones are the common basement rocks under the dunes of the Otindag, and extensive volcanic basalts forming flat terrains are to the north (Zhu et al., 1980; Li et al., 1995).

Hydrology and hydrogeology. The Otindag Desert originated during the Late Quaternary (Yang et al., 2015) and various alluvial fans formed at the margins of this desert during the early to middle Holocene. These are composed of conglomerate and sand deposits, where major periodic streams or wadis debouched into the Otindag. At present two rivers run through the eastern margin of the Otindag Desert, i.e. the Xilamulun River in the north and the Shandian River and its two tributaries, the Shepi River and Tuligen River in the south. Both stem from the eastern and southeastern parts of the Otindag (Fig. 1). The Xilamulun River, 380 km in length and  $32.54 \times 10^3 \text{ km}^2$  in area, is a neighboring river both to the northeastern Otindag and the southeastern Dali Basin, the northern catchment of the Otindag Desert. The Xilamulun River flows to the east and finally goes into the Xiliao River, with an annual mean runoff of  $6.58 \times 10^8 \text{ m}^3$  (Wu et al., 2014). The Shandian River is the upper reach of the Luan River, with a length of 254 km and a catchment area of  $4.11 \times 10^3 \text{ km}^2$  (Yao et al., 2013). Spotted salt crusts can extensively develop on land surface due to the high rate of evaporation. Sabkhas and salt pans often form in areas surrounding the flat shorelines of some lakes in the Otindag. During rainy season, some rain and floodwaters (generally coming from the Yinshan piedmonts) are retained in low-lying areas, which may temporarily recharge shallow aquifers. Under storm conditions, fast-flowing floods often form in some wadi channels with rich soil due to the occasional short, heavy rainstorms.

Groundwater resources in the Otindag Desert and its surrounding areas depend on several kinds of aquifers with different water-bearing formations and units (Fig. 3). Coarse- to fine-grained sedimentary rocks, magmatic rocks and metamorphic rocks of the Inner Mongolia-Daxing'Anling Orogenic Belt (Zhang et al., 2015) form the major regional aquifer unit (Fig. 3). They are composed mainly of alluvial sediments (mid-Permian Zhesi Formation), melange (Solonker suture zone), A-type granite (early Permian), bimodal volcanic rocks with sedimentary intercalations (early Permian Dashizhai Formation), diorite-quartz diorite-granodiorite rocks (Carboniferous-Permian) and metamorphic complex (predominantly gneiss, early Paleozoic) (Fig. 2). The aquifer is generally unconfined in dune fields of the Otindag Desert, unconfined to semi-confined in the Yinshan Mountains' piedmont, and semi-confined to confined in the Daxing'Anling uplands (Fig. 3). Water-level measurement in June 2010 indicated that the general depth of unconfined groundwater level ranges between 10 to 70 m in the Otindag Desert (Fig. 3). Local granular aquifers in the central desert are composed of coarse fluvial, lacustrine and aeolian sediments, but their extent and thickness vary throughout the watershed (Zhu et al., 1980; Li et al., 1995). The generally coarse-grained texture of the unconsolidated rock formations provides primary porosity in terms of groundwater flow in the desert.

### 3. Methods

The isotopes and ion chemistries of different water samples in the Otindag Desert, including natural samples collected from local and regional precipitation, depression springs, shallow and deep aquifers, perpetual lakes and outflowing rivers,

are analyzed here and discussed. Relationships between the study area and the regional prevailing EASM climate, the dominant topographical, geological (tectonic) and hydrogeological conditions, are also explored and interpreted, using multiple graphs and diagrams. Fieldworks took place during the summer season of 2011 and the spring season of 2012. Water samples were mainly retrieved from shallow and deep wells located over a wide area in dune fields of the study regions. The detailed locations of the sampling sites are shown in Fig. 4.

In this study, we designed two groups of parameters to characterize the physiochemistry of each water sample. One is the field-measured parameters and another is the lab-measured parameters. The former includes those parameters that will change in a shorter period of time when they are not directly measured in the field, such as the total dissolved solid (TDS, mg/L), electrical conductivity (EC in micro-Siemens per centimeter or  $\mu\text{S}/\text{cm}$ ), hydrogen-ion concentration (pH) and temperature ( $^{\circ}\text{C}$ ). The analysis for major cations ( $\text{F}^{-}$ ,  $\text{Cl}^{-}$ ,  $\text{NO}_2^{-}$ ,  $\text{NO}_3^{-}$ ,  $\text{SO}_4^{2-}$ ,  $\text{HCO}_3^{-}$ ,  $\text{CO}_3^{2-}$  and  $\text{H}_2\text{PO}_4^{-}$ ) and anions ( $\text{Li}^{+}$ ,  $\text{Na}^{+}$ ,  $\text{NH}_4^{+}$ ,  $\text{K}^{+}$ ,  $\text{Mg}^{2+}$  and  $\text{Ca}^{2+}$ ) are determined for all of the water samples collected. Contents of stable ( $^2\text{H}$  and  $^{18}\text{O}$ ) and radioactive isotopes ( $^3\text{H}$ ) in the rain and groundwater samples are precisely measured. The analytical data of the physiochemical parameters and the stable and radioactive isotopes of the water samples collected in this study are listed in Tables 1, 2 and 3, respectively.

## 4. Results and Discussions

### 4. 1. Hydrochemical characteristics of natural waters

The natural water samples collected in this study are generally neutral to slightly alkaline, with the pH values varying between 6.26 and 9.44 (except the precipitation sample p1, 4.61) (Table 1) and a median value of 7.27. The TDS values range between 67 and 660 mg/L (average 211 mg/L) (Table 1), all belonging to fresh water (TDS < 1000 mg/L) in the salination classification of natural water (Meybeck, 2004). The variations in ion concentrations of the major cations and anions in the studied water samples were displayed in a fingerprint diagram with a semi-logarithm y-axis (Fig. 5). The rain water sample is the most depleted in ions among these samples. The groundwater samples have the highest concentrations of cations and anions and the lake, river and spring waters had intermediate values. The calcium concentration is the highest among cations in almost all of the water samples, and the  $\text{HCO}_3^{-} + \text{CO}_3^{2-}$  concentration (bicarbonate + carbonate, alkalinity) is the highest among anions in most of the water samples. For several groundwater samples (g3, g4, g5, g6 and g11), spring sample (s1) and precipitation sample (p1), they have higher  $\text{SO}_4^{2-}$  concentrations than alkalinity (Fig. 5).

Two chemically distinct water types are recognized for the studied waters via a Piper diagram (Fig. 6), calcium bicarbonate and calcium sulphate. No Chloride-type and sodium-type waters occur in the study area (Fig. 6). It has been reported that the global groundwater tends to evolve chemically towards the composition of seawater (Chebotarev, 1955), and this evolution is associated with regional changes in dominant anions but not cations. This general evolution of groundwater can be illustrated as an anion evolution line (Freeze and Cherry, 1979):  $\text{HCO}_3^{-} \rightarrow \text{HCO}_3^{-} + \text{SO}_4^{2-} \rightarrow \text{SO}_4^{2-} + \text{HCO}_3^{-} \rightarrow \text{SO}_4^{2-} + \text{Cl}^{-} \rightarrow \text{Cl}^{-} + \text{SO}_4^{2-} \rightarrow \text{Cl}^{-}$ , which travels along the flow paths

and increasing ages. It can be deduced from this line that bicarbonate water is the early product of groundwater evolution with low salinity, renewable water resources or low residence time, while sulfate waters is the intermediate or advanced product of groundwater evolution with higher salinity passing through gypsum and anhydrite aquifers (Clark, 2015). The distribution pattern of water chemical types occurred in the study area indicates a primary stage of groundwater evolution in the Otindag Desert.

The  $\delta D$  values of the groundwater samples collected in this study varied from -63.42‰ to -75.92‰ (Table 3), with an average -69.53‰. The  $\delta^{18}O$  values ranged between -8.64‰ and -11.26‰ (Table 3), with an average -10.17‰. The spring water samples were relatively concentrated in  $\delta D$  and  $\delta^{18}O$  and were greatly similar to those of the groundwater samples (Fig. 7). The  $\delta D$  and  $\delta^{18}O$  values in the river water samples were slightly more variable and were also similar to those of the groundwater (Fig. 7). The lake water samples were enriched in  $\delta D$  and  $\delta^{18}O$  by comparison to the groundwater samples (Fig. 6). The precipitation sample p1 was also enriched in  $\delta D$  and  $\delta^{18}O$  by comparison to the groundwater samples (Fig. 7). The content of radioactive isotope of tritium ( $^3H$ ) measured in seven well groundwater samples with 6-60 m depth ranged from 1.86 to 24.35 TU (Table 3), with an average 14.95 TU, higher than the mean tritium concentration (9.8 TU) of groundwater in the Vienna Basin, Austria (Stolp et al., 2010), the seat of the International Atomic Energy Agency (IAEA).

If we plot the relationships between oxygen and hydrogen isotopes of groundwater, spring, river and lake water samples, we observed that most of the data points fell on a straight line that can be expressed by a regression equation:  $\delta D = 4.09\delta^{18}O - 28.31$  ( $R^2=0.93$ ,  $n=24$ ) (EL1 in Fig. 7). This local groundwater line (LGWL) is different from the Global Meteoric Water Line (GMWL,  $\delta D = 8\delta^{18}O + 10$ ) and the Mediterranean Meteoric Water Line (MMWL,  $\delta D = 8\delta^{18}O + 20$ ) estimated by Craig (1961), but it is similar to the local groundwater lines established for other deserts in northern China and central Asia with a same slope but different Y-intercepts, such as  $\delta D = 4.17\delta^{18}O - 31.3$  for the Badanjilin Desert (Jin et al., 2018),  $\delta D = 4.8\delta^{18}O - 15.2$  for the Ejina Desert in China (Wang et al., 2013), and  $\delta D = 4.26\delta^{18}O + 9.23$  for the Rub Al Khal Desert in the United Arab Emirates (Rizk and El-Etr, 1997). The data points are scattered for the lake water samples (Fig. 7) in the Otindag, suggesting that the lake waters are affected by evaporation, but the other waters in the desert are not so.

#### 4. 2. **Summer pP**precipitation recharge on groundwater in the Otindag

In order to compare the isotopic signals between groundwater and precipitation at a regional scale, the isotopic analysis of precipitation from similar areas surrounding the study area, such as Baotou, were incorporated with local data of **summer** precipitation (p1) in this study (Fig. 7). The Baotou station is the nearest long-term station to the Otindag Desert and was monitored for the isotopic composition of rainfall for the period 1986-2001 within the International Atomic Energy Agency Global Network of Isotopes in Precipitation (IAEA-GNIP) database. The stable isotope data from Baotou was used to represent the regional background of stable isotopic compositions of the present-day **summer** meteoric water, especially in the westward inland areas of the Otindag Desert (Fig. 1). In addition, stable isotope data of the



Tianjin station was also used to represent the regional background of [summer](#) precipitation in the eastern coastal areas of the Otindag Desert (Fig. 1).

Based on the isotopic data from the Baotou station, the local meteoric water lines can be statistically expressed as the isotopic regression equation of  $\delta D = 6.36\delta^{18}O - 5.21$  (LMWL-B). It can also be expressed as  $\delta D = 6.57\delta^{18}O + 0.31$  (LWML-T), based on the data from the Tianjin station (Fig. 7). The precipitation sample p1 collected in this study fell onto the GMWL (Fig. 7). It also showed similar  $\delta D$  and  $\delta^{18}O$  values to those of the precipitation collected in the GNIP stations of Baotou and Tianjin (Fig. 7).

Compared to the [summer](#) precipitation data from the GNIP stations and from the local [summer](#) precipitation (p1), the groundwater, spring, and river water samples were evidently depleted in heavy stable isotopes in the Otindag (Fig. 7). Except for the lake water samples, most of the groundwater, river water and spring water samples in the Otindag fall on or lay between the LMWL-B and the LMWL-T lines, and are located at the lower left area of the precipitation points (Fig. 7).

Because the isotopic evolution of  $\delta D$  and  $\delta^{18}O$  in water illustrated in the Craig line represents a one-way and irreversible process, the water bodies distributed at the upper right area of the Craig line can not be recharge sources for the water bodies distributed at the lower left area of the line. Such results indicate that the groundwater, river water and spring water in the Otindag are not recharged by the regional precipitation, namely no significant modern direct recharge has taken place for groundwater in the Otindag.

Dogramaci et al. (2012) documented that only intense and remarkable rainfall events >20 mm could recharge groundwater in the semi-arid Hamersley Basin of northwest Australia, while the rainfall events <20 mm had limited influences on groundwater recharge. Chen et al. (2014) described that rainfall events  $\leq 5$  mm in the [summer](#) arid and semi-arid region of northern China would be evaporated into the atmosphere rapidly before it is infiltrated into the groundwater system. Based on the analysis on the data records from two meteorological stations around the Otindag, i.e. the Duolun and Xilinhaote stations (see Fig. 1a), we observed that [summer](#) rainfall events >20 mm on average only occur 2.5-3.4 times per year (Table 4). In some years (e.g. from 2005 to 2007 at the Xilinhaote Station), no [summer](#) rainfall events >20 mm even occurred. It further indicated the limited contribution of regional [summer](#) precipitation on groundwater recharge in the Otindag.

In addition to groundwater, the river and spring water samples from the Otindag also deviated from the local precipitation in the Craig diagram (Fig. 7). These water samples came from the Xilamulun, Shepi and Tuligen rivers. They shared the same evaporation line (EL1) with the groundwater and lake water samples (Fig. 7). Generally speaking, natural waters that have a same recharge source are distributed on a same line of evaporation in the  $\delta^2$  and  $\delta^{18}O$  diagram (Chen et al., 2012b). This indicates that the recharge sources of groundwater, river water, spring water and lake water in the Otindag are genetically associated each other and differ from the local precipitation.

#### 4. 3. Winter precipitation and palaeowater recharge on groundwater in the Otindag

Since the groundwater samples in the Otindag are depleted in their  $\delta D$  and  $\delta^{18}O$  values even more than those of the local rainfall (Fig. 7), they must be sourced from

other waters characterized by similar or more depleted signals in their stable isotopes compositions. Due to the temperature effect (such as evaporation) on isotopic fractionation, only the waters issued from colder environments can be more depleted in their  $\delta D$  and  $\delta^{18}O$  values even more than those of the local rainfall.

Because the Otindag Desert is under the control of the EASM climate (Fig. 1), the local rainfall in the desert is mainly sourced from summer precipitation. This can also be illustrated by the seasonal distributions in annual mean precipitation (Fig. 8a), in annual mean air temperature (Fig. 8b) and in annual mean water vapor pressure (Fig. 8c) over the last forty years at the two surrounding GNIP weather stations in Baotou and Tianjin. The seasonal distributions of stable isotopes in the two stations (Fig. 8d-e) show that the summer rainfall is evidently positive in its signals of  $\delta D$  and  $\delta^{18}O$  by comparison with those of the winter rainfall, further suggesting that the waters issued from cold environments can be more depleted in their  $\delta D$  and  $\delta^{18}O$  values than those of the summer rainfall. Thus we speculate that groundwater in the Otindag can be potentially derived from (1) modern precipitation in winter, (2) palaeowater formed in the past glacial period, or (3) remote/mountains waters that emanate in colder and wetter conditions.

The annual mean values of  $\delta D$  and  $\delta^{18}O$  over the last forty years are more depleted in winter precipitation than in summer precipitation at the Baotou and Tianjin stations (Fig. 8d-e). This isotopic signal qualifies the regional winter precipitation to be a potential source of groundwaters in the Otindag. However, the precipitation amounts and the water vapor pressures (effective moisture) in winter months are much lower than those in the summer months at both the Baotou and Tianjin stations (Fig. 8a and 8c). It indicates that the winter seasons in these regions are relatively colder and drier but not colder and wetter. A colder-wetter winter season is a necessary condition for winter precipitation to be a water source for the formation of groundwater under a summer monsoon climate. This is because the bigger amounts of summer precipitation will easily remove or weaken the depleted isotopic signals of winter precipitation in groundwater. In this regard, modern winter precipitation is unlikely to be an important source of groundwater in the Otindag.

As to the palaeowaters formed in colder and wetter periods such as the last glacial, it has been proposed to be a potential water source for groundwaters in the wide arid lands of the world. The depleted signals of stable isotopes ( $\delta D$  and  $\delta^{18}O$ ) in groundwater have been recognized in global arid and semi-arid regions, such as the Sinai Desert in Egypt (Gat and Issar, 1974), Israel (Gat, 1983), South Australia (Love et al., 1994, 2000), northern China (Ma et al., 2010), Saudi Arabia (Bazuhaier and Wood, 1996) and North Africa (Guendouz et al., 2003). These signals are very often explained as palaeo-groundwater that recharged by precipitation during past wetter and colder periods (Love et al., 1994, 2000; Herczeg and Leaney, 2011).

Here we use the tritium data as an environmental tracer to estimate the groundwater age in the Otindag. The tritium data at the GNIP stations of the Baotou and Tianjin are also referenced as the background values in precipitation of recent years. The residence time of groundwater in aquifer and the residual tritium of a water body can be calculated by  $N = N_0 e^{-\lambda t}$  (Yang and Williams, 2003). Where  $N$  = content of residual tritium in water sample,  $\lambda = 0.0565$ , the radioactive decay constant,  $N_0$  = content of tritium at the time of rainfall and  $t$  = years after precipitation. Based on this equation, the residual tritium was theoretically

calculated and the standard for tritium dating was established for seven groundwater samples in the Otindag Desert (Table 3). As a result, ages of 0-60 years were obtained for these groundwater samples (Table 5). This indicates that recent recharge took place several decades after the peak in global nuclear tests. We thus conclude that groundwater is generally not older than 70 years in the study area. It means that groundwater in the Otindag are not palaeowater recharged.

Both the modern summer and winter precipitation recharge and the palaeowater recharge can be refuted, indicating that direct recharge is not a major mechanism controlling the groundwater recharge in the Otindag.

#### 4. 4. ~~External Remote~~ water recharge on groundwater in the Otindag: Dali Basin

The third hypothesis that “remote/mountains waters emanate under colder and wetter conditions” is further considered here. In essence, it is an indirect recharge mechanisms as water originates from remote areas (Healy, 2010; Herczeg and Leaney, 2011).

It is worth noting that the values of deuterium and oxygen-18 for groundwater in the north part of the study area are more depleted in  $\delta D$  and  $\delta^{18}O$  than those in the south part (Table 3). It suggests that the Otindag groundwater might be potentially recharged by water resources coming from the northern neighboring catchment, such as the Dali Basin.

Recently published data of  $\delta D$  and  $\delta^{18}O$  in groundwater, lake water, river water and spring water sampled from the Dali Basin (e.g., Chen et al., 2008; Zhen et al., 2014) were compiled in this study and were co-analyzed with the data from the Otindag. About 70 natural water samples from the Dali and Otindag with  $\delta D$  and  $\delta^{18}O$  values are shown in a Craig diagram (Fig. 9). All of these samples fell on or lied near the evaporation line EL2 in the Craig diagram (Fig. 9), with a regression equation of  $\delta D = 4.81\delta^{18}O - 21.55$  and a high correlation coefficient ( $R^2=0.98$ ,  $n=70$ ). Compared to the groundwater samples in the Otindag, water samples from the groundwaters, rivers and springs from the Dali Basin are more depleted in  $\delta^{18}O$  and  $\delta D$  (Fig. 9). Such results further indicate that, in terms of its isotopic signature, the groundwater in the Otindag has a close relationship with the natural waters in the Dali Basin.

The similar signals of  $\delta D$  and  $\delta^{18}O$  between the groundwater in the Otindag and the river water in the Dali (Fig. 9) point towards the idea that the groundwater in the Otindag might be sourced from the river water in the Dali Basin, since the Dali has more depleted isotopic signals in water than the Otindag (Fig. 9). Considering the topographical gradient of elevations between the two regions, however, river water in the Dali Basin cannot flow into the eastern Otindag, because the terrain elevation of the Dali Basin is lower than that of the Otindag (Fig. 1). This is also the reason why the huge Dali Lake that lies in the Dali Basin has no equivalent in the Otindag (Fig. 1). If there is a hydraulic linkage between the two regions, water should flow from the Otindag into the the Dali, but not conversely.

In view of the hydraulic gradient, river water in the Dali Basin could not be a recharge source for groundwater in the Otindag. However, in view of the isotopic gradients, groundwater in the Otindag could not conversely be the source of river water in the Dali (Fig. 9). Thus, the similar isotopic signals between the river water in Dali and the groundwater in Otindag indicate that these waters might be recharged

468 from a common source.

469 Similar isotopic signals also occurred in the groundwaters between the Otindag  
470 and the Dali Basin (Fig. 9). In order to understand the linkage of groundwaters  
471 between the two regions, the potential movement of groundwater in the transition  
472 zone of the two regions need to be known. In this study, a groundwater-sampling  
473 project was designed in the field along a N-S section of a palaeo-channel located at  
474 the transition zone between the Dali and Otindag (Figs. 1, 2). The channel was  
475 named "PCSX" in this study, with its north part named "NPCSX" and the south part  
476 named "SPCSX".

477 The GPS elevation of the northernmost sampling site in the NPCSX (g11, about  
478 1317 m a.s.l.) was much lower than that of the southernmost site in the SPCSX (g1,  
479 1396 m a.s.l.) (Fig. 2 and Table 1). Regarding to the topographical gradient in the  
480 channel, there is a drop of about 80 m between the NPCSX and the SPCSX. Under  
481 such slope, the underground hydraulic gradient for groundwater flow can be roughly  
482 parallel with that of the surface water flow, namely that the groundwaterflow should  
483 move downwards from the SPCSX area into the NPCSX area. Thus we can speculate  
484 that groundwater in the NPCSX would have higher salinity than those in the SPCSX  
485 under such flowing direction. In order to verify this speculation, actual variations of  
486 water salinity (chloride and TDS) were detected along the PCSX section. The sampling  
487 site g1 was defined as the initial point and the distances between g1 and other  
488 sampling sites along the PCSX section were calculated, based on their GPS  
489 geographical coordinates measured in the field. The results are shown in Fig. 10a-b.  
490 It is clear that the variations of chloride and TDS concentrations in groundwater do  
491 not increase along the palaeo-channel from south to north (Fig. 10a-b). On the  
492 contrary, both the values of chloride and TDS are lower in the NPCSX area than those  
493 in the SPCSX area. Such kind of spatial variations in the chloride and TDS values  
494 contradict the speculated patterns abovementioned, suggesting that the hydraulic  
495 gradient of groundwater flowing path in this region is not controlled by the  
496 topographical gradient between the NPCSX and SPCSX areas.

497 Compared between the NPCSX and SPCSX regions, the stable isotopic values  
498 ( $\delta^{18}\text{O}$  and  $\delta\text{D}$ ) of groundwaters in the SPCSX region vary greatly with a large  
499 amplitude, while those in the NPCSX are relatively constant (Fig. 10c-d). The constant  
500 variations indicate that the recharge source of groundwater in the NPCSX is relatively  
501 unitary. The isotopic values in the SPCSX are much lighter than those in the NPCSX  
502 along the distance section from south to north (Fig. 10c-d). The heaviest values  
503 occurred in the sample g11 collected from the NPCSX (Fig. 10c-d), indicating a water  
504 being earlier recharged. The spring water sample s2, a representation of discharge  
505 water, is characterized by medium values of  $\delta\text{D}$  and  $\delta^{18}\text{O}$ . These results indicate that  
506 the groundwaters in the SPCSX area, with relatively enriched isotopic signals in  $\delta\text{D}$   
507 and  $\delta^{18}\text{O}$  by comparison with those in the NPCSX area, are composed of a mixture of  
508 the groundwaters in the NPCSX with other waters.

509 The tritium contents were broadly and positively related to the values of  
510 deuterium excess in the groundwater samples in the PCSX (Fig. 10e). For water that  
511 experiences an evaporation process, the d-excess value will increase in the  
512 evaporated water vapor, but will decrease in the residual water body (Dansgaard,  
513 1964; Merlivat and Jouzel, 1979). In this study, except for sample g11 (a sample very  
514 close to the riverhead area), the positive relationship between the tritium and the

deuterium excess generally shows that the d-excess values are higher in the groundwaters collected from the NPCSX, but are lower in those from the SPCSX (Fig. 10e). This distribution pattern indicates that the groundwaters in the NPCSX are relatively younger and experienced a lower degree of evaporation than those in the SPCSX. The d-excess gradient, increasing from south to north in the PCSX, further suggests that groundwater does not flow from the SPCSX area to the NPCSX area, namely out of the topographical control.

Many studies (e.g., Boronina et al., 2005; Kazemi et al., 2006) have demonstrated that groundwater flows in the direction in which it gets older. In view of this point, groundwaters in the PCSX region should flow from the NPCSX area to the SPCSX area, in opposition to the S-N topographical gradient between the Otindag and Dali regions. Thus groundwater in the Dali are not the source of groundwater in the Otindag. The similar isotopic signals between groundwaters in the two regions indicate that these waters might be recharged from a common source in other place.

#### **4. 5. Remote-Water sources recharge from remote areas for groundwater in the Otindag: mountains waters**

The discussions above revealed that both the groundwaters in the Otindag and DaliBasin might be recharged from a common source derived from another place. Considering the third hypothesis abovementioned that “remote/mountains waters emanate under colder and wetter conditions”, we propose that this “common source” of the two regions are from mountains areas surrounding the Otindag and Dali Basin.

There are two large permanent rivers and lots of small intermittent streams entering the Dali Basin (Xiao et al., 2008), including the Xilamulun River to the south and the Gongger River to the north, both of which are stemming from the Greater Khingan Mountains (Daxing’Anling Mountains in Chinese pinyin, 1,100-1,400 m above seal level) (Fig. 1). The Xilamulun River carries a large amount of water (about  $6.58 \times 10^8 \text{ m}^3/\text{y}$ ) from the Daxing’Anling Mountains flowing through the east margins of the Dali and Otindag (Wu et al., 2014). This is an important clue linking natural waters between the Otindag and Dali Basin.

Variation in the elevation from the Dali Lake to the riverhead of the Xilamulun River can be clearly found along a land surface topographical section (Fig. 11). The channel of the Xilamulun River is located in the Xar Moron Fault (Fig. 1), which is a part of the Solonker Suture Zone (Eizenhöfer et al., 2014) or the Xilamulun-Changchun-Yanji plate suture zone (Sun et al., 2004) in the regional tectonical settings (Fig. 2). Outcrop observations indicate that fault zones commonly have a permeability structure suggesting they should act as complex conduit–barrier systems in which along-fault flow is encouraged and across-fault flow is impeded (Bense et al., 2013). Thus the hydraulic gradient of groundwater flow in the Eastern margins of the Otindag and Dali Basin must be controlled by the fault zone hydrogeology. This may be the reason why the hydraulic gradient of groundwater represented by the isotopic and hydrogeochemical gradients of groundwater samples in this study is not consistent with the local topographical gradient in the Otindag Desert. On the other hand, the regional aquifer is generally unconfined in dune fields of the Otindag Desert but semi-confined to confined in the Daxing’Anling uplands (Fig. 3), thus the thick unconsolidated aquifers in the study area (Figs. 3 and 11) will be favourable conditions for groundwater storage and transportation along the Solonker

Suture Zone. When rivers stem from the Daxing'Anling Mountains and flow downward to the marginal areas of the Dali and Otindag, leakage water from these rivers can recharge the desert land through thick unconsolidated aquifers. A strong isotopic evidence is that the lake and river waters in the Dali Basin share the same evaporation line (EL2) with the groundwaters in the PCSX area.

Although groundwaters in the SPCSX area are different from those in the NPCSX area, their isotopic data points still fell onto the EL2 (Fig. 9), which further indicates that the groundwaters in the SPCSX are a mixture of waters from the Daxing'Anling Mountain and other sources. Another source for groundwater recharge in the SPCSX could be represented by remote water such as flash floods coming from the north Yinshan Mountains, because it can be clearly observed from digital maps that many transient rivers or streams originated from the Yinshan Mountains flow into the south and southeastern Otindag (Fig. 1). Supportive evidence for this idea can also be observed in the summer rainy season. During rainy days or under storm conditions, fast-flowing floods caused by occasional short, heavy rainstorms can form in playas, wadi channels and low-lying depressions in the unconfined to semi-confined areas of the Yinshan Mountains' piedmont. These waters may temporarily recharge shallow aquifers in the SPCSX area.

#### 4. 6. Speciation modeling and hydrogeological conceptual model

Speciation modeling. Selected results of speciation modeling are provided in Table 6. All samples are undersaturated with respect to calcite, aragonite, dolomite, halite and gypsum. The values of  $\log P_{CO_2}$ , ranging between -4.77 and -1.45 in the samples from the sedimentary sandy aquifer, indicating that groundwater in the study area is not at equilibrium with atmospheric  $P_{CO_2}$ .

Based on the above analyses, a conceptual model of groundwater recharge was suggested to facilitate understanding of the hydrogeological conditions in the study area. Local and regional modern precipitation is a negligible source. Quaternary unconsolidated sediments with large exposed area form the main aquifer in the study area. Groundwater is recharged by cold water from remote mountain areas, and it flows from east to west along the Solonker Suture Zone. Evaporation is a minor process during groundwater hydrogeochemical evolution. Mineral dissolution may contribute to groundwater salinization, because saturation indices of all minerals are less than zero, indicating that these minerals still can dissolve into groundwater. These clues mean that the origin of groundwater in the desert is mainly controlled by geological structures and processes. The tectonic settings are more important than climatic and topographical settings to explain the origin of groundwater in the desert.

In a view of orogenic belt of the global middle-latitude regions, various groundwater and hydrogeological case studies have established a link between geological perspectives and origin of groundwater flows. Tague and Grant (2004) identify, for instance, the dominant control of a young volcanic geological unit on the groundwater regime of the studied region in Oregon, this geological formation having an exceptionally high permeability. Pfister et al. (2017) show that bedrock permeability significantly influences the ratio between average summer and winter run-off of 16 investigated catchments in Luxembourg. For a selection of Swiss catchments, Naef et al. (2015) associate lower groundwater flow with slowly draining

带格式的：字体：加粗

带格式的：缩进：首行缩进： 0 字符

带格式的：字体：加粗

带格式的：图案：清除

带格式的：下标

带格式的：图案：15%（自动设置前景，白色 背景）

porous bedrock and low streamflow during dry periods for catchments dominated by Moraine deposits. Kaser and Hunkeler (2016) have shown that alluvial aquifers, even if they represent only a small portion of the catchment surface, can contribute significantly to the catchment groundwater outflow especially during low-flow periods. Alluvial aquifers can thus also be relevant for total catchment groundwater storage. Chen and Wang (2009) proposed that earthquake is a possible mechanism for groundwater releasing in the Qilian Mountains and discharging it in the Hexi Corridor. Carlier et al. (2018) statistically analyzed 22 catchments of the Swiss Plateau and Prealpes to establish relationships between streamflow indicators and various geological and hydrogeological properties of the bedrock and Quaternary deposits, along with meteorological, soil, land use, and topographical characteristics. The study shows that the geological characteristics dominate catchment response during high and low groundwater flow conditions.

These studies focused the influence of base/surrounding rock, topography, recharge source and permeability on groundwater flow in orogeny area. According to the hydrologically active bedrock hypothesis (Uchida et al. 2008) the bedrock is an active reservoir that significantly contributes to baseflow (Tague and Grant 2004; Andermann et al. 2012; Welch and Allen 2012; Birkel et al. 2014). The hydraulic conductivity of the bedrock controls storage processes (Hale et al. 2016; Pfister et al. 2017). Most importantly, the ratio of the hydraulic conductivity to recharge rates has been shown to be relevant for water table elevation (Gleeson and Manning 2008). Haitjema and Mitchell-Bruker (2005) propose a criterion based on the Dupuit-Forchheimer approximation combining this ratio with geometrical aquifer properties and topographical characteristics to determine whether the water table is controlled by the topography or the recharge. From the above review it can be seen that various studies have used spatially distributed, synthetic groundwater models to identify and explore how topography, recharge and/or bedrock permeability influence groundwater fluxes and flow patterns (e.g., Gleeson and Manning 2008; Welch et al. 2012; Welch and Allen 2012; Welch and Allen 2014).

These studies highlight the complex interplay of topography and hydrogeology on groundwater flow. They, however, mainly focus on the geology of the bedrock, no studies mentioned the important role of tectonic structure on the groundwater flow. Thus, based on this study in the Otindag Desert, we proposed a simple conceptual model of multiprocesses that constrain the mechanism of groundwater recharge in the desert, namely mountain water (M) – tectonic fault hydrology (T) – unconfined vadose zone with underlying buried fault (V) – groundwater formation and recharge (G), i.e. the MTVG mechanism. Although the model is still conceptual but not practical at present, it provides a new perspective into the origin and evolution of groundwater resources in the middle-latitude deserts of the arid Asia.

## 5. Conclusions

In the middle-latitude desert zone of northern China, many deserts such as the Otindag and Badanjilin Deserts, are unexpectedly rich in groundwater resources, although they have no surface runoff and have been under an arid or hyper-arid climate for a long period of time. How groundwaters originated and recharged in these deserts are thus key questions that are still under debate. For some earth scientists, the direct recharge is thought to be very important for groundwaters in

带格式的: 图案: 清除

带格式的: 图案: 清除



the wide desert lands of northern China, due to the lack of surface runoffs. However, groundwater availability is very much a function of the local- and regional-scale geological and climatic settings. To achieve an integrated understanding of the groundwater recharge and its controlling mechanisms is of great significance. In this study, groundwater recharge was explored using multiple environmental tracers in the Otindag Desert of northern China, a region that is under the influence of the East Asian Summer Monsoon (EASM) climate. Compared to modern summer precipitation, the groundwaters, river waters and spring waters are depleted in  $\delta D$  and  $\delta^{18}O$ . All these waters shared a same Craig line, indicating a genetic relationship on their recharge sources. The stable isotopic signals of the groundwaters is more depleted than those of the modern summer precipitation and this suggests that the groundwaters studied could only be sourced from cold water different from the EASM precipitation. In general, the analyses revealed that the highland remote water resources from the Daxing'anling and Yinshan Mountains were isotopically and geochemically traced to be a major source for the groundwater in the Otindag. It suggests that the modern indirect recharge mechanism, instead of the direct recharge and the palaeo-water recharge, is the most significant for groundwater recharge in the eastern Otindag. This study provides a new perspective into the origin and evolution of groundwater resources in the middle-latitude desert zone of northern China.

#### Acknowledgements

This study was financially supported by the National Natural Science Foundation of China (41771014 and 41602196), and the National Key Research and Development Program of China (2016YFA0601900), and the National Natural Science Foundation of China (41602196). We thank the China Meteorological Data Sharing Service system for providing the weather data. Sincere thanks are also extended to Profs. Xiaoping Yang, Xunming Wang, Jule Xiao and other workmates, e.g., Ziting Liu, Hongwei Li, and Deguo Zhang for their generous help in the research work.

#### References:

- Andermann, C., Longuevergne, L., Bonnet, S., Crave, A., Davy, P., and Gloaguen, R.: [Impact of transient groundwater storage on the discharge of Himalayan rivers. Nature Geoscience, 5, 127-132, 2012.](#)
- Bazuhair, A.S., and Wood, W.W.: Chloride mass-balance method for estimating ground water recharge in arid areas: examples from western Saudi Arabia. *Journal of Hydrology*, 186, 153-159, 1996.
- Bense, V.F., Gleeson, T., Loveless, S.E., Bour, O., and Scibek, J.: Fault zone hydrogeology. *Earth-Science Reviews*, 127, 171-192, 2013.
- Birkel, C., Soulsby, C., and Tetzlaff, D.: [Developing a consistent process-based conceptualization of catchment functioning using measurements of internal state variables. Water Resources Research, 50, 3481-3501, 2014.](#)
- Blasch, K.W., and Bryson, J.R.: Distinguishing sources of ground water recharge by using  $\delta^2H$  and  $\delta^{18}O$ . *Ground Water*, 45, 294-308, 2007.
- Boronina, A., Renard, P., Balderer, W., and Stichler, W.: Application of tritium in precipitation and in groundwater of the Kouris catchment (Cyprus) for description of the regional groundwater flow. *Applied Geochemistry*, 20,

1292-1308, 2005.

[Carlier, C., Wirth, S.B., Cochand, F., Hunkeler, D., and Brunner, P.: Geology controls streamflow dynamics. Journal of Hydrology, 566, 756–769, 2018.](#)

Chebotarev, I.I.: Metamorphism of natural waters in the crust of weathering. *Geochimica et Cosmochimica Acta*, 8, 22-32, 1955.

Chen, F., Chen, J., Holmes, J., Boomer, I., Austin, P., Gates, J.B., Wang, N., Brooks, S.J., and Zhang, J.: Moisture changes over the last millennium in arid central Asia: a review, synthesis and comparison with monsoon region. *Quaternary Science Reviews*, 29, 1055-1068, 2010.

Chen, J., Chen, X., and Wang, T.: Isotopes tracer research of wet sand layer water sources in Alxa Desert. *Advances in Water Science*, 25, 196-206, 2014 (in Chinese).

Chen, J., Li, L., Wang, J., Barry, D.A., Sheng, X., Gu, W., Zhao, X., and Chen, L.: Water resources: groundwater maintains dune landscape. *Nature*, 432, 459-460, 2004.

Chen, J., Liu, X., Wang, C., Rao, W., Tan, H., Dong, H., Sun, X., Wang, Y., and Su, Z.: Isotopic constraints on the origin of groundwater in the Ordos Basin of northern China. *Environmental Earth Sciences*, 66, 505-517, 2012a.

Chen, J., Sun, X., Gu, W., Tan, H., Rao, W., Dong, H., Liu, X., and Su, Z.: Isotopic and hydrochemical data to restrict the origin of the groundwater in the Badain Jaran Desert, Northern China. *Geochemistry International* 50, 455-465, 2012b.

[Chen, J.S., and Wang, C.Y.: Rising springs along the Silk Road. Geology 37, 243-246, 2009.](#)

Chen, J., Yang, Q., and Hao, G.: Using hydrochemical and environmental isotopical data to analyse groundwater recharge in the Hunshandake Sandy Land. *Inner Mongolia Science Technology & Economy*, 17, 9-12, 2008 (in Chinese).

Clark, I.D.: *Groundwater Geochemistry and Isotopes*. CRC Press, Boca Raton, 2015.

Craig, H.: Isotopic Variations in Meteoric Waters. *Science*, 133, 1702-1703, 1961.

Dansgaard, W.: Stable isotopes in precipitation. *Tellus*, 16, 436-468, 1964.

Dogramaci, S., Skrzypek, G., Dodson, W., and Grierson, P.F.: Stable isotope and hydrochemical evolution of groundwater in the semi-arid Hamersley Basin of subtropical northwest Australia. *Journal of hydrology*, 475, 281-293, 2012.

Doll, P., and Fiedler, K.: Global-scale modeling of groundwater recharge. *Hydrology and Earth System Sciences*, 12, 863-885, 2008.

Doll, P.: Vulnerability to the impact of climate change on renewable groundwater resources: a global-scale assessment. *Environmental Research Letters*, 4, 035006, doi:10.1088/1748-9326/4/3/035006, 2009.

Drever, J.I.: Catchment mass balance. In: Saether, O.M., and de Caritat, P. (Eds.), *Geochemical Processes, Weathering and Groundwater Recharge in Catchments*. A.A. Balkema, Rotterdam, pp. 241-261, 1997.

Edmunds, W.M., Ma, J., Aeschbach-Hertig, W., Kipfer, R., and Darbyshire, D.P.F.: Groundwater recharge history and hydrogeochemical evolution in the Minqin Basin, North West China. *Applied Geochemistry*, 21, 2148-2170, 2006.

Eizenhöfer, P.R., Zhao, G., Zhang, J., and Sun, M.: Final closure of the Paleo-Asian Ocean along the Solonker Suture Zone: Constraints from geochronological and geochemical data of Permian volcanic and sedimentary rocks. *Tectonics*, 33, 441-463, 2014.

Freeze, R.A., and Cherry, J.A.: Groundwater. Prentice-Hall, Inc, New Jersey, 1979.

Gat, J.R.: Precipitation, groundwater and surface waters: control of climate parameters on their isotopic composition and their utilization as palaeoclimatological tools. In: Palaeoclimates and palaeowaters: a collection of environmental isotope studies. Proc. Adv. Gp. Meeting, Vienna, 25–28 Nov 1980, pp 3–12, IAEA, Vienna, 1983.

Gat, J.R., and Issar, A.: Desert isotope hydrology: water sources of the Sinai Desert. *Geochimica et Cosmochimica Acta*, 38, 1117-1131, 1974.

Gates, J., Edmunds, W.M., Ma, J., and Scanlon, B.: Estimating groundwater recharge in a cold desert environment in northern China using chloride. *Hydrogeology Journal*, 16, 893-910, 2008.

Giordano, M.: Global groundwater? Issues and solutions. *Annual Review of Environment and Resources*, 34, 153-178, 2009.

[Gleeson, T., and Manning, A.H.: Regional groundwater flow in mountainous terrain: Three-dimensional simulations of topographic and hydrogeologic controls. \*Water Resources Research\*, 44, 1-16, 2008.](#)

Guendouz, A., Moulla, A.S., Edmunds, W.M., Zouari, K., Shand, P., and Mamou, A.: Hydrogeochemical and isotopic evolution of water in the Complexe Terminal aquifer in the Algerian Sahara. *Hydrogeology Journal*, 11, 483-495, 2003.

[Haitjema, H.M., and Mitchell-Bruker, S.: Are water tables a subdued replica of the topography? \*Ground Water\*, 43, 781-786, 2005.](#)

[Hale, V.C., McDonnell, J.J., Stewart, M.K., Solomon, D.K., Doolittle, J., Ice, G.G., and Pack, R.T.: Effect of bedrock permeability on stream base flow mean transit time scaling relationships: 2. Process study of storage and release. \*Water Resources Research\*, 52, 1375-1397, 2016.](#)

Healy, R.W.: Estimating groundwater recharge. Cambridge University Press, New York, 2010.

Herczeg, A.L., and Leaney, F.: Review: environmental tracers in arid-zone hydrology. *Hydrogeology Journal*, 19, 17-29, 2011.

Jahn, B.M.: The Central Asian Orogenic Belt and growth of the continental crust in the Phanerozoic. *Geological Society London Special Publications*, 226, 73-100, 2004.

Jian, P., Liu, D., Kroner, A., Windley, B.F., Shi, Y., Zhang, W., Zhang, F., Miao, L., Zhang, L., and Tomurhuu, D.: Evolution of a Permian intraoceanic arc-trench system in the Solonker suture zone, Central Asian Orogenic Belt, China and Mongolia. *Lithos*, 118, 169-190, 2010.

Jin, K., Rao, W., Tan, H., Song, Y., Yong, B., Zheng, Y., Chen, T., and Han, L.: H-O isotopic and chemical characteristics of a precipitation-lake water-groundwater system in a desert area. *Journal of Hydrology*, 559, 848-860, 2018.

Jobbágy, E., Noretto, M., Villagra, P., and Jackson, R.: Water subsidies from mountains to deserts: their role in sustaining groundwater-fed oases in a sandy landscape. *Ecological Applications*, 21, 678-694, 2011.

[Kaser, D., and Hunkeler, D.: Contribution of alluvial groundwater to the outflow of mountainous catchments. \*Water Resources Research\*, 52, 680-697, 2016.](#)

Kazemi, G.A., Lehr, J.H., and Perrochet, P.: Groundwater age. John Wiley & Sons, Hoboken, 2006.

Li, J.: Permian geodynamic settings of Northeast China and adjacent regions: closure

- of the Paleo-Asian Ocean and subduction of the Paleo-Pacific Plate. *Journal of Asian Earth Sciences*, 26, 207-224.
- Li, S., Sun, W., Li, X., and Zhang, B.: Sedimentary characteristics and environmental evolution of Otindag sandy land in Holocene. *Journal of Desert Research*, 15, 323-331, 1995 (in Chinese).
- Liu, Z., and Yang, X.: Geochemical-geomorphological evidence for the provenance of aeolian sands and sedimentary environments in the Hunshandake Sandy Land, eastern Inner Mongolia, China. *Acta Geologica Sinica (English Edition)*, 87, 871-884, 2013.
- Love, A.J., Herczeg, A.L., Leaney, F.W., Stadter, M.H., Dighton, J.C., and Armstrong, D.: Groundwater residence time and palaeohydrology in the Otway Basin, South Australia. *Journal of Hydrology*, 153, 157-187, 1994.
- Love, A.J., Herczeg, A.L., Sampson, L., Cresswell, R.G., and Fifield, L.K.: Sources of chloride and implications for <sup>36</sup>Cl dating of old groundwater, south-western Great Artesian basin, Australia. *Water Resources Research*, 36(6), 1561-1574, 2000.
- Ma, J., Ding, Z., Gates, J.B., and Su, Y.: Chloride and the environmental isotopes as the indicators of the groundwater recharge in the Gobi Desert, northwest China. *Environmental Geology*, 55, 1407-1419, 2008.
- Ma, J., and Edmunds, W.M.: Groundwater and lake evolution in the BadainJaran Desert ecosystem, Inner Mongolia. *Hydrogeology Journal*, 14, 1231-1243, 2006.
- Ma, J., Pan, F., Chen, L., Edmunds, W.M., Ding, Z., He, J., Zhou, K., and Huang, T.: Isotopic and geochemical evidence of recharge sources and water quality in the Quaternary aquifer beneath Jinchang city, NW China. *Applied Geochemistry*, 25, 996-1007, 2010.
- Merlivat, L., and Jouzel, J.: Global climatic interpretation of the deuterium-oxygen 18 relationship for precipitation. *Journal of Geophysical Research*, 84, 5029-5033, 1979.
- Meybeck, M.: Global occurrence of major elements in rivers. In: Drever, J.I. (Ed.), *Surface and Ground Water, Weathering, and Soils*. Holland, H.D., and Turekian, K.K. (Exec.Eds), *Treatise on Geochemistry*, vol. 5. Elsevier-Pergamon, Oxford, pp. 207-223, 2004.
- [Naef, F., Margreth, M., and Floriancic, M.: Festlegung von Restwassermengen: Q347, eine entscheidende, aber schwer zu fassende Größe. Wasser Energie Luft, Heft 4\(107. Jahrgang\), 277-284, 2015.](#)
- Petrides, B., Cartwright, I., and Weaver, T.R.: The evolution of groundwater in the Tyrrell catchment, south-central Murray Basin, Victoria, Australia. *Hydrogeology Journal*, 14, 1522-1543, 2006.
- [Pfister, L., Martinez-Carreras, N., Hissler, C., Klaus, J., Carrer, G.E., Stewart, M.K., and McDonnell, J.J.: Bedrock geology controls on catchment storage, mixing, and release: A comparative analysis of 16 nested catchments. Hydrological Processes, 31, 1828-1845, 2017.](#)
- Rizk, Z.S., and El-Etr, H.A.: Hydrogeology and hydrogeochemistry of some springs in the United Arab Emirates. *Arabian Journal for Science and Engineering*, 22, 95-111, 1997.
- Scanlon, B.R., Keese, K.E., Flint, A.L., Flint, L.E., Gaye, C.B., Edmunds, W.M., and Simmers, I.: Global synthesis of groundwater recharge in semiarid and arid

- regions. *Hydrological Processes*, 20, 3335-3370, 2006.
- Seiler, K.P., and Gat, J.R.: Groundwater Recharge From Run-Off, Infiltration and Percolation. Springer, The Netherlands, 2007.
- Stolp, B.J., Solomon, D.K., Suckow, A., Vitvar, T., Rank, D., Aggarwal, P.K., and Han, L.F.: Age dating base flow at springs and gaining streams using helium-3 and tritium: Fischa-Dagnitz system, southern Vienna Basin, Austria. *Water Resources Research*, 46, W07503, doi:10.1029/2009WR008006, 2010.
- Sultan, M., Sturchio, N., Gheith, H., Hady, Y.A., and Anbeawy, M.: Chemical and Isotopic Constraints on the Origin of Wadi EliTarma Ground Water, Eastern Desert, Egypt. *Ground Water*, 38, 743-751, 2000.
- Sun, D., Wu, F., Zhang, Y., and Gao, S.: The final closing time of the west Lamulun River-Changchun-Yanji plate suture zone-Evidence from the Dayushan granitic pluton, Jilin Province. *Journal of Jilin University (Earth Science Edition)*, 34, 174-181, 2004 (in Chinese).
- Sun, J., Ye, J., Wu, W., Ni, X., Bi, S., Zhang, Z., Liu, W., and Meng, J.: Late Oligocene-Miocene mid-latitude aridification and wind patterns in the Asian interior. *Geology*, 38, 515-518, 2010.
- [Tague, C., and Grant G.E.: A geological framework for interpreting the low-flow regimes of Cascade streams, Willamette River basin, Oregon. \*Water Resources Research\*, 40\(4\), 1-9, 2004.](#)
- Tian, F., Wang, Y., Liu, J., Tang, W., and Jiang, N.: Late Holocene climate change inferred from a lacustrine sedimentary sequence in southern Inner Mongolia, China. *Quaternary International*, 452, 22-32, 2017.
- [Uchida, T., Miyata, S., and Asano Y.: Effects of the lateral and vertical expansion of the water flowpath in bedrock on temporal changes in hillslope discharge. \*Geophysical Research Letters\*, 35, 2-6, 2008.](#)
- Wang, P., Yu, J., Zhang, Y., and Liu, C.: Groundwater recharge and hydrogeochemical evolution in the Ejina Basin, northwest China. *Journal of Hydrology*, 476, 72-86, 2013.
- Wang, Q., and Liu, X.Y.: Paleoplate tectonics between Cathaysia and Angaraland in Inner Mongolia of China. *Tectonics*, 5, 1073-1088, 1986.
- Wang, W., and Feng, Z.D.: Holocene moisture evolution across the Mongolian Plateau and its surrounding areas: a synthesis of climatic records. *Earth-Science Reviews*, 122, 38-57, 2013.
- [Welch, L.A., and Allen, D.M.: Consistency of groundwater flow patterns in mountainous topography: Implications for valley bottom water replenishment and for defining groundwater flow boundaries. \*Water Resources Research\*, 48, 1-17, 2012.](#)
- [Welch, L.A.A., Allen, D.M.M., and van Meerveld, H.J.: Topographic controls on deep groundwater contributions to mountain headwater streams and sensitivity to available recharge. \*Canadian Water Resources Journal\*, 37, 349-371, 2012.](#)
- [Welch, L.A., and Allen, D.M.: Hydraulic conductivity characteristics in mountains and implications for conceptualizing bedrock groundwater flow. \*Hydrogeology Journal\*, 22, 1003-1026, 2014.](#)
- Wu, J., An, N., Ji, Y., and Wei, X.: Analysis on Characteristics of Precipitation and Runoff in Silas MuLun River Basin. *Meteorology Journal of Inner Mongolia*,

891 23-25, 2014 (in Chinese).  
 892 Xiao, J., Si, B., Zhai, D., Itoh, S., and Lomtatidze, Z.: Hydrology of Dali Lake in  
 893 central-eastern Inner Mongolia and Holocene East Asian monsoon variability.  
 894 *Journal of Paleolimnology*, 40, 519-528, 2008.  
 895 Yang, X., Li, H., and Conacher, A.: Large-scale controls on the development of sand  
 896 seas in northern China. *Quaternary International*, 250, 74-83, 2012.  
 897 Yang, X., Ma, N., Dong, J., Zhu, B., Xu, B., Ma, Z., and Liu, J.: Recharge to the  
 898 inter-dune lakes and Holocene climatic changes in the BadainJaran Desert,  
 899 western China. *Quaternary Research*, 73, 10-19, 2010.  
 900 Yang, X., Scuderi, L.A., Wang, X., Scuderi, L.J., Zhang, D., Li, H., Forman, S., Xu, Q.,  
 901 Wang, R., Huang, W., and Yang, S.: Groundwater sapping as the cause of  
 902 irreversible desertification of Hunshandake Sandy Lands, Inner Mongolia,  
 903 northern China. *PNAS*, 112, 702-706, 2015.  
 904 Yang, X., Wang, X., Liu, Z., Li, H., Ren, X., Zhang, D., Ma, Z., Rioual, P., Jin, X., and  
 905 Scuderi, L.: Initiation and variation of the dune fields in semi-arid China – with a  
 906 special reference to the Hunshandake Sandy Land, Inner Mongolia. *Quaternary*  
 907 *Science Reviews*, 78, 369-380, 2013.  
 908 Yang, X., and Williams, M.A.J.: The ion chemistry of lakes and late Holocene  
 909 desiccation in the BadainJaran Desert, Inner Mongolia, China. *Catena*, 51, 45-60,  
 910 2003.  
 911 Yang, X., Zhu, B., Wang, X., Li, C., Zhou, Z., Chen, J., Yin, J., and Lu, Y.: Late Quaternary  
 912 environmental changes and organic carbon density in the Hunshandake Sandy  
 913 Land, eastern Inner Mongolia, China. *Global and Planetary Change*, 61, 70-78,  
 914 2008.  
 915 Yao, S., Zhu, Z., Zhang, S., Zhang, S., and Li, Y.: Using SWAT model to simulate the  
 916 discharge of the river Shandianhe in Inner Mongolia. *Journal of Arid Land*  
 917 *Resources and Environment*, 27, 175-180, 2013 (in Chinese).  
 918 Zhang, Z., Li, K., Li, J., Tang, W., Chen, Y., and Luo, Z.: Geochronology and  
 919 geochemistry of the Eastern Erenhot ophiolitic complex: implications for the  
 920 tectonic evolution of the Inner Mongolia-Daxinganling Orogenic Belt. *Journal of*  
 921 *Asian Earth Sciences*, 97, 279-293, 2015.  
 922 Zhao, J., Ma, Y., Luo, X., Yue, D., Shao, T., and Dong, Z.: The discovery of surface runoff  
 923 in the megadunes of BadainJaran Desert, China, and its significance. *Science*  
 924 *China Earth Sciences*, 60, 707-719, 2017.  
 925 Zhao, L., Xiao, H., Dong, Z., Xiao, S., Zhou, M., Cheng, G., Yin, L., and Yin, Z.: Origins of  
 926 groundwater inferred from isotopic patterns of the Badain Jaran Desert,  
 927 Northwestern China. *Ground Water*, 50, 715-725, 2012.  
 928 Zhen, Z., Li, C., Li, W., Hu, Q., Liu, X., Liu, Z., and Yu, R.: Characteristics of  
 929 environmental isotopes of surface water and groundwater and their recharge  
 930 relationships in Lake Dali basin. *Journal of Lake Sciences*, 26, 916-922, 2014 (in  
 931 Chinese).  
 932 Zhu, B.Q., Yu, J.J., Rioual, P., Gao, Y., Zhang, Y.C., and Xiong, H.G.: Climate effects on  
 933 recharge and evolution of natural water resources in middle-latitude  
 934 watersheds under arid climate. In: Ramkumar, M. U., Kumaraswamy, K., and  
 935 Mohanraj, R. (Eds.), *Environmental Management of River Basin Ecosystems*.  
 936 Springer Earth System Sciences, Springer-Verlag, Heidelberg, pp. 91-109, 2015.  
 937 Zhu, B.Q., Wang, X.M., and Rioual, P.: Multivariate indications between environment

938 and ground water recharge in a sedimentary drainage basin in northwestern  
939 China. *Journal of Hydrology*, 2017, 549, 92-113, 2017.  
940 Zhu, G.F., Li, Z.Z., Su, Y.H., Ma, J.Z., and Zhang, Y.Y.: Hydrogeochemical and isotope  
941 evidence of groundwater evolution and recharge in Minqin Basin, Northwest  
942 China. *Journal of Hydrology*, 333, 239-251, 2007.  
943 Zhu, G.F., Su, Y.H., and Feng, Q.: The hydrochemical characteristics and evolution of  
944 groundwater and surface water in the Heihe River Basin, northwest China.  
945 *Hydrogeology Journal*, 16, 167-182, 2008.  
946 Zhu, Z., Wu, Z., Liu, S., and Di, X.: *An Outline of Chinese Deserts*. Science Press,  
947 Beijing, 1980 (in Chinese).  
948  
949



**Figure Captions:**

**Fig. 1.** The Geographical location of the Otindag Desert in northern China. (a) The study area shown at a large scale, and (b) the study area shown at a smaller scale, with detailed information about the boundary and tectonic settings of the desert land. 1, the palaeo lake area of the megalake Dali; 2, the boundary of the Otindag; 3, the modern lake area; 4, the boundary of Fig. 2; 5, the boundary between the westerlies and the East Asian Summer Monsoon (EASM) climate systems. ①, the Xilamulun River. ②, the Gonggeer River. ③, the Shepi River. ④, the Tuligen River. The boundary between the westerlies and the EASMin (a) and (b) is modified from Chen et al. (2010). The palaeo lake area of the megalake Dali and the palaeo channel in (b) is modified from Yang et al. (2015). The location of the Xar Moron Fault is referenced from Eizenhöfer et al. (2014). Section S1 is an elevation section starting from the upstream of the Dali Lake and ending with a spring sample (s2) in the riverhead of Xilamulun River.

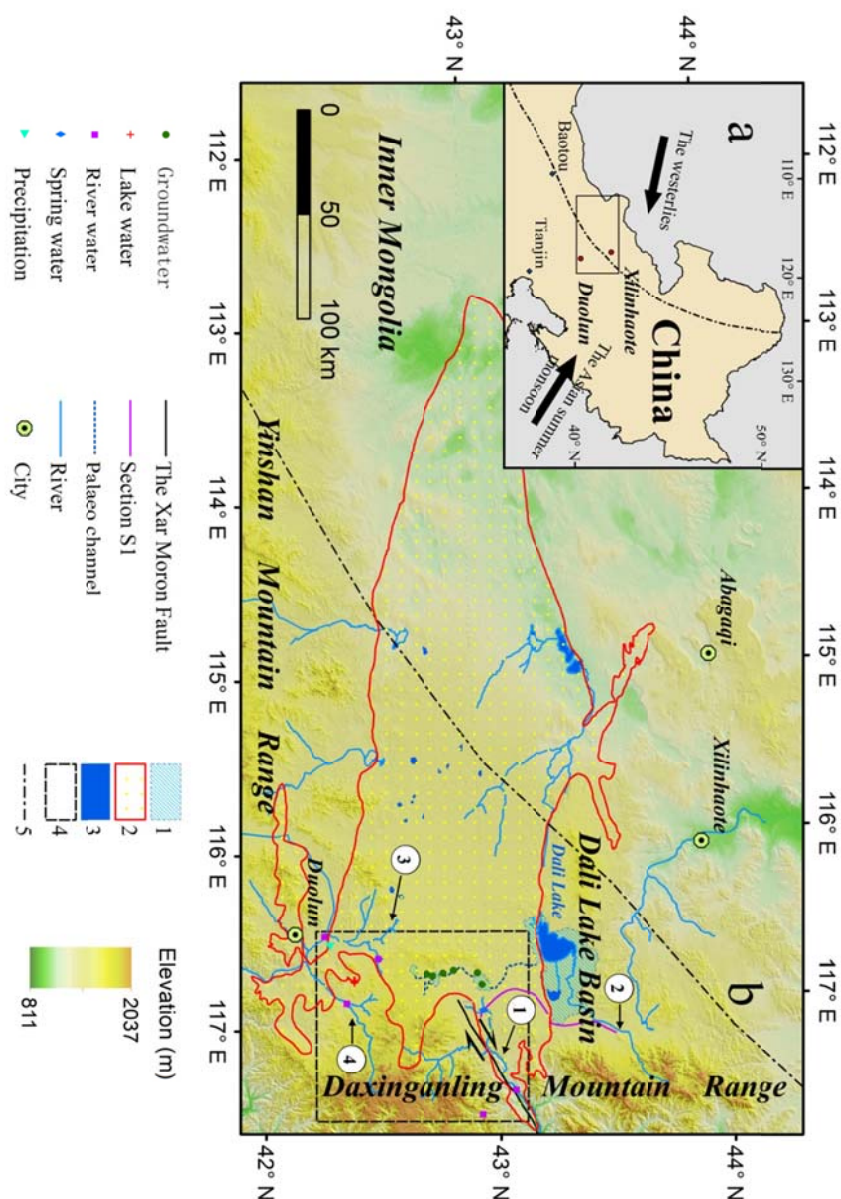


**Fig. 2.** (a) Tectonic framework of the north China-Mongolian segment of the Central Asian Orogenic Belt (modified after Jahn, 2004). (b) Geological sketch map of the northern China-Mongolia tract (modified after Jian et al., 2010). The Solonker suture zone represents the tectonic boundary between the northern (Hutag Uul Block-Northern orogen) and the southern (southern orogen-Northern margin of North China craton) continental blocks. Note that the red line marks the early Permian paleobiogeographical boundary (Wang and Liu, 1986; Li, 2006), which coincides with the northern boundary of the suture zone.

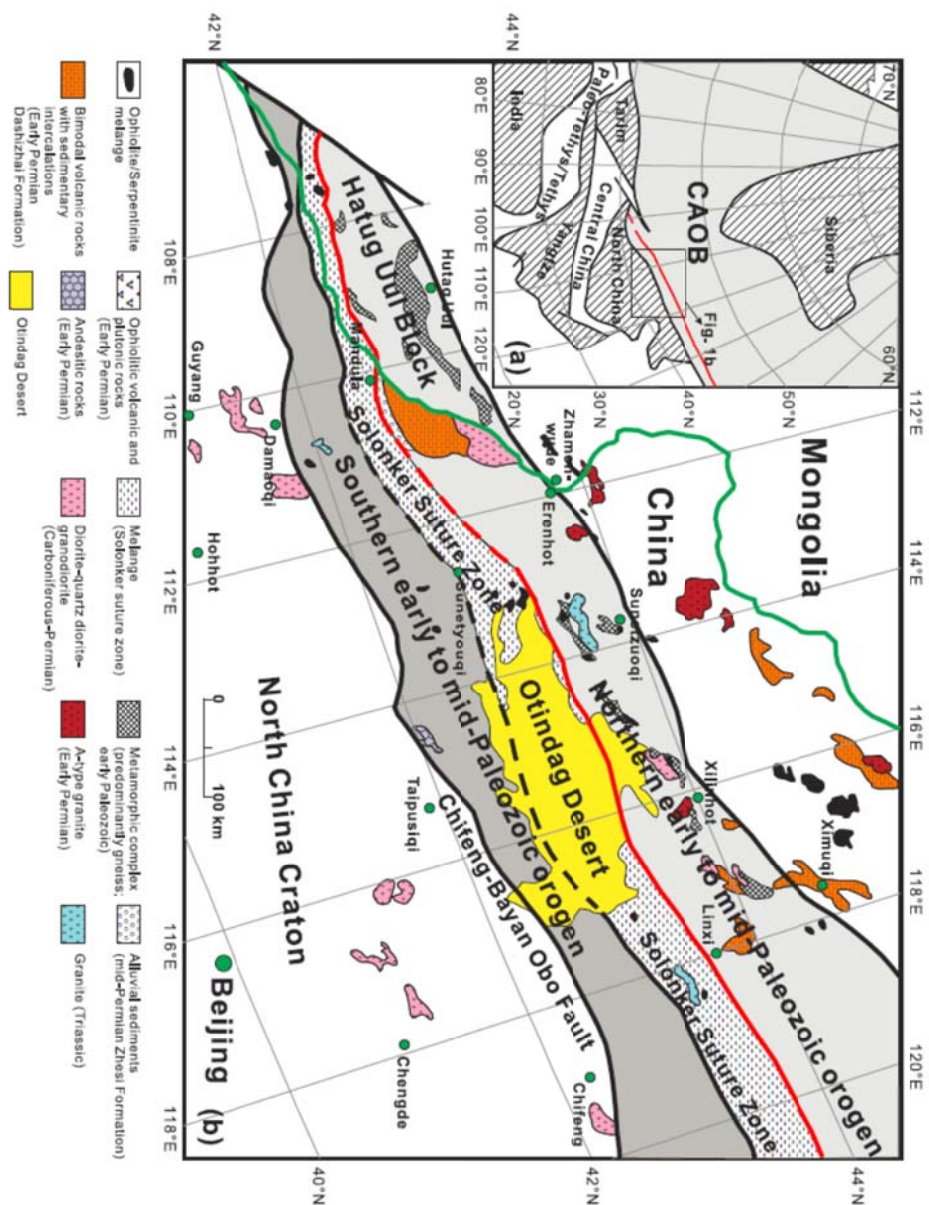


**Fig. 3.** The hydrogeological division map of the Otindag Desert.

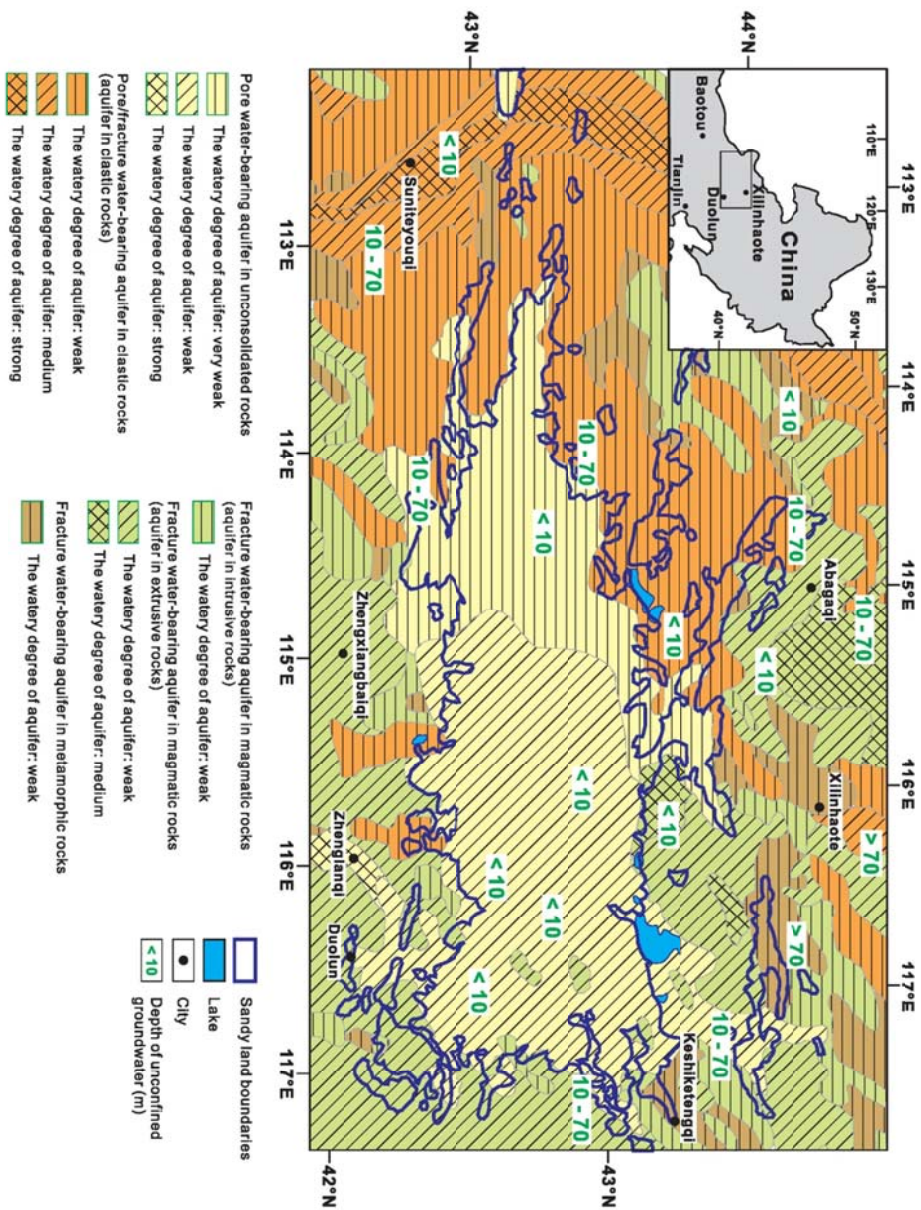
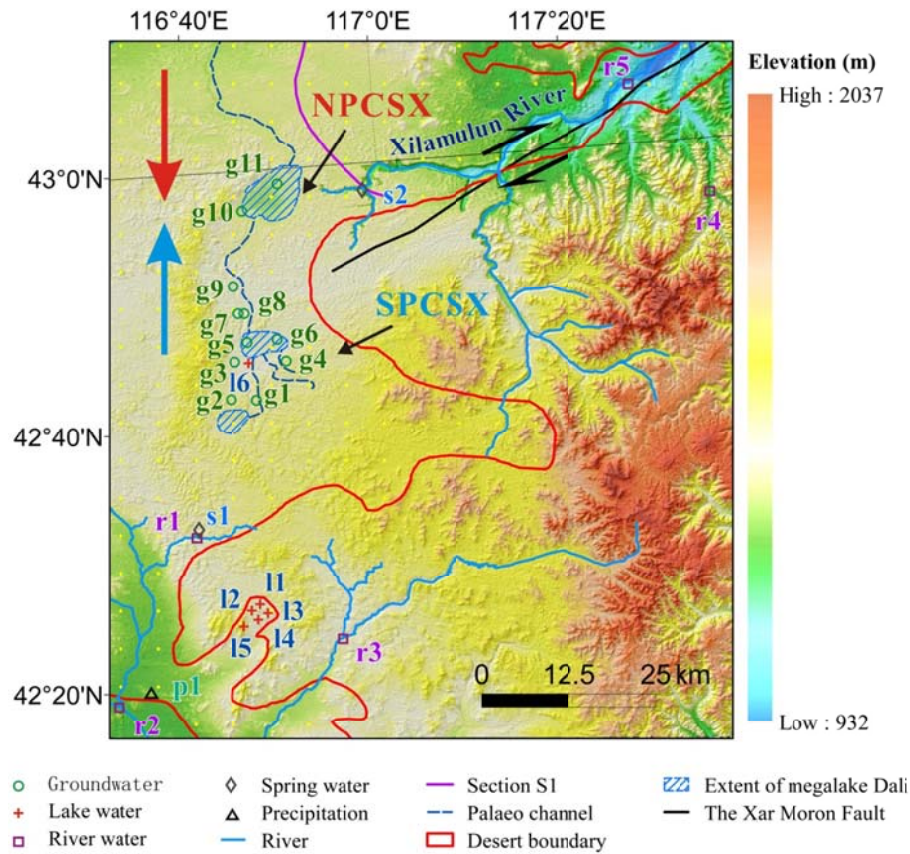


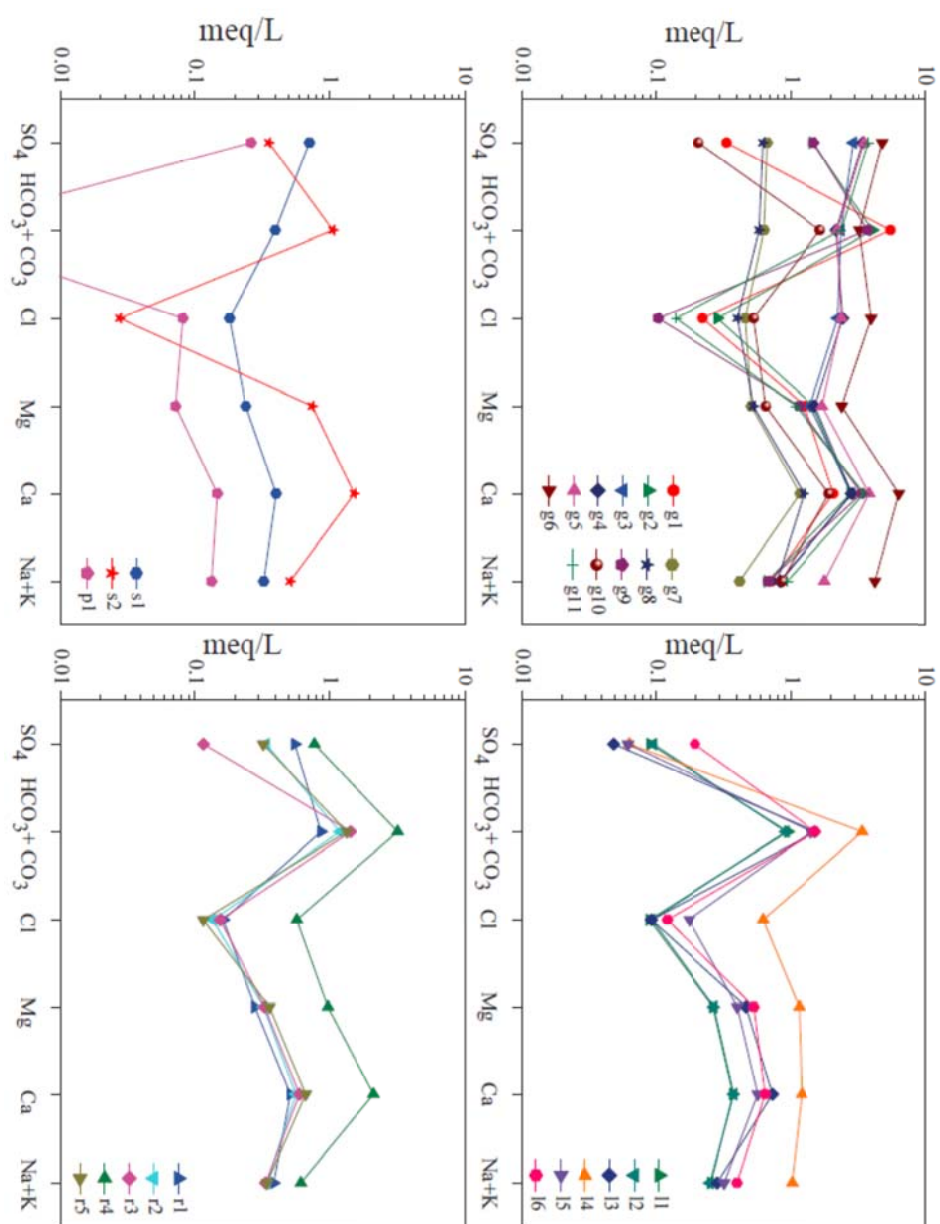


**Fig. 4.** The locations of the water sampling sites in this study.



1015  
1016  
1017  
1018  
1019  
1020  
1021  
1022

1023 **Fig. 5.** The fingerprint diagram showing the variations of multiple ions'  
1024 concentrations in the studied water samples in an equivalent unit. The  $\text{HCO}_3+\text{CO}_3$   
1025 concentration in the sample p1 was not shown, due to its value being lower than the  
1026 detection limit.



1028  
1029  
1030  
1031  
1032  
1033  
1034  
1035  
1036  
1037  
1038



**Fig. 6.** The Piper diagram showing the relative abundances of major cations and anions in the studied water samples. Major water types are also shown in this diagram.

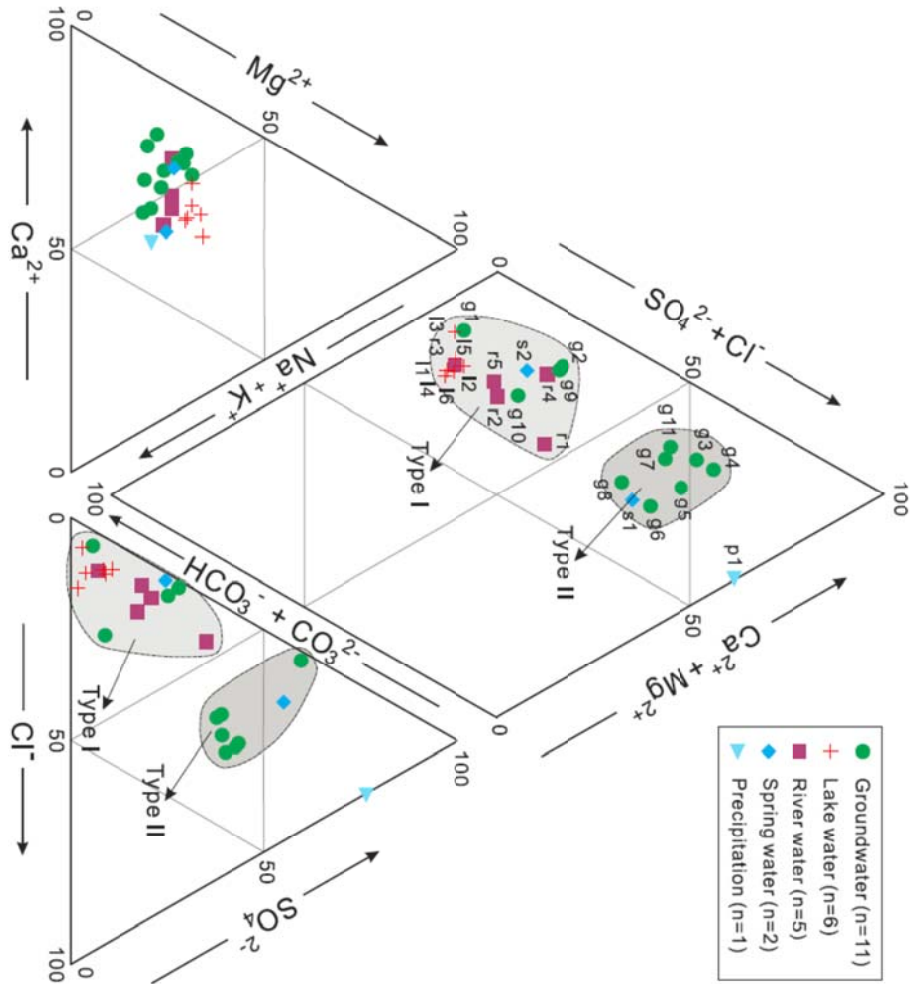


**Fig. 7.** The bivariate diagram of  $\delta D$  and  $\delta^{18}O$ , i.e. the Craig diagram, for the natural water samples in this study. Different relationships between the groundwaters, lake waters, river waters, spring waters and the precipitation waters are illustrated. AWMB, the annual weighted mean value at the Baotou station; AWMT, the annual weighted mean value at the Tianjin station; LWMB, the long-term weighted means at the Baotou station; LWMT, the long-term weighted means at the Tianjin station; GMWL, the Global Meteoric Water Line; LMWL-B, the local meteoric water line calculated based on the data from the Baotou station; LWML-T, the local meteoric water line calculated based on the data from the Tianjin station; EL1, the evaporation line calculated based on the data of water samples collected in this study.

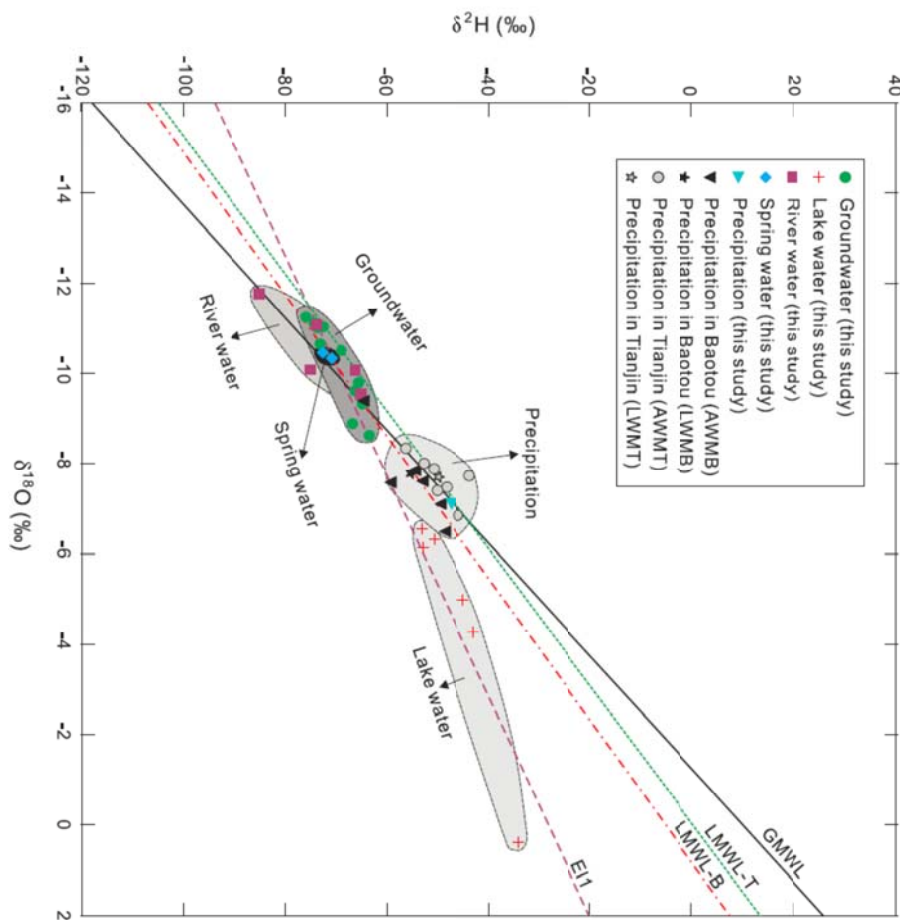


**Fig. 8.** The seasonal mean distributions of (a) precipitation, (b) surface air temperature and (c) water vapor pressure from the Baotou and Tianjin weather stations (station sites seen in **Fig. 1a**) in the surrounding areas of the Otindag for the period 1981-2010. The seasonal mean distributions of (d)  $\delta^{18}\text{O}$  and (e)  $\delta\text{D}$  values in precipitation from the Baotou and Tianjin weather stations in the surrounding areas of the Otindag for the period 1986-2001.

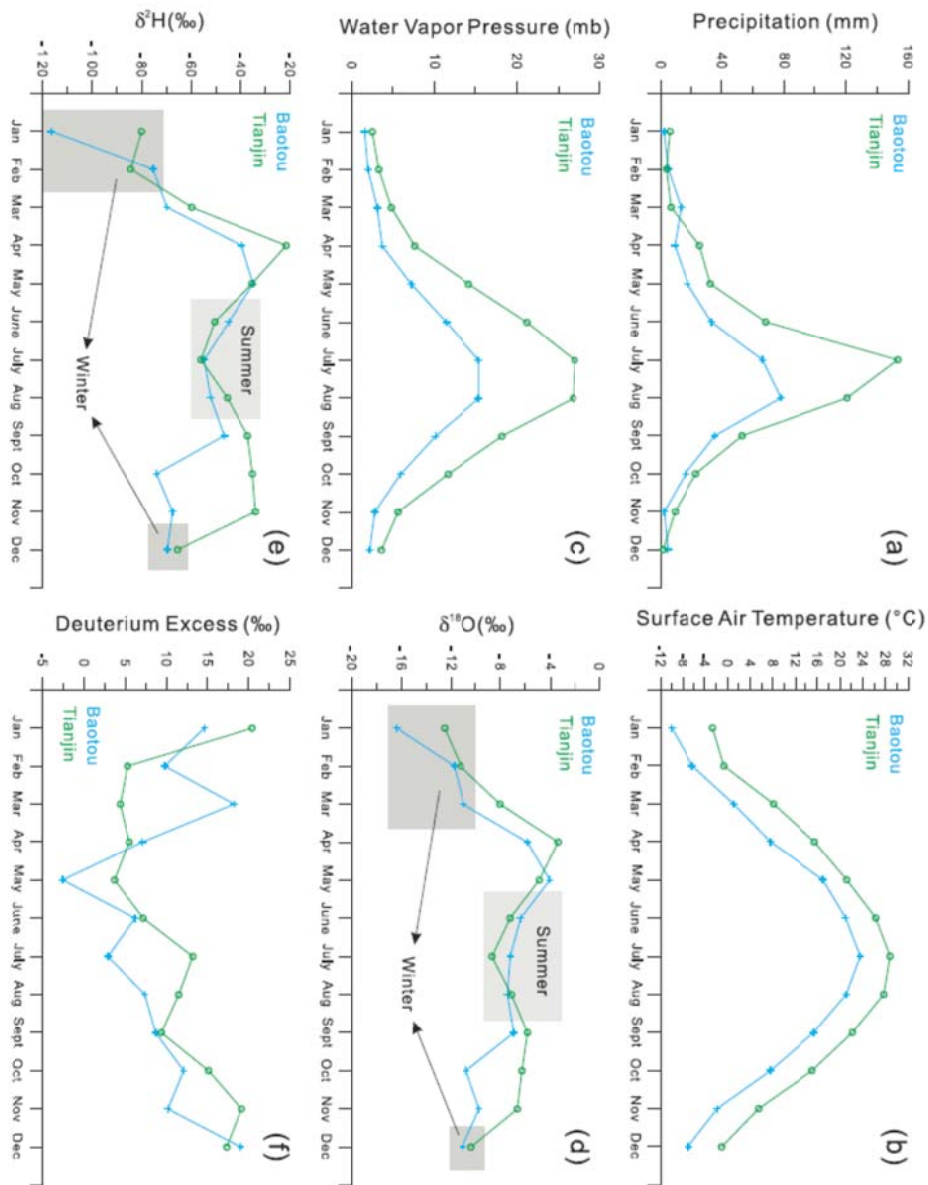


**Fig. 9.** The bivariate diagram of  $\delta\text{D}$  and  $\delta^{18}\text{O}$ , i.e. the Craig diagram, for the natural water samples collected in the Otindag (this study) and the Dali Basin. Different

relationships between the groundwaters, lake waters, river waters, spring waters and the precipitation waters are clearly illustrated. AWMB, AWMT, LWMB, LWMT, GMWL, LMWL-B, LWML-T, and EL1 are the same as in Fig. 7. EL2, the evaporation line calculated based on the data from the groundwater, lake water, river water and spring water samples collected from the Otindag and Dali Basin. The data for the Dali were taken from Chen et al. (2008) and Zhen et al. (2014).

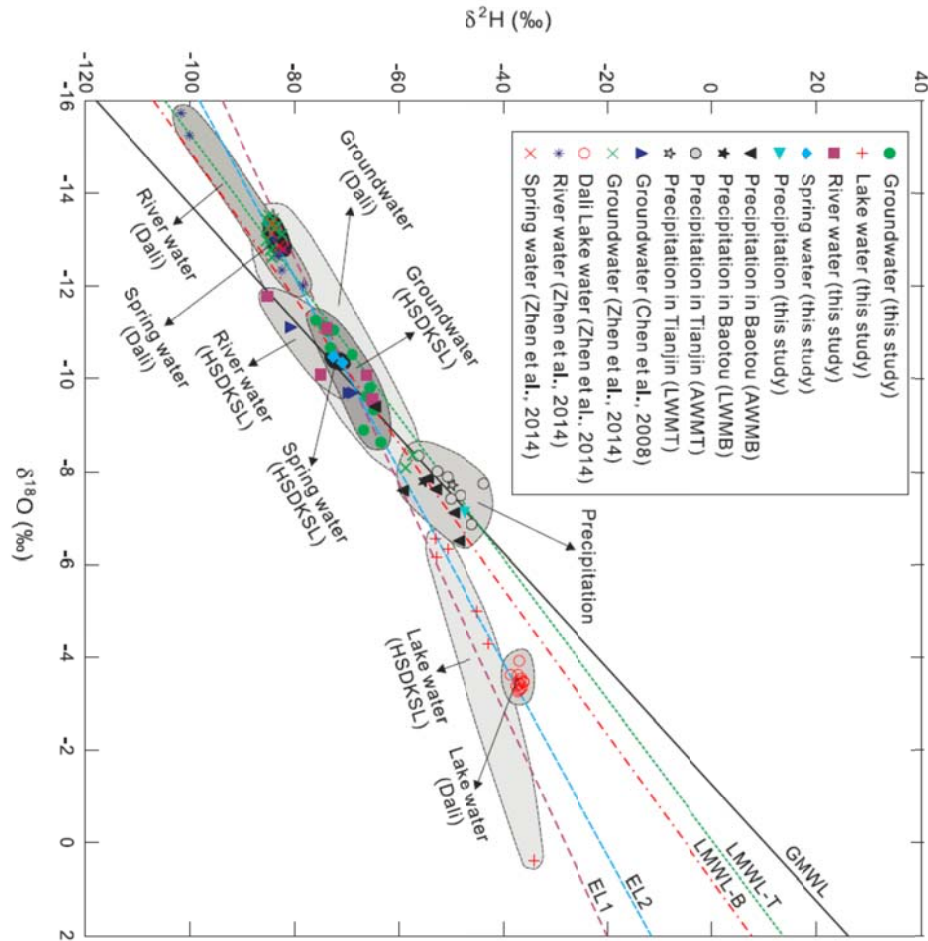


**Fig. 10.** (a) Sketch map showing the relationship between the groundwaters in the NPCSX and SPCSX areas, based on variations of (a) the chloride concentrations, (b) the TDS concentrations, (c) the  $\delta^{18}\text{O}$  values and (d) the  $\delta\text{D}$  values of these water samples versus their distances away from the water sample g1 along the palaeo river channel (PCSX) from south to north. The dashed line in (c) and (d) represents the corresponding values of the spring water sample s2, and divides samples into the NPCSX and SPCSX parts. (e) Variations of tritium contents vs. deuterium excess for the groundwater samples in the study area. The sample g6 was omitted due to its potential contamination.

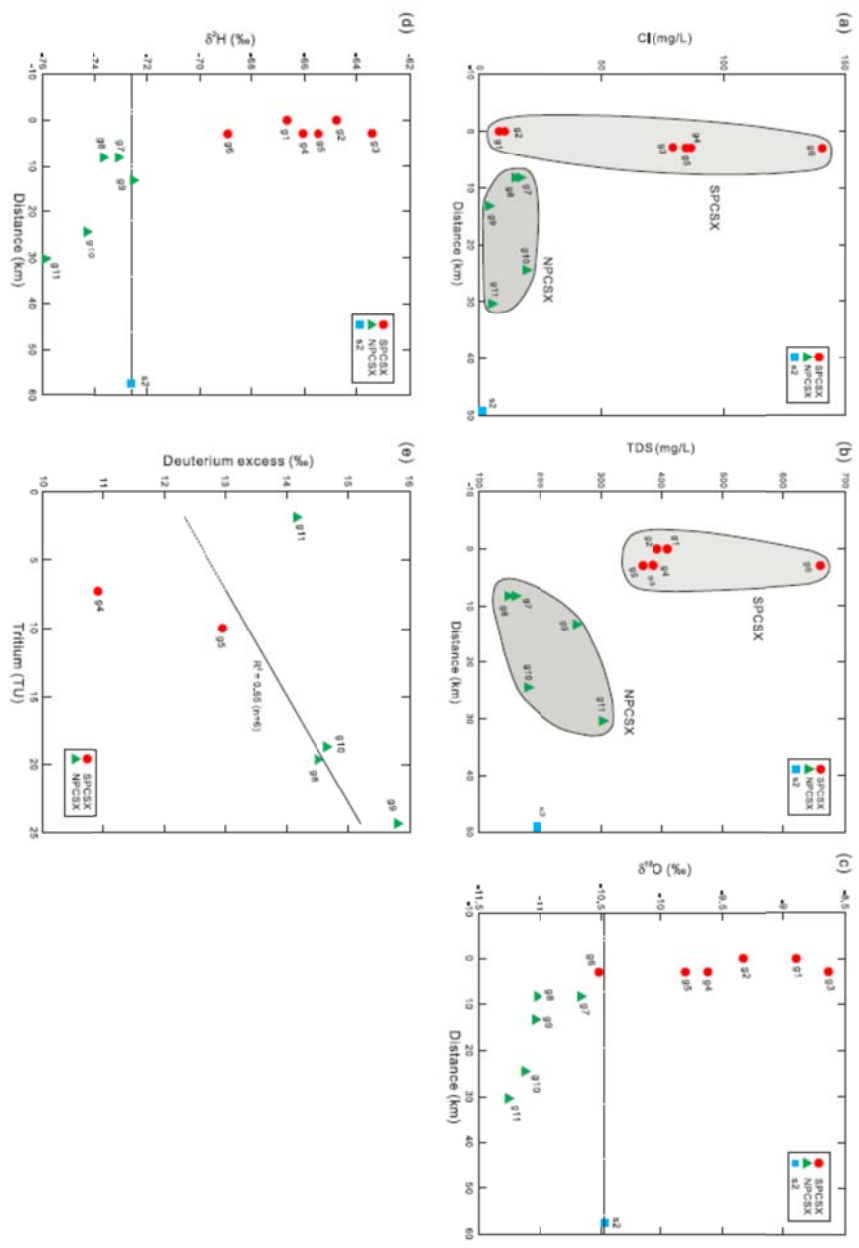
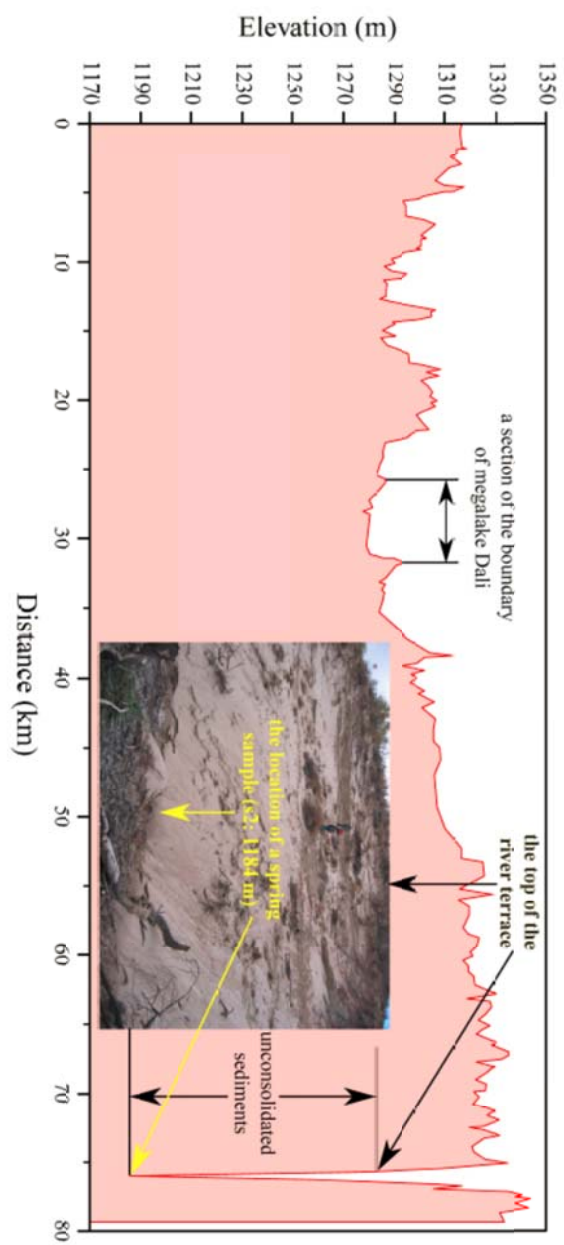


**Fig. 11.** Variation of the topographical elevation along the section S1 (see Fig. 1b) from the upstream of the Dali Lake to the location site of the spring water sample (s2) in the riverhead of the Xilamulun River. Note that no river water samples are shown in this figure.



1147  
1148



1148 **Table Captions:**  
1149 **Table 1.**The physical parameters measured for the natural water samples in the study area.

Sample ID	Water type	Latitude (N, degree)	Longitude (E, degree)	Elevation (m a.s.l)	Depth (m)	Temperature (°C)	pH	Eh (mV)	EC (μS/cm)	TDS (mg/L)	Salinity (%)	Alkalinity (meq/L)	Hardness (°dH)
g1	Groundwater	42.736306	116.747333	1396	12	5.8	6.72	3	769	410	0.6	5.47	9.42
g2	Groundwater	42.736306	116.747333	1396	26	6.0	6.91	-10	736	393	0.5	4.07	12.0
g3	Groundwater	42.760194	116.760139	1355	32	7.7	6.88	-6	725	384	0.5	2.39	11.9
g4	Groundwater	42.759694	116.760417	1360	7	10.0	6.74	1	725	387	0.5	2.20	12.3
g5	Groundwater	42.759556	116.760556	1362	27	7.6	6.46	16	691	368	0.5	2.23	15.6
g6	Groundwater	42.760111	116.760250	1365	7	10.3	6.26	22	1240	660	0.8	3.25	24.5
g7	Groundwater	42.806361	116.747806	1352	20	6.8	6.71	2	297	158	0.2	0.63	4.70
g8	Groundwater	42.806361	116.747806	1352	16	6.5	6.92	-8	276	147	0.2	0.58	5.00
g9	Groundwater	42.850333	116.735722	1347	30	7.2	6.74	-1	487	260	0.4	3.73	12.7
g10	Groundwater	42.949861	116.759194	1321	37	9.9	6.75	-2	337	179	0.2	1.66	7.23
g11	Groundwater	42.967111	116.827528	1317	60	8.6	6.99	-14	571	302	0.4	2.40	12.9
l1	Lake water	42.424611	116.769194	1368	/	16.9	9.44	-151	126	67	0.1	0.95	1.79

l2	Lake water	42.424611	116.769194	1368	/	19.6	9.18	-137	132	70	0.1	0.92	1.82
l3	Lake water	42.424611	116.757806	1365	/	20.2	7.38	-36	196	105	0.1	1.53	3.36
l4	Lake water	42.427083	116.757639	1366	/	20.5	7.87	-64	448	238	0.2	3.42	6.61
l5	Lake water	42.421806	116.756917	1360	/	20.1	8.23	-83	173	92	0.1	1.43	2.73
l6	Lake water	42.736389	116.747222	1374	/	10.7	8.35	-89	194	103	0.1	1.53	3.30
r1	River water	42.530917	116.641250	1355	/	20.6	7.31	-33	180	96	0.1	0.88	2.23
r2	River water	42.310883	116.494817	1231	/	14.9	7.67	-52	178	95	0.1	1.21	2.50
r3	River water	42.385778	116.886194	1362	/	9.5	7.62	-48	177	94	0.1	1.45	2.62
r4	River water	42.931417	117.585306	1217	/	10.5	7.97	-69	474	252	0.3	3.22	8.73
r5	River water	43.079083	117.457389	1006	/	12.9	7.87	-62	191	101	0.1	1.37	2.88
s1	Spring water	42.530917	116.641250	1359	/	20.9	6.63	5	165	88	0.1	0.40	1.81
s2	Spring water	42.965417	116.975361	1184	/	19.0	7.47	-46	371	195	0.2	1.07	6.40
p1	Precipitation	42.330750	116.551694	1260	/	20.2	4.61	109	78	42	0.0	/	0.61

1150

1151 **Table 2.** The concentrations of major cations and anions measured for the water samples in the study area.

Sample	F <sup>-</sup> (mg/L)	Cl <sup>-</sup> (mg/L)	NO <sub>2</sub> <sup>-</sup> (mg/L)	NO <sub>3</sub> <sup>-</sup> (mg/L)	SO <sub>4</sub> <sup>2-</sup> (mg/L)	CO <sub>3</sub> <sup>2-</sup> (mg/L)	HCO <sub>3</sub> <sup>-</sup> (mg/L)	Li <sup>+</sup> (mg/L)	Na <sup>+</sup> (mg/L)	NH <sub>4</sub> <sup>+</sup> (mg/L)	K <sup>+</sup> (mg/L)	Mg <sup>2+</sup> (mg/L)	Ca <sup>2+</sup> (mg/L)
g1	0.13	7.90	2.32	0.48	16.1	0.00	335	0.02	13.8	10.5	4.59	15.5	41.8
g2	0.21	10.2	0.00	6.15	70.6	0.10	248	0.02	13.4	6.56	3.45	17.9	56.0
g3	0.11	79.6	0.00	0.00	141	0.00	145	0.01	17.9	2.28	1.76	17.1	57.3
g4	0.10	86.9	0.00	5.73	165	0.00	134	0.02	18.0	0.00	2.02	18.5	57.3
g5	0.07	84.8	0.00	0.76	169	0.00	136	0.00	39.7	1.02	2.72	20.9	76.9
g6	0.07	141	0.00	111	229	0.00	198	0.00	79.8	0.00	29.47	29.3	126.7
g7	0.37	16.3	0.00	306	32.0	0.00	38.7	0.06	7.83	0.00	3.09	6.21	23.4
g8	0.29	14.3	0.00	35.5	29.9	0.00	35.5	0.02	16.2	0.11	3.38	6.44	25.1
g9	0.10	3.66	0.15	1.19	71.6	0.00	227	0.06	12.9	0.55	4.50	14.1	67.5
g10	0.24	18.8	0.00	49.5	9.97	0.00	101	0.00	18.5	0.00	2.09	7.92	38.7
g11	0.28	4.94	0.00	0.00	182	0.00	146	0.05	20.4	2.59	2.06	13.3	70.6

l1	0.16	3.15	0.00	0.07	4.32	0.00	57.9	0.01	5.42	0.00	0.86	3.24	7.49
l2	0.16	3.30	0.00	1.66	4.57	0.00	55.8	0.00	5.33	0.00	0.84	3.29	7.61
l3	0.11	3.27	0.00	0.61	2.33	0.00	93.3	0.01	5.88	0.00	1.19	5.68	14.7
l4	0.17	22.1	0.00	0.39	3.04	0.10	208	0.00	9.21	0.70	24.2	14.1	24.2
l5	0.09	6.24	0.00	0.65	2.97	0.10	86.8	0.01	6.72	0.00	1.16	4.91	11.4
l6	0.18	4.29	0.00	0.80	9.34	0.10	93.0	0.01	8.41	0.00	1.36	6.47	13.0
r1	0.30	5.76	0.00	2.38	26.7	0.30	52.4	0.01	7.15	0.00	2.99	3.41	10.3
r2	0.19	4.82	0.00	0.65	16.4	0.10	73.1	0.01	6.82	0.00	1.92	3.96	11.4
r3	0.64	5.46	0.00	0.43	5.57	0.00	88.1	0.01	7.11	0.00	1.13	4.04	12.1
r4	1.08	20.4	0.00	19.3	37.3	0.50	195	0.01	13.0	0.00	1.96	11.9	42.8
r5	0.19	4.10	0.00	1.08	15.6	0.00	82.6	0.01	6.71	0.00	2.08	4.38	13.4
s1	0.16	6.44	0.00	1.95	34.3	0.00	24.3	0.02	6.56	0.00	1.62	2.92	8.10
s2	0.05	0.98	0.00	0.45	17.2	0.00	64.9	0.02	9.87	0.00	3.32	9.10	30.8
p1	0.61	2.90	0.00	9.46	12.7	0.00	0.00	0.00	2.09	2.07	1.64	0.88	2.95

1152

1153

1154

1155 **Table 3.** The analytical data of stable and radioactive isotopes measured for the water samples in this study.

Sample ID	$\delta D$ (‰)	$\sigma$ ‰	$\delta^{18}O$ (‰)	$\sigma$ ‰	deuterium excess (d)	Tritium ( $^3H$ ) (TU)
g1	-66.7	0.199	-8.90	0.026	4.50	/
g2	-64.8	0.291	-9.34	0.039	9.93	/
g3	-63.4	0.269	-8.64	0.008	5.66	/
g4	-66.1	0.149	-9.62	0.062	10.9	7.25
g5	-65.5	0.111	-9.80	0.027	13.0	9.98
g6	-68.9	0.287	-10.5	0.039	15.2	22.9
g7	-73.1	0.298	-10.7	0.041	12.2	/

g8	-73.7	0.220	-11.0	0.037	14.5	19.6
g9	-72.5	0.181	-11.0	0.015	15.8	24.3
g10	-74.4	0.201	-11.1	0.026	14.7	18.7
g11	-75.9	0.340	-11.3	0.015	14.2	1.86
l1	-53.1	0.229	-6.55	0.002	-0.704	/
l2	-50.7	0.304	-6.32	0.026	-0.161	/
l3	-42.9	0.239	-4.29	0.034	-8.55	/
l4	-34.2	0.243	0.381	0.040	-37.2	/
l5	-45.1	0.206	-4.99	0.009	-5.16	/
l6	-52.9	0.187	-6.15	0.049	-3.67	/
r1	-66.2	0.118	-10.1	0.015	14.4	/
r2	-65.0	0.148	-9.55	0.012	11.4	/
r3	-73.8	0.315	-11.1	0.021	14.9	/
r4	-85.2	0.244	-11.8	0.005	9.09	/
r5	-75.0	0.195	-10.1	0.003	5.69	/
s1	-70.8	0.074	-10.3	0.007	11.9	/
s2	-72.6	0.281	-10.5	0.046	11.1	/
p1	-47.4	0.374	-7.14	0.017	9.69	/

**Table 4.** The statistical frequency of rainfall events being >20 mm per year during the recent 30 years from 1985 to 2014. The data come from the China Meteorological Data Sharing Service System.

Station	One time/year	Two times/year	Three times/year	Four times/year	Five times/year	Six times/year	Seven times/year	Mean times/year
Duolun	2	8	8	4	4	3	1	3.4
Xilinhaote	8	5	2	6	3	2	0	2.5

1161  
1162

**Table 5.** The measured contents of tritium in the groundwater samples studied and the calculated ages of these samples.

Sample-ID	Tritium content (T.U.)	Possible ages (years)
g1	not measured	not clear
g2	not measured	not clear
g3	not measured	not clear
g4	7.25	20-40
g5	9.97	13-33
g6	22.9	0-20
g7	not measured	not clear
g8	19.6	0-20
g9	24.3	0-17
g10	18.7	0-22
g11	1.86	40-65

1163  
1164

**Table 6.** Mineral saturation Index (MSI) of the water samples studied.

Sample-ID	Mineral (Formula)	Anhydrite (CaSO <sub>4</sub> )	Aragonite (CaCO <sub>3</sub> )	Calcite (CaCO <sub>3</sub> )	Dolomite (CaMg(CO <sub>3</sub> ) <sub>2</sub> )	Fluorite (CaF <sub>2</sub> )	Gypsum (CaSO <sub>4</sub> ·2H <sub>2</sub> O)	Halite (NaCl)	CH <sub>4</sub> (g) (CH <sub>4</sub> )	CO <sub>2</sub> (g) (CO <sub>2</sub> )	H <sub>2</sub> (g) (H <sub>2</sub> )	H <sub>2</sub> O(g) (H <sub>2</sub> O)	NH <sub>3</sub> (g) (NH <sub>3</sub> )	O <sub>2</sub> (g) (O <sub>2</sub> )
g1	SI	-2.76	-1.21	-1.05	-2.5	-2.69	-2.5	-8.48	-58.68	-1.5	-21.44	-2.04	-8.5	-47.28
	Log IAP	-7.1	-9.45	-9.45	-19.11	-13.56	-7.1	-6.95	-61.37	-2.71	-24.5	0	-6.32	-50
	Log KT	-4.34	-8.24	-8.4	-16.61	-10.86	-4.6	1.54	-2.69	-1.2	-3.06	2.04	2.18	-2.72
g2	SI	-2.04	-0.99	-0.83	-2.12	-2.19	-1.79	-8.39	-60.49	-1.76	-21.82	-2.04	-8.51	-46.44
	Log IAP	-6.39	-9.23	-9.23	-18.74	-13.05	-6.39	-6.86	-63.18	-2.97	-24.88	0	-6.33	-49.16
	Log KT	-4.34	-8.24	-8.4	-16.62	-10.86	-4.6	1.54	-2.69	-1.21	-3.06	2.04	2.18	-2.73
g3	SI	-1.77	-1.25	-1.09	-2.62	-2.8	-1.51	-7.38	-60.71	-1.96	-21.76	-1.99	-8.9	-45.9
	Log IAP	-6.11	-9.49	-9.49	-19.29	-13.63	-6.11	-5.84	-63.41	-3.2	-24.83	0	-6.77	-48.65
	Log KT	-4.34	-8.25	-8.4	-16.66	-10.83	-4.6	1.54	-2.71	-1.23	-3.07	1.99	2.14	-2.74

带格式的：字体：加粗

g4	SI	-1.72	-1.43	-1.27	-2.92	-2.94	-1.47	-7.35	-59.85	-1.88	-21.48	-1.92	-45.59	
	Log IAP	-6.06	-9.69	-9.69	-19.64	-13.73	-6.06	-5.8	-62.58	-3.15	-24.56	0	-48.35	
	Log KT	-4.34	-8.26	-8.41	-16.72	-10.8	-4.59	1.55	-2.73	-1.27	-3.08	1.92	-2.77	
g5	SI	-1.6	-1.74	-1.59	-3.66	-3.09	-1.35	-7.02	-57.1	-1.73	-20.92	-1.99	-9.68	-47.62
	Log IAP	-5.94	-9.99	-9.99	-20.32	-13.93	-5.94	-5.48	-59.81	-2.96	-23.99	0	-7.54	-50.36
	Log KT	-4.34	-8.25	-8.4	-16.66	-10.83	-4.6	1.54	-2.71	-1.23	-3.07	1.99	2.14	-2.74
g6	SI	-1.39	-1.67	-1.52	-3.54	-3.01	-1.13	-6.53	-55.63	-1.45	-20.52	-1.91	-47.4	
	Log IAP	-5.73	-9.93	-9.93	-20.27	-13.8	-5.73	-4.98	-58.36	-2.73	-23.6	0	-50.16	
	Log KT	-4.34	-8.26	-8.41	-16.73	-10.79	-4.59	1.55	-2.73	-1.27	-3.08	1.91	-2.77	
g7	SI	-2.79	-2.45	-2.29	-5.1	-2.12	-2.54	-8.44	-59.68	-2.43	-21.42	-2.01	-46.93	
	Log IAP	-7.13	-10.69	-10.69	-21.74	-12.97	-7.13	-6.91	-62.38	-3.65	-24.49	0	-49.66	
	Log KT	-4.34	-8.24	-8.4	-16.64	-10.85	-4.6	1.54	-2.7	-1.22	-3.07	2.01	-2.73	
g8	SI	-2.65	-2.11	-1.95	-4.43	-2.19	-2.4	-8.15	-61.48	-2.6	-21.84	-2.02	-10.23	-46.21
	Log IAP	-6.99	-10.35	-10.35	-21.06	-13.04	-6.99	-6.61	-64.18	-3.82	-24.9	0	-8.07	-48.94
	Log KT	-4.34	-8.24	-8.4	-16.63	-10.85	-4.6	1.54	-2.7	-1.22	-3.06	2.02	2.17	-2.73
g9	SI	-1.96	-1.14	-0.98	-2.58	-2.77	-1.7	-8.85	-59.22	-1.67	-21.48	-2	-9.68	-46.66
	Log IAP	-6.3	-9.38	-9.38	-19.23	-13.6	-6.3	-7.31	-61.92	-2.9	-24.55	0	-7.53	-49.39
	Log KT	-4.34	-8.24	-8.4	-16.65	-10.84	-4.6	1.54	-2.7	-1.23	-3.07	2	2.15	-2.74
g10	SI	-2.99	-1.63	-1.47	-3.51	-2.24	-2.73	-7.98	-60.04	-2	-21.5	-1.92	-45.59	
	Log IAP	-7.32	-9.88	-9.88	-20.23	-13.04	-7.32	-6.44	-62.77	-3.27	-24.58	0	-48.35	
	Log KT	-4.34	-8.25	-8.41	-16.72	-10.8	-4.59	1.55	-2.73	-1.27	-3.08	1.92	-2.76	
g11	SI	-1.59	-1.01	-0.86	-2.34	-1.92	-1.33	-8.54	-61.8	-2.04	-21.98	-1.96	-8.69	-45.12
	Log IAP	-5.92	-9.26	-9.26	-19.02	-12.74	-5.92	-6.99	-64.51	-3.29	-25.05	0	-6.57	-47.87
	Log KT	-4.34	-8.25	-8.41	-16.69	-10.82	-4.59	1.54	-2.72	-1.25	-3.07	1.96	2.12	-2.75
l1	SI	-3.95	0.37	0.52	0.92	-5.34	-3.7	-9.28	-85.36	-4.77	-26.88	-1.73	-32.25	
	Log IAP	-8.29	-7.92	-7.92	-15.97	-16.04	-8.29	-7.72	-88.15	-6.14	-29.99	0	-35.08	
	Log KT	-4.34	-8.29	-8.44	-16.9	-10.7	-4.58	1.56	-2.79	-1.37	-3.11	1.73	-2.83	
l2	SI	-3.9	0.18	0.33	0.58	-3.36	-3.66	-9.27	-83.39	-4.49	-26.36	-1.65	-32.33	
	Log IAP	-8.24	-8.12	-8.12	-16.38	-14.02	-8.24	-7.7	-86.2	-5.89	-29.49	0	-35.18	
	Log KT	-4.34	-8.3	-8.45	-16.96	-10.66	-4.58	1.57	-2.81	-1.4	-3.13	1.65	-2.85	
l3	SI	-3.92	-1.1	-0.95	-2.03	-3.4	-3.69	-9.24	-67.05	-2.47	-22.76	-1.64	-39.32	
	Log IAP	-8.27	-9.4	-9.4	-19	-14.06	-8.27	-7.67	-69.87	-3.88	-25.89	0	-42.18	

	<u>Log KT</u>	<u>-4.34</u>	<u>-8.31</u>	<u>-8.45</u>	<u>-16.98</u>	<u>-10.66</u>	<u>-4.58</u>	<u>1.57</u>	<u>-2.82</u>	<u>-1.41</u>	<u>-3.13</u>	<u>1.64</u>		<u>-2.86</u>
<u>l4</u>	<u>SI</u>	<u>-3.7</u>	<u>-0.07</u>	<u>0.07</u>	<u>0.2</u>	<u>-2.9</u>	<u>-3.46</u>	<u>-8.24</u>	<u>-71.14</u>	<u>-2.6</u>	<u>-23.74</u>	<u>-1.63</u>	<u>-7.72</u>	<u>-37.26</u>
	<u>Log IAP</u>	<u>-8.04</u>	<u>-8.38</u>	<u>-8.38</u>	<u>-16.78</u>	<u>-13.55</u>	<u>-8.04</u>	<u>-6.67</u>	<u>-73.96</u>	<u>-4.01</u>	<u>-26.87</u>	<u>0</u>	<u>-5.86</u>	<u>-40.11</u>
	<u>Log KT</u>	<u>-4.35</u>	<u>-8.31</u>	<u>-8.46</u>	<u>-16.98</u>	<u>-10.65</u>	<u>-4.58</u>	<u>1.57</u>	<u>-2.82</u>	<u>-1.41</u>	<u>-3.13</u>	<u>1.63</u>	<u>1.86</u>	<u>-2.86</u>
<u>l5</u>	<u>SI</u>	<u>-3.92</u>	<u>-0.36</u>	<u>-0.21</u>	<u>-0.51</u>	<u>-3.69</u>	<u>-3.68</u>	<u>-8.9</u>	<u>-74.69</u>	<u>-3.32</u>	<u>-24.46</u>	<u>-1.64</u>		<u>-35.96</u>
	<u>Log IAP</u>	<u>-8.26</u>	<u>-8.67</u>	<u>-8.67</u>	<u>-17.48</u>	<u>-14.34</u>	<u>-8.26</u>	<u>-7.33</u>	<u>-77.51</u>	<u>-4.73</u>	<u>-27.59</u>	<u>0</u>		<u>-38.81</u>
	<u>Log KT</u>	<u>-4.34</u>	<u>-8.31</u>	<u>-8.45</u>	<u>-16.97</u>	<u>-10.66</u>	<u>-4.58</u>	<u>1.57</u>	<u>-2.82</u>	<u>-1.41</u>	<u>-3.13</u>	<u>1.64</u>		<u>-2.86</u>
<u>l6</u>	<u>SI</u>	<u>-3.39</u>	<u>-0.32</u>	<u>-0.16</u>	<u>-0.49</u>	<u>-2.91</u>	<u>-3.13</u>	<u>-8.95</u>	<u>-74.42</u>	<u>-3.47</u>	<u>-24.7</u>	<u>-1.9</u>		<u>-38.88</u>
	<u>Log IAP</u>	<u>-7.72</u>	<u>-8.58</u>	<u>-8.58</u>	<u>-17.23</u>	<u>-13.7</u>	<u>-7.72</u>	<u>-7.4</u>	<u>-77.16</u>	<u>-4.74</u>	<u>-27.79</u>	<u>0</u>		<u>-41.66</u>
	<u>Log KT</u>	<u>-4.34</u>	<u>-8.26</u>	<u>-8.41</u>	<u>-16.74</u>	<u>-10.79</u>	<u>-4.59</u>	<u>1.55</u>	<u>-2.74</u>	<u>-1.28</u>	<u>-3.09</u>	<u>1.9</u>		<u>-2.77</u>
<u>r1</u>	<u>SI</u>	<u>-3.01</u>	<u>-1.57</u>	<u>-1.43</u>	<u>-3.05</u>	<u>-2.69</u>	<u>-2.77</u>	<u>-8.91</u>	<u>-66.73</u>	<u>-2.65</u>	<u>-22.62</u>	<u>-1.63</u>		<u>-39.46</u>
	<u>Log IAP</u>	<u>-7.36</u>	<u>-9.88</u>	<u>-9.88</u>	<u>-20.03</u>	<u>-13.35</u>	<u>-7.36</u>	<u>-7.34</u>	<u>-69.55</u>	<u>-4.06</u>	<u>-25.75</u>	<u>0</u>		<u>-42.32</u>
	<u>Log KT</u>	<u>-4.35</u>	<u>-8.31</u>	<u>-8.46</u>	<u>-16.99</u>	<u>-10.65</u>	<u>-4.58</u>	<u>1.57</u>	<u>-2.82</u>	<u>-1.41</u>	<u>-3.13</u>	<u>1.63</u>		<u>-2.86</u>
<u>r2</u>	<u>SI</u>	<u>-3.18</u>	<u>-1.09</u>	<u>-0.94</u>	<u>-2.14</u>	<u>-2.97</u>	<u>-2.94</u>	<u>-9</u>	<u>-69.01</u>	<u>-2.88</u>	<u>-23.34</u>	<u>-1.78</u>		<u>-40.05</u>
	<u>Log IAP</u>	<u>-7.52</u>	<u>-9.37</u>	<u>-9.37</u>	<u>-18.98</u>	<u>-13.7</u>	<u>-7.52</u>	<u>-7.44</u>	<u>-71.79</u>	<u>-4.22</u>	<u>-26.44</u>	<u>0</u>		<u>-42.86</u>
	<u>Log KT</u>	<u>-4.34</u>	<u>-8.28</u>	<u>-8.43</u>	<u>-16.85</u>	<u>-10.73</u>	<u>-4.58</u>	<u>1.56</u>	<u>-2.77</u>	<u>-1.34</u>	<u>-3.1</u>	<u>1.78</u>		<u>-2.81</u>
<u>r3</u>	<u>SI</u>	<u>-3.62</u>	<u>-1.12</u>	<u>-0.97</u>	<u>-2.3</u>	<u>-1.8</u>	<u>-3.36</u>	<u>-8.91</u>	<u>-67.72</u>	<u>-2.78</u>	<u>-23.24</u>	<u>-1.93</u>		<u>-42.26</u>
	<u>Log IAP</u>	<u>-7.95</u>	<u>-9.38</u>	<u>-9.38</u>	<u>-19.01</u>	<u>-12.61</u>	<u>-7.95</u>	<u>-7.36</u>	<u>-70.44</u>	<u>-4.04</u>	<u>-26.32</u>	<u>0</u>		<u>-45.02</u>
	<u>Log KT</u>	<u>-4.34</u>	<u>-8.25</u>	<u>-8.41</u>	<u>-16.71</u>	<u>-10.8</u>	<u>-4.59</u>	<u>1.55</u>	<u>-2.72</u>	<u>-1.26</u>	<u>-3.08</u>	<u>1.93</u>		<u>-2.76</u>
<u>r4</u>	<u>SI</u>	<u>-2.41</u>	<u>0.06</u>	<u>0.21</u>	<u>0</u>	<u>-0.93</u>	<u>-2.15</u>	<u>-8.11</u>	<u>-70.67</u>	<u>-2.78</u>	<u>-23.94</u>	<u>-1.9</u>		<u>-40.48</u>
	<u>Log IAP</u>	<u>-6.74</u>	<u>-8.2</u>	<u>-8.2</u>	<u>-16.73</u>	<u>-11.72</u>	<u>-6.75</u>	<u>-6.56</u>	<u>-73.4</u>	<u>-4.06</u>	<u>-27.02</u>	<u>0</u>		<u>-43.25</u>
	<u>Log KT</u>	<u>-4.34</u>	<u>-8.26</u>	<u>-8.41</u>	<u>-16.74</u>	<u>-10.79</u>	<u>-4.59</u>	<u>1.55</u>	<u>-2.73</u>	<u>-1.28</u>	<u>-3.08</u>	<u>1.9</u>		<u>-2.77</u>
<u>r5</u>	<u>SI</u>	<u>-3.15</u>	<u>-0.8</u>	<u>-0.65</u>	<u>-1.61</u>	<u>-2.88</u>	<u>-2.89</u>	<u>-9.07</u>	<u>-70.47</u>	<u>-3.03</u>	<u>-23.74</u>	<u>-1.84</u>		<u>-39.99</u>
	<u>Log IAP</u>	<u>-7.48</u>	<u>-9.07</u>	<u>-9.07</u>	<u>-18.4</u>	<u>-13.63</u>	<u>-7.48</u>	<u>-7.52</u>	<u>-73.23</u>	<u>-4.34</u>	<u>-26.84</u>	<u>0</u>		<u>-42.78</u>
	<u>Log KT</u>	<u>-4.33</u>	<u>-8.27</u>	<u>-8.42</u>	<u>-16.8</u>	<u>-10.75</u>	<u>-4.59</u>	<u>1.55</u>	<u>-2.76</u>	<u>-1.31</u>	<u>-3.1</u>	<u>1.84</u>		<u>-2.79</u>
<u>s1</u>	<u>SI</u>	<u>-2.99</u>	<u>-2.83</u>	<u>-2.68</u>	<u>-5.51</u>	<u>-3.34</u>	<u>-2.76</u>	<u>-8.9</u>	<u>-61.12</u>	<u>-2.44</u>	<u>-21.26</u>	<u>-1.62</u>		<u>-42.08</u>
	<u>Log IAP</u>	<u>-7.34</u>	<u>-11.14</u>	<u>-11.14</u>	<u>-22.5</u>	<u>-13.99</u>	<u>-7.34</u>	<u>-7.33</u>	<u>-63.95</u>	<u>-3.86</u>	<u>-24.39</u>	<u>0</u>		<u>-44.94</u>
	<u>Log KT</u>	<u>-4.35</u>	<u>-8.31</u>	<u>-8.46</u>	<u>-16.99</u>	<u>-10.65</u>	<u>-4.58</u>	<u>1.57</u>	<u>-2.83</u>	<u>-1.42</u>	<u>-3.13</u>	<u>1.62</u>		<u>-2.86</u>
<u>s2</u>	<u>SI</u>	<u>-2.8</u>	<u>-0.89</u>	<u>-0.74</u>	<u>-1.73</u>	<u>-3.79</u>	<u>-2.56</u>	<u>-9.55</u>	<u>-67.85</u>	<u>-2.72</u>	<u>-22.94</u>	<u>-1.67</u>		<u>-39.38</u>
	<u>Log IAP</u>	<u>-7.14</u>	<u>-9.19</u>	<u>-9.19</u>	<u>-18.68</u>	<u>-14.46</u>	<u>-7.14</u>	<u>-7.98</u>	<u>-70.66</u>	<u>-4.12</u>	<u>-26.06</u>	<u>0</u>		<u>-42.23</u>
	<u>Log KT</u>	<u>-4.34</u>	<u>-8.3</u>	<u>-8.45</u>	<u>-16.95</u>	<u>-10.67</u>	<u>-4.58</u>	<u>1.57</u>	<u>-2.81</u>	<u>-1.39</u>	<u>-3.12</u>	<u>1.67</u>		<u>-2.85</u>

1165  
1166

	<u>SI</u>	<u>-3.81</u>		<u>-2.59</u>	<u>-3.57</u>	<u>-9.73</u>		<u>-17.22</u>	<u>-1.64</u>	<u>-10.5</u>	<u>-50.4</u>
<u>p1</u>	<u>Log IAP</u>	<u>-8.15</u>		<u>-13.25</u>	<u>-8.15</u>	<u>-8.16</u>		<u>-20.35</u>	<u>0</u>	<u>-8.63</u>	<u>-53.26</u>
	<u>Log KT</u>	<u>-4.34</u>		<u>-10.66</u>	<u>-4.58</u>	<u>1.57</u>		<u>-3.13</u>	<u>1.64</u>	<u>1.87</u>	<u>-2.86</u>



# Potential source of groundwater recharge in the middle-latitude desert of Otindag, China?

Bing-Qi Zhu<sup>1\*</sup>, Xiao-Zong Ren<sup>2</sup>, Patrick Rioual<sup>3</sup>

<sup>1</sup>KLWCRES, IGSNRR, CAS, Beijing, China

<sup>2</sup>SGS, TYN, Jinzhong, China

<sup>3</sup>KLCGE, IGCCAS, Beijing, China

Correspondence to: Bing-Qi Zhu ([zhubingqi@sina.com](mailto:zhubingqi@sina.com))

**Abstract.** The Otindag Desert in the middle-latitude desert zone of northern Hemisphere (NH) is essential to livestock-economy and environment of northern China. Many areas in this zone are unexpectedly rich with groundwater resources although they have been under arid or hyper-arid climate. Widespread fresh groundwater deep to 60 m was found at the eastern part of the Otindag Desert. The occurrence of this massive fresh groundwater raises doubts on the long-lasting hypothesis in academic circles that regional atmospheric precipitation or palaeowater is the source of water in the middle-latitude desert aquifers of northern China. Understanding of the recharge sources of this fresh groundwater is important in evaluating the feasibility of groundwater exploitation and utilization. In this study we conducted hydrogeochemical and isotopical analyses to assess possible origin and recharge of these groundwaters. The analytical results indicate that the fresh groundwater is neither originated from regional atmospheric precipitation derived from the Asian Summer Monsoon system, nor from palaeowater that formed during the last glacial period. These findings suggest that the groundwater in this desert is possible to originate from remote mountain areas via the faults of the Solonker Suture zone. In addition, it is concluded that the hydrogeological linkage between desert aquifers and mountain systems through the suture zone is crucial to the hydrological functioning of the Otindag aquifer. This suggests that the modern indirect recharge mechanism, instead of the direct recharge and the palaeo-water recharge, is the most significant for groundwater recharge in the Otindag Desert. This study provides a new perspective into the origin and evolution of groundwater resources in the middle-latitude desert zone of HA.

**Keywords:** fresh groundwater recharge; atmospheric precipitation; direct recharge; indirect recharge; palaeowater recharge; fault hydrology; middle-latitude desert; Otindag Desert.

## 1. Introduction

The deficit of rainfall occurs globally in semi-arid to arid regions. It is usually made up by extracting groundwater to supply the needs of a growing population and a higher standard of living. Many areas in the middle-latitude desert zone of northern China such as the Badanjilin Desert, the Mu US sandy Land and the Hobq Desert (Chen et al., 2012a; Chen et al., 2012b), are unexpectedly rich with large groundwater resources although they have been under arid or hyper-arid climate for a long time (Sun et al., 2010). How these groundwaters originated and how they are recharged in these deserts are thus fundamental scientific questions. Until now,

45 however, no consensus has been achieved in academic circles.

46 The Otindag Desert is one of the largest sandy lands located at the monsoon  
47 margin of northern China and is the geographical centre of the northeastern Asian  
48 Continent (Fig. 1), which can be regarded as a significant repository of information  
49 relating to the groundwater recharge in the arid Inner Asia. At present, the eastern  
50 Otindag is also a typical case for its unexpected groundwater resources, because  
51 there is abundant groundwater in this desert land and even rivers originate there due  
52 to the spillover of spring water, such as the tributaries of Xilamulun River in its north  
53 and the Shandian River in its south (Fig. 1). Climatically, the monsoon margin of  
54 northern China refers to a strip along the present East Asian Summer Monsoon  
55 (EASM) limits and is considered to be sensitive to climate change (Wang and Feng,  
56 2013). Geologically, the Otindag Desert lies in a tectonic depression of the central  
57 Solonker suture zone with a few faults stretching east and west (Fig. 2), with its  
58 northern margin along a fault marked by a series of lake basins. Thus, the large-scale  
59 hydrogeological conditions of the Otindag Desert belong to a fault zone under the  
60 influence of the EASM climate.

61 Until now, however, whether the climate or other factors affected the  
62 groundwater recharge in the Otindag is still not known. Little data about the  
63 groundwater and its origin is available in the literature, and knowledge and reliable  
64 data on various hydrogeological characteristics of the desert such as the catchment  
65 extent, input/output, the hysteretic hydraulic functions, the transient hydraulic  
66 conditions, in-homogeneities, and on transfer functions to overcome scale problems  
67 are also missing. Under such conditions, conventional methods such as water  
68 balance and hydraulic methods sometimes fail in determining groundwater recharge,  
69 particularly in extreme environments (arid, semi-arid, or cold) (Drever, 1997).  
70 Because pristine aquatic conditions may significantly differ from managed conditions  
71 in arid environment, and thus groundwater recharge is not a fixed number, but may  
72 vary with the boundary conditions of the recharge system (Seiler and Gat, 2007).

73 Groundwater recharge can be broadly classified into two categories: the direct  
74 recharge by native water resources and the indirect recharge by external water  
75 resources (Herczeg and Leaney, 2011). Water infiltration of atmospheric precipitation  
76 through the unsaturated zone to the groundwater is hydrologically defined as the  
77 direct recharge, and the indirect recharge is defined as recharge from mappable  
78 features such as rivers, canals, lakes and originates from remote areas (Scanlon et al.,  
79 2006; Healy, 2010). It is well known that groundwater recharge can be influenced by  
80 environmental factors, including climate change, underlying soil and geology, land  
81 cover and the growth in human population that affects withdrawal and economic  
82 development (Zhu et al., 2015, 2017). Among these environmental factors, climate  
83 and land cover largely determine precipitation and evapotranspiration, whereas the  
84 underlying soil and geology dictate whether a water surplus (precipitation minus  
85 evapotranspiration) can be transmitted and stored in the subsurface (Doll, 2008,  
86 2009; Giordano, 2009).

87 For some earth scientists, the direct recharge is thought to be very important  
88 for groundwaters in the wide desert lands of north China due to the lack of surface  
89 runoffs (Yang et al., 2010; Yang and Williams, 2003; Zhao et al., 2017). They argued  
90 that although the amount of atmospheric precipitation is small, the vast catchment  
91 area in the desert region could concentrate the rainfall into large inland basins,

creating an aquifer with large storage capacity and great thickness. However, some hydrologists estimated by the chloride mass balance method that the direct recharge was 1.4 mm/year, which represents approximately only 1.7% of the mean annual precipitation in a cold large desert (Badanjilin) in northern China (Gates et al., 2008). A similar estimation of 1 mm/year was given for Gobi deserts from the Hexi Corridor to the Inner Mongolia Plateau in northwestern China (Ma et al., 2008). Consequently, they thought that heavy potential evaporation and little precipitation make it difficult for direct recharge to meet the supply of groundwater in these desert areas. Thus, the indirect recharge is considered to be an important mechanism for groundwater recharge in these desert areas. For example, Zhao et al. (2012) suggested that little precipitation had recharged into groundwaters in the Badain Jaran Desert. Chen et al. (2004) argued that the groundwaters in the Badanjilin Desert were recharged by palaeo-glacial melt water through faults and deep carbonate layers far away from the local desert. Many studies also suggested that palaeowaters stored in an aquifer during wetter climate periods could recharge to groundwater under certain conditions in arid lands (Edmunds et al., 2006; Ma and Edmunds, 2006). Other kinds of indirect recharge, such as mountain front recharge from adjacent mountain blocks, are also proposed to offer an important inflow to aquifers within arid to semiarid catchments (Blasch and Bryson, 2007).

In this paper, we focus to answer the question that whether groundwater recharge in Otindag is mainly direct or indirect, using hydrochemical and isotopic indicators as tracers to offer a valuable support for identifying the contributions of precipitation recharge on groundwater, since these indicators reflect the composition of water molecules and are sensitive to physical processes such as mixing and evaporation (Sultan et al., 2000; Guendouz et al., 2003; Petrides et al., 2006; Scanlon et al., 2006; Zhu et al., 2007, 2008; Jobbágy et al., 2011). The detailed objectives are: (1) to recognize the major sources of groundwater in the area, and (2) to identify the key mechanism of groundwater recharge in the desert.

## 2. Regional settings

**Geographical location.** The Otindag Desert lies between latitudes 42° and 44°N and longitudes 112° and 118° E (Fig. 1). It is an east part of the great middle-latitude desert zone between northwestern and northeastern China which extends from the Taklamakan Desert in northwestern China to the Kelqin Desert in northeastern China, near the west coast of the Pacific Ocean. The desert has an area of approximately 21,400 square kilometers located in the eastern Inner Mongolia and at the monsoon margin of northern China (Fig. 1). It is the fourth largest sandy lands in China (Yang et al., 2012) and is bordered by a flat steppe terrain of Dali Basin to the north, the Yinshan Mountains and mountainous loess landscape to the south, and the the Greater Khingan (Daxing'Anling) Mountains to the east (Fig. 1). The Otindag Desert is essential to livestock-economy and ecoenvironment of northern China. Settlements in this desert are constrained to oases to frequent springs, groundwater with high level and areas where cultivation and irrigation are feasible. Some herdsmen live a precarious life by grazing livestock in the desert.

**Topography and geomorphology.** The relief in the Otindag Desert is varied with a combination of extensive dune fields and rugged piedmonts and mountains along the eastern and southern rims. In the east, the Daxing'Anling Mountains has an

average elevation ranging from 1,100 to 1,400 m and extend from the Heilong River Valley into the upper reach valleys of the Xilumulun River from northeast to southwest, with a gradual increase in height northwards from about 180 m near Huma to Huanggangliang, where the highest mountaintop reach 2,029 m. In the south and southeast, the Yinshan Mountains decline gradually near Duolun and Zhenglanqi, and in some areas leave wide alluvial plains. The terrain of the Otindag Desert is less rough and elevations decrease from ca. 1300 m in the southeast to ca. 1000 m in the northwest. Over the greater part of this desert the ground cover consists of fixed and semi-fixed sandy dunes, with a few mobile dunes in area of little vegetation. The dominated dune types are represented from parabolic to barchans, linear and grid-formed types, ranging from a few meters to over 40 m in height (Zhu et al., 1980; Yang et al., 2008).

Climate, vegetation and soil. The climate of the Otindag Desert was not uniform in geological period, with much sand movement, occasional rainy years, and several wetter intervals during the Holocene (Yang et al., 2015; Tian et al., 2017). At present the whole desert belongs to the arid and semi-arid temperate zone, with a mean annual temperature of 2 °C in the north and 4°C in the south (Liu and Yang, 2013). At the regional scale, the climate of the desert is typically controlled by the East Asian Monsoon system, characterized by a warm summer, with precipitation transported by the EASM, and by a cold and dry winter under the influence of the East Asian Winter Monsoon (EAWM). The rainfall in the desert exhibits a wide variation in space and time. Influence of the EASM changes from southeast to northwest in the desert, varying with the distance increase from the Pacific Ocean and leading to the mean annual rainfall decreasing from ~450 mm in the southeast to ~150 mm in the northwest (Yang et al., 2013). The spatial inequality of rainfall makes a great impact on the availability of near-surface moisture, consequently on the distribution of vegetation, soil and the animal husbandry potential of local communities. The major soil type is the grey desert soil in the west and changes to the sierozems and chernozem or chestnut soil in the east. Through the desert, vegetation is sparse in the west and relatively abundant in the east. The native vegetation is scrub woodland in the east and is steppe in the west, showing a natural characteristic of the temperate desert or semi-desert. It is greatly affected by temperature, rainfall and elevation in the growing season due to the scarcity of surface runoff.

Geology. The Otindag Desert is located in a tectonic depression of the Solonker Suture Zone (Jian et al., 2010) bounded by the Northern Early to Mid-Paleozoic Orogen Zone and the Hatug Uul Block to the north, the Southern Early to Mid-Paleozoic Orogen Zone and the North China Craton system to the south (Fig. 2). A few faults such as the Xar Moron Fault and Chifeng-Bayan Obo Fault stretch east and west, with its northern margin along the Solonker Suture Zone marked by a series of lake basins (Figs. 1 and 2). The tectonostratigraphic units and overall structural trends are mainly oriented NE–SW (Fig. 2), which may be interpreted as resulting from overall compressive stresses oriented principally in the NW–SE quadrants during orogenesis (Jian et al., 2010; Zhang et al., 2015). Diverse rock types from unlithified and lithified clastic sediments through to carbonate, crystalline, and volcanic rocks are distributed in and around the Otindag Desert (Zhang et al., 2015) (Figs. 2 and 3). Tertiary and Quaternary sandstones and mudstones are the common basement rocks under the dunes of the Otindag, and extensive volcanic basalts

forming flat terrains are to the north (Zhu et al., 1980; Li et al., 1995).

Hydrology and hydrogeology. The Otindag Desert originated during the Late Quaternary (Yang et al., 2015) and various alluvial fans formed at the margins of this desert during the early to middle Holocene. These are composed of conglomerate and sand deposits, where major periodic streams or wadis debouched into the Otindag. At present two rivers run through the eastern margin of the Otindag Desert, i.e. the Xilamulun River in the north and the Shandian River and its two tributaries, the Shepi River and Tuligen River in the south. Both stem from the eastern and southeastern parts of the Otindag (Fig. 1). The Xilamulun River, 380 km in length and  $32.54 \times 10^3 \text{ km}^2$  in area, is a neighboring river both to the northeastern Otindag and the southeastern Dali Basin, the northern catchment of the Otindag Desert. The Xilamulun River flows to the east and finally goes into the Xiliao River, with an annual mean runoff of  $6.58 \times 10^8 \text{ m}^3$  (Wu et al., 2014). The Shandian River is the upper reach of the Luan River, with a length of 254 km and a catchment area of  $4.11 \times 10^3 \text{ km}^2$  (Yao et al., 2013). Spotted salt crusts can extensively develop on land surface due to the high rate of evaporation. Sabkhas and salt pans often form in areas surrounding the flat shorelines of some lakes in the Otindag. During rainy season, some rain and floodwaters (generally coming from the Yinshan piedmonts) are retained in low-lying areas, which may temporarily recharge shallow aquifers. Under storm conditions, fast-flowing floods often form in some wadi channels with rich soil due to the occasional short, heavy rainstorms.

Groundwater resources in the Otindag Desert and its surrounding areas depend on several kinds of aquifers with different water-bearing formations and units (Fig. 3). Coarse- to fine-grained sedimentary rocks, magmatic rocks and metamorphic rocks of the Inner Mongolia-Daxing'Anling Orogenic Belt (Zhang et al., 2015) form the major regional aquifer unit (Fig. 3). They are composed mainly of alluvial sediments (mid-Permian Zhesi Formation), melange (Solonker suture zone), A-type granite (early Permian), bimodal volcanic rocks with sedimentary intercalations (early Permian Dashizhai Formation), diorite-quartz diorite-granodiorite rocks (Carboniferous-Permian) and metamorphic complex (predominantly gneiss, early Paleozoic) (Fig. 2). The aquifer is generally unconfined in dune fields of the Otindag Desert, unconfined to semi-confined in the Yinshan Mountains' piedmont, and semi-confined to confined in the Daxing'Anling uplands (Fig. 3). Water-level measurement in June 2010 indicated that the general depth of unconfined groundwater level ranges between 10 to 70 m in the Otindag Desert (Fig. 3). Local granular aquifers in the central desert are composed of coarse fluvial, lacustrine and aeolian sediments, but their extent and thickness vary throughout the watershed (Zhu et al., 1980; Li et al., 1995). The generally coarse-grained texture of the unconsolidated rock formations provides primary porosity in terms of groundwater flow in the desert.

### 3. Methods

The isotopes and ion chemistries of different water samples in the Otindag Desert, including natural samples collected from local and regional precipitation, depression springs, shallow and deep aquifers, perpetual lakes and outflowing rivers, are analyzed here and discussed. Relationships between the study area and the regional prevailing EASM climate, the dominant topographical, geological (tectonic)

and hydrogeological conditions, are also explored and interpreted, using multiple graphs and diagrams. Fieldworks took place during the summer season of 2011 and the spring season of 2012. Water samples were mainly retrieved from shallow and deep wells located over a wide area in dune fields of the study regions. The detailed locations of the sampling sites are shown in Fig. 4.

In this study, we designed two groups of parameters to characterize the physiochemistry of each water sample. One is the field-measured parameters and another is the lab-measured parameters. The former includes those parameters that will change in a shorter period of time when they are not directly measured in the field, such as the total dissolved solid (TDS, mg/L), electrical conductivity (EC in micro-Siemens per centimeter or  $\mu\text{S}/\text{cm}$ ), hydrogen-ion concentration (pH) and temperature ( $^{\circ}\text{C}$ ). The analysis for major cations ( $\text{F}^{-}$ ,  $\text{Cl}^{-}$ ,  $\text{NO}_2^{-}$ ,  $\text{NO}_3^{-}$ ,  $\text{SO}_4^{2-}$ ,  $\text{HCO}_3^{-}$ ,  $\text{CO}_3^{2-}$  and  $\text{H}_2\text{PO}_4^{-}$ ) and anions ( $\text{Li}^{+}$ ,  $\text{Na}^{+}$ ,  $\text{NH}_4^{+}$ ,  $\text{K}^{+}$ ,  $\text{Mg}^{2+}$  and  $\text{Ca}^{2+}$ ) are determined for all of the water samples collected. Contents of stable ( $^2\text{H}$  and  $^{18}\text{O}$ ) and radioactive isotopes ( $^3\text{H}$ ) in the rain and groundwater samples are precisely measured. The analytical data of the physiochemical parameters and the stable and radioactive isotopes of the water samples collected in this study are listed in Tables 1, 2 and 3, respectively.

## 4. Results and Discussions

### 4. 1. Hydrochemical characteristics of natural waters

The natural water samples collected in this study are generally neutral to slightly alkaline, with the pH values varying between 6.26 and 9.44 (except the precipitation sample p1, 4.61) (Table 1) and a median value of 7.27. The TDS values range between 67 and 660 mg/L (average 211 mg/L) (Table 1), all belonging to fresh water (TDS < 1000 mg/L) in the salination classification of natural water (Meybeck, 2004). The variations in ion concentrations of the major cations and anions in the studied water samples were displayed in a fingerprint diagram with a semi-logarithm y-axis (Fig. 5). The rain water sample is the most depleted in ions among these samples. The groundwater samples have the highest concentrations of cations and anions and the lake, river and spring waters had intermediate values. The calcium concentration is the highest among cations in almost all of the water samples, and the  $\text{HCO}_3^{-} + \text{CO}_3^{2-}$  concentration (bicarbonate + carbonate, alkalinity) is the highest among anions in most of the water samples. For several groundwater samples (g3, g4, g5, g6 and g11), spring sample (s1) and precipitation sample (p1), they have higher  $\text{SO}_4^{2-}$  concentrations than alkalinity (Fig. 5).

Two chemically distinct water types are recognized for the studied waters via a Piper diagram (Fig. 6), calcium bicarbonate and calcium sulphate. No Chloride-type and sodium-type waters occur in the study area (Fig. 6). It has been reported that the global groundwater tends to evolve chemically towards the composition of seawater (Chebotarev, 1955), and this evolution is associated with regional changes in dominant anions but not cations. This general evolution of groundwater can be illustrated as an anion evolution line (Freeze and Cherry, 1979):  $\text{HCO}_3^{-} \rightarrow \text{HCO}_3^{-} + \text{SO}_4^{2-} \rightarrow \text{SO}_4^{2-} + \text{HCO}_3^{-} \rightarrow \text{SO}_4^{2-} + \text{Cl}^{-} \rightarrow \text{Cl}^{-} + \text{SO}_4^{2-} \rightarrow \text{Cl}^{-}$ , which travels along the flow paths and increasing ages. It can be deduced from this line that bicarbonate water is the early product of groundwater evolution with low salinity, renewable water resources

or low residence time, while sulfate waters is the intermediate or advanced product of groundwater evolution with higher salinity passing through gypsum and anhydrite aquifers (Clark, 2015). The distribution pattern of water chemical types occurred in the study area indicates a primary stage of groundwater evolution in the Otindag Desert.

The  $\delta D$  values of the groundwater samples collected in this study varied from -63.42‰ to -75.92‰ (Table 3), with an average -69.53‰. The  $\delta^{18}O$  values ranged between -8.64‰ and -11.26‰ (Table 3), with an average -10.17‰. The spring water samples were relatively concentrated in  $\delta D$  and  $\delta^{18}O$  and were greatly similar to those of the groundwater samples (Fig. 7). The  $\delta D$  and  $\delta^{18}O$  values in the river water samples were slightly more variable and were also similar to those of the groundwater (Fig. 7). The lake water samples were enriched in  $\delta D$  and  $\delta^{18}O$  by comparison to the groundwater samples (Fig. 6). The precipitation sample p1 was also enriched in  $\delta D$  and  $\delta^{18}O$  by comparison to the groundwater samples (Fig. 7). The content of radioactive isotope of tritium ( $^3H$ ) measured in seven well groundwater samples with 6-60 m depth ranged from 1.86 to 24.35 TU (Table 3), with an average 14.95 TU, higher than the mean tritium concentration (9.8 TU) of groundwater in the Vienna Basin, Austria (Stolp et al., 2010), the seat of the International Atomic Energy Agency (IAEA).

If we plot the relationships between oxygen and hydrogen isotopes of groundwater, spring, river and lake water samples, we observed that most of the data points fell on a straight line that can be expressed by a regression equation:  $\delta D = 4.09\delta^{18}O - 28.31$  ( $R^2=0.93$ ,  $n=24$ ) (EL1 in Fig. 7). This local groundwater line (LGWL) is different from the Global Meteoric Water Line (GMWL,  $\delta D = 8\delta^{18}O + 10$ ) and the Mediterranean Meteoric Water Line (MMWL,  $\delta D = 8\delta^{18}O + 20$ ) estimated by Craig (1961), but it is similar to the local groundwater lines established for other deserts in northern China and central Asia with a same slope but different Y-intercepts, such as  $\delta D = 4.17\delta^{18}O - 31.3$  for the Badanjilin Desert (Jin et al., 2018),  $\delta D = 4.8\delta^{18}O - 15.2$  for the Ejina Desert in China (Wang et al., 2013), and  $\delta D = 4.26\delta^{18}O + 9.23$  for the Rub Al Khal Desert in the United Arab Emirates (Rizk and El-Etr, 1997). The data points are scattered for the lake water samples (Fig. 7) in the Otindag, suggesting that the lake waters are affected by evaporation, but the other waters in the desert are not so.

#### 4. 2. Summer precipitation recharge on groundwater in the Otindag

In order to compare the isotopic signals between groundwater and precipitation at a regional scale, the isotopic analysis of precipitation from similar areas surrounding the study area, such as Baotou, were incorporated with local data of summer precipitation (p1) in this study (Fig. 7). The Baotou station is the nearest long-term station to the Otindag Desert and was monitored for the isotopic composition of rainfall for the period 1986-2001 within the International Atomic Energy Agency Global Network of Isotopes in Precipitation (IAEA-GNIP) database. The stable isotope data from Baotou was used to represent the regional background of stable isotopic compositions of the present-day summer meteoric water, especially in the westward inland areas of the Otindag Desert (Fig. 1). In addition, stable isotope data of the Tianjin station was also used to represent the regional background of summer precipitation in the eastern coastal areas of the Otindag Desert (Fig. 1).



Based on the isotopic data from the Baotou station, the local meteoric water lines can be statistically expressed as the isotopic regression equation of  $\delta D = 6.36\delta^{18}O - 5.21$  (LMWL-B). It can also be expressed as  $\delta D = 6.57\delta^{18}O + 0.31$  (LWML-T), based on the data from the Tianjin station (Fig. 7). The precipitation sample p1 collected in this study fell onto the GMWL (Fig. 7). It also showed similar  $\delta D$  and  $\delta^{18}O$  values to those of the precipitation collected in the GNIP stations of Baotou and Tianjin (Fig. 7).

Compared to the summer precipitation data from the GNIP stations and from the local summer precipitation (p1), the groundwater, spring, and river water samples were evidently depleted in heavy stable isotopes in the Otindag (Fig. 7). Except for the lake water samples, most of the groundwater, river water and spring water samples in the Otindag fall on or lay between the LMWL-B and the LMWL-T lines, and are located at the lower left area of the precipitation points (Fig. 7).

Because the isotopic evolution of  $\delta D$  and  $\delta^{18}O$  in water illustrated in the Craig line represents a one-way and irreversible process, the water bodies distributed at the upper right area of the Craig line can not be recharge sources for the water bodies distributed at the lower left area of the line. Such results indicate that the groundwater, river water and spring water in the Otindag are not recharged by the regional precipitation, namely no significant modern direct recharge has taken place for groundwater in the Otindag.

Dogramaci et al. (2012) documented that only intense and remarkable rainfall events  $>20$  mm could recharge groundwater in the semi-arid Hamersley Basin of northwest Australia, while the rainfall events  $<20$  mm had limited influences on groundwater recharge. Chen et al. (2014) described that rainfall events  $\leq 5$  mm in the summer arid and semi-arid region of northern China would be evaporated into the atmosphere rapidly before it is infiltrated into the groundwater system. Based on the analysis on the data records from two meteorological stations around the Otindag, i.e. the Duolun and Xilinhaote stations (see Fig. 1a), we observed that summer rainfall events  $>20$  mm on average only occur 2.5-3.4 times per year (Table 4). In some years (e.g. from 2005 to 2007 at the Xilinhaote Station), no summer rainfall events  $>20$  mm even occurred. It further indicated the limited contribution of regional summer precipitation on groundwater recharge in the Otindag.

In addition to groundwater, the river and spring water samples from the Otindag also deviated from the local precipitation in the Craig diagram (Fig. 7). These water samples came from the Xilamulun, Shepi and Tuligen rivers. They shared the same evaporation line (EL1) with the groundwater and lake water samples (Fig. 7). Generally speaking, natural waters that have a same recharge source are distributed on a same line of evaporation in the  $\delta^2$  and  $\delta^{18}O$  diagram (Chen et al., 2012b). This indicates that the recharge sources of groundwater, river water, spring water and lake water in the Otindag are genetically associated each other and differ from the local precipitation.

#### **4. 3. Winter precipitation and palaeowater recharge on groundwater in the Otindag**

Since the groundwater samples in the Otindag are depleted in their  $\delta D$  and  $\delta^{18}O$  values even more than those of the local rainfall (Fig. 7), they must be sourced from other waters characterized by similar or more depleted signals in their stable isotopes compositions. Due to the temperature effect (such as evaporation) on

isotopic fractionation, only the waters issued from colder environments can be more depleted in their  $\delta D$  and  $\delta^{18}O$  values even more than those of the local rainfall.

Because the Otindag Desert is under the control of the EASM climate (Fig. 1), the local rainfall in the desert is mainly sourced from summer precipitation. This can also be illustrated by the seasonal distributions in annual mean precipitation (Fig. 8a), in annual mean air temperature (Fig. 8b) and in annual mean water vapor pressure (Fig. 8c) over the last forty years at the two surrounding GNIP weather stations in Baotou and Tianjin. The seasonal distributions of stable isotopes in the two stations (Fig. 8d-e) show that the summer rainfall is evidently positive in its signals of  $\delta D$  and  $\delta^{18}O$  by comparison with those of the winter rainfall, further suggesting that the waters issued from cold environments can be more depleted in their  $\delta D$  and  $\delta^{18}O$  values than those of the summer rainfall. Thus we speculate that groundwater in the Otindag can be potentially derived from (1) modern precipitation in winter, (2) palaeowater formed in the past glacial period, or (3) remote/mountain waters that emanate in colder and wetter conditions.

The annual mean values of  $\delta D$  and  $\delta^{18}O$  over the last forty years are more depleted in winter precipitation than in summer precipitation at the Baotou and Tianjin stations (Fig. 8d-e). This isotopic signal qualifies the regional winter precipitation to be a potential source of groundwaters in the Otindag. However, the precipitation amounts and the water vapor pressures (effective moisture) in winter months are much lower than those in the summer months at both the Baotou and Tianjin stations (Fig. 8a and 8c). It indicates that the winter seasons in these regions are relatively colder and drier but not colder and wetter. A colder-wetter winter season is a necessary condition for winter precipitation to be a water source for the formation of groundwater under a summer monsoon climate. This is because the bigger amounts of summer precipitation will easily remove or weaken the depleted isotopic signals of winter precipitation in groundwater. In this regard, modern winter precipitation is unlikely to be an important source of groundwater in the Otindag.

As to the palaeowaters formed in colder and wetter periods such as the last glacial, it has been proposed to be a potential water source for groundwaters in the wide arid lands of the world. The depleted signals of stable isotopes ( $\delta D$  and  $\delta^{18}O$ ) in groundwater have been recognized in global arid and semi-arid regions, such as the Sinai Desert in Egypt (Gat and Issar, 1974), Israel (Gat, 1983), South Australia (Love et al., 1994, 2000), northern China (Ma et al., 2010), Saudi Arabia (Bazuhaier and Wood, 1996) and North Africa (Guendouz et al., 2003). These signals are very often explained as palaeo-groundwater that recharged by precipitation during past wetter and colder periods (Love et al., 1994, 2000; Herczeg and Leaney, 2011).

Here we use the tritium data as an environmental tracer to estimate the groundwater age in the Otindag. The tritium data at the GNIP stations of the Baotou and Tianjin are also referenced as the background values in precipitation of recent years. The residence time of groundwater in aquifer and the residual tritium of a water body can be calculated by  $N = N_0 e^{-\lambda t}$  (Yang and Williams, 2003). Where  $N$  = content of residual tritium in water sample,  $\lambda = 0.0565$ , the radioactive decay constant,  $N_0$  = content of tritium at the time of rainfall and  $t$  = years after precipitation. Based on this equation, the residual tritium was theoretically calculated and the standard for tritium dating was established for seven groundwater samples in the Otindag Desert (Table 3). As a result, ages of 0-60 years were obtained

for these groundwater samples (Table 5). This indicates that recent recharge took place several decades after the peak in global nuclear tests. We thus conclude that groundwater is generally not older than 70 years in the study area. It means that groundwater in the Otindag are not palaeowater recharged.

Both the modern summer and winter precipitation recharge and the palaeowater recharge can be refuted, indicating that direct recharge is not a major mechanism controlling the groundwater recharge in the Otindag.

#### **4. 4. External water recharge on groundwater in the Otindag: Dali Basin**

The third hypothesis that “remote/mountains waters emanate under colder and wetter conditions” is further considered here. In essence, it is an indirect recharge mechanisms as water originates from remote areas (Healy, 2010; Herczeg and Leaney, 2011).

It is worth noting that the values of deuterium and oxygen-18 for groundwater in the north part of the study area are more depleted in  $\delta D$  and  $\delta^{18}O$  than those in the south part (Table 3). It suggests that the Otindag groundwater might be potentially recharged by water resources coming from the northern neighboring catchment, such as the Dali Basin.

Recently published data of  $\delta D$  and  $\delta^{18}O$  in groundwater, lake water, river water and spring water sampled from the Dali Basin (e.g., Chen et al., 2008; Zhen et al., 2014) were compiled in this study and were co-analyzed with the data from the Otindag. About 70 natural water samples from the Dali and Otindag with  $\delta D$  and  $\delta^{18}O$  values are shown in a Craig diagram (Fig. 9). All of these samples fell on or lied near the evaporation line EL2 in the Craig diagram (Fig. 9), with a regression equation of  $\delta D = 4.81\delta^{18}O - 21.55$  and a high correlation coefficient ( $R^2=0.98$ ,  $n=70$ ). Compared to the groundwater samples in the Otindag, water samples from the groundwaters, rivers and springs from the Dali Basin are more depleted in  $\delta^{18}O$  and  $\delta D$  (Fig. 9). Such results further indicate that, in terms of its isotopic signature, the groundwater in the Otindag has a close relationship with the natural waters in the Dali Basin.

The similar signals of  $\delta D$  and  $\delta^{18}O$  between the groundwater in the Otindag and the river water in the Dali (Fig. 9) point towards the idea that the groundwater in the Otindag might be sourced from the river water in the Dali Basin, since the Dali has more depleted isotopic signals in water than the Otindag (Fig. 9). Considering the topographical gradient of elevations between the two regions, however, river water in the Dali Basin cannot flow into the eastern Otindag, because the terrain elevation of the Dali Basin is lower than that of the Otindag (Fig. 1). This is also the reason why the huge Dali Lake that lies in the Dali Basin has no equivalent in the Otindag (Fig. 1). If there is a hydraulic linkage between the two regions, water should flow from the Otindag into the the Dali, but not conversely.

In view of the hydraulic gradient, river water in the Dali Basin could not be a recharge source for groundwater in the Otindag. However, in view of the isotopic gradients, groundwater in the Otindag could not conversely be the source of river water in the Dali (Fig. 9). Thus, the similar isotopic signals between the river water in Dali and the groundwater in Otindag indicate that these waters might be recharged from a common source.

Similar isotopic signals also occurred in the groundwaters between the Otindag

and the Dali Basin (Fig. 9). In order to understand the linkage of groundwaters between the two regions, the potential movement of groundwater in the transition zone of the two regions need to be known. In this study, a groundwater-sampling project was designed in the field along a N-S section of a palaeo-channel located at the transition zone between the Dali and Otindag (Figs. 1, 2). The channel was named “PCSX” in this study, with its north part named “NPCSX” and the south part named “SPCSX”.

The GPS elevation of the northernmost sampling site in the NPCSX (g11, about 1317 m a.s.l.) was much lower than that of the southernmost site in the SPCSX (g1, 1396 m a.s.l.) (Fig. 2 and Table 1). Regarding to the topographical gradient in the channel, there is a drop of about 80 m between the NPCSX and the SPCSX. Under such slope, the underground hydraulic gradient for groundwater flow can be roughly parallel with that of the surface water flow, namely that the groundwaterflow should move downwards from the SPCSX area into the NPCSX area. Thus we can speculate that groundwater in the NPCSX would have higher salinity than those in the SPCSX under such flowing direction. In order to verify this speculation, actual variations of water salinity (chloride and TDS) were detected along the PCSX section. The sampling site g1 was defined as the initial point and the distances between g1 and other sampling sites along the PCSX section were calculated, based on their GPS geographical coordinates measured in the field. The results are shown in Fig. 10a-b. It is clear that the variations of chloride and TDS concentrations in groundwater do not increase along the palaeo-channel from south to north (Fig. 10a-b). On the contrary, both the values of chloride and TDS are lower in the NPCSX area than those in the SPCSX area. Such kind of spatial variations in the chloride and TDS values contradict the speculated patterns abovementioned, suggesting that the hydraulic gradient of groundwater flowing path in this region is not controlled by the topographical gradient between the NPCSX and SPCSX areas.

Compared between the NPCSX and SPCSX regions, the stable isotopic values ( $\delta^{18}\text{O}$  and  $\delta\text{D}$ ) of groundwaters in the SPCSX region vary greatly with a large amplitude, while those in the NPCSX are relatively constant (Fig. 10c-d). The constant variations indicate that the recharge source of groundwater in the NPCSX is relatively unitary. The isotopic values in the SPCSX are much lighter than those in the NPCSX along the distance section from south to north (Fig. 10c-d). The heaviest values occurred in the sample g11 collected from the NPCSX (Fig. 10c-d), indicating a water being earlier recharged. The spring water sample s2, a representation of discharge water, is characterized by medium values of  $\delta\text{D}$  and  $\delta^{18}\text{O}$ . These results indicate that the groundwaters in the SPCSX area, with relatively enriched isotopic signals in  $\delta\text{D}$  and  $\delta^{18}\text{O}$  by comparison with those in the NPCSX area, are composed of a mixture of the groundwaters in the NPCSX with other waters.

The tritium contents were broadly and positively related to the values of deuterium excess in the groundwater samples in the PCSX (Fig. 10e). For water that experiences an evaporation process, the d-excess value will increase in the evaporated water vapor, but will decrease in the residual water body (Dansgaard, 1964; Merlivat and Jouzel, 1979). In this study, except for sample g11 (a sample very close to the riverhead area), the positive relationship between the tritium and the deuterium excess generally shows that the d-excess values are higher in the groundwaters collected from the NPCSX, but are lower in those from the SPCSX (Fig.

10e). This distribution pattern indicates that the groundwaters in the NPCSX are relatively younger and experienced a lower degree of evaporation than those in the SPCSX. The d-excess gradient, increasing from south to north in the PCSX, further suggests that groundwater does not flow from the SPCSX area to the NPCSX area, namely out of the topographical control.

Many studies (e.g., Boronina et al., 2005; Kazemi et al., 2006) have demonstrated that groundwater flows in the direction in which it gets older. In view of this point, groundwaters in the PCSX region should flow from the NPCSX area to the SPCSX area, in opposition to the S-N topographical gradient between the Otindag and Dali regions. Thus groundwater in the Dali are not the source of groundwater in the Otindag. The similar isotopic signals between groundwaters in the two regions indicate that these waters might be recharged from a common source in other place.

#### **4. 5. Water sources from remote areas for groundwater in the Otindag: mountain waters**

The discussions above revealed that both the groundwaters in the Otindag and DaliBasin might be recharged from a common source derived from another place. Considering the third hypothesis abovementioned that “remote/mountains waters emanate under colder and wetter conditions”, we propose that this “common source” of the two regions are from mountains areas surrounding the Otindag and Dali Basin.

There are two large permanent rivers and lots of small intermittent streams entering the Dali Basin (Xiao et al., 2008), including the Xilamulun River to the south and the Gongger River to the north, both of which are stemming from the Greater Khingan Mountains (Daxing’Anling Mountains in Chinese pinyin, 1,100-1,400 m above seal level) (Fig. 1). The Xilamulun River carries a large amount of water (about  $6.58 \times 10^8 \text{ m}^3/\text{y}$ ) from the Daxing’Anling Mountains flowing through the east margins of the Dali and Otindag (Wu et al., 2014). This is an important clue linking natural waters between the Otindag and Dali Basin.

Variation in the elevation from the Dali Lake to the riverhead of the Xilamulun River can be clearly found along a land surface topographical section (Fig. 11). The channel of the Xilamulun River is located in the Xar Moron Fault (Fig. 1), which is a part of the Solonker Suture Zone (Eizenhöfer et al., 2014) or the Xilamulun-Changchun-Yanji plate suture zone (Sun et al., 2004) in the regional tectonical settings (Fig. 2). Outcrop observations indicate that fault zones commonly have a permeability structure suggesting they should act as complex conduit–barrier systems in which along-fault flow is encouraged and across-fault flow is impeded (Bense et al., 2013). Thus the hydraulic gradient of groundwater flow in the Eastern margins of the Otindag and Dali Basin must be controlled by the fault zone hydrogeology. This may be the reason why the hydraulic gradient of groundwater represented by the isotopic and hydrogeochemical gradients of groundwater samples in this study is not consistent with the local topographical gradient in the Otindag Desert. On the other hand, the regional aquifer is generally unconfined in dune fields of the Otindag Desert but semi-confined to confined in the Daxing’Anling uplands (Fig. 3), thus the thick unconsolidated aquifers in the study area (Figs. 3 and 11) will be favourable conditions for groundwater storage and transportation along the Solonker Suture Zone. When rivers stem from the Daxing’Anling Mountains and flow downward to the marginal areas of the Dali and Otindag, leakage water from these

rivers can recharge the desert land through thick unconsolidated aquifers. A strong isotopic evidence is that the lake and river waters in the Dali Basin share the same evaporation line (EL2) with the groundwaters in the PCSX area.

Although groundwaters in the SPCSX area are different from those in the NPCSX area, their isotopic data points still fell onto the EL2 (Fig. 9), which further indicates that the groundwaters in the SPCSX are a mixture of waters from the Daxing'Anling Mountain and other sources. Another source for groundwater recharge in the SPCSX could be represented by remote water such as flash floods coming from the north Yinshan Mountains, because it can be clearly observed from digital maps that many transient rivers or streams originated from the Yinshan Mountains flow into the south and southeastern Otindag (Fig. 1). Supportive evidence for this idea can also be observed in the summer rainy season. During rainy days or under storm conditions, fast-flowing floods caused by occasional short, heavy rainstorms can form in playas, wadi channels and low-lying depressions in the unconfined to semi-confined areas of the Yinshan Mountains' piedmont. These waters may temporarily recharge shallow aquifers in the SPCSX area.

#### **4. 6. Speciation modeling and hydrogeological conceptual model**

Speciation modeling. Selected results of speciation modeling are provided in Table 6. All samples are undersaturated with respect to calcite, aragonite, dolomite, halite and gypsum. The values of  $\log P_{CO_2}$ , ranging between -4.77 and -1.45 in the samples from the sedimentary sandy aquifer, indicating that groundwater in the study area is not at equilibrium with atmospheric  $P_{CO_2}$ .

Based on the above analyses, a conceptual model of groundwater recharge was suggested to facilitate understanding of the hydrogeological conditions in the study area. Local and regional modern precipitation is a negligible source. Quaternary unconsolidated sediments with large exposed area form the main aquifer in the study area. Groundwater is recharged by cold water from remote mountain areas, and it flows from east to west along the Solonker Suture Zone. Evaporation is a minor process during groundwater hydrogeochemical evolution. Mineral dissolution may contribute to groundwater salinization, because saturation indices of all minerals are less than zero, indicating that these minerals still can dissolve into groundwater. These clues mean that the origin of groundwater in the desert is mainly controlled by geological structures and processes. The tectonic settings are more important than climatic and topographical settings to explain the origin of groundwater in the desert.

In a view of orogenic belt of the global middle-latitude regions, various groundwater and hydrogeological case studies have established a link between geological perspectives and origin of groundwater flows. Tague and Grant (2004) identify, for instance, the dominant control of a young volcanic geological unit on the groundwater regime of the studied region in Oregon, this geological formation having an exceptionally high permeability. Pfister et al. (2017) show that bedrock permeability significantly influences the ratio between average summer and winter run-off of 16 investigated catchments in Luxembourg. For a selection of Swiss catchments, Naef et al. (2015) associate lower groundwater flow with slowly draining porous bedrock and low streamflow during dry periods for catchments dominated by Moraine deposits. Kaser and Hunkeler (2016) have shown that alluvial aquifers, even

if they represent only a small portion of the catchment surface, can contribute significantly to the catchment groundwater outflow especially during low-flow periods. Alluvial aquifers can thus also be relevant for total catchment groundwater storage. Chen and Wang (2009) proposed that earthquake is a possible mechanism for groundwater releasing in the Qilian Mountains and discharging it in the Hexi Corridor. Carlier et al. (2018) statistically analyzed 22 catchments of the Swiss Plateau and Prealpes to establish relationships between streamflow indicators and various geological and hydrogeological properties of the bedrock and Quaternary deposits, along with meteorological, soil, land use, and topographical characteristics. The study shows that the geological characteristics dominate catchment response during high and low groundwater flow conditions.

These studies focused the influence of base/surrounding rock, topography, recharge source and permeability on groundwater flow in orogeny area. According to the hydrologically active bedrock hypothesis (Uchida et al. 2008) the bedrock is an active reservoir that significantly contributes to baseflow (Tague and Grant 2004; Andermann et al. 2012; Welch and Allen 2012; Birkel et al. 2014). The hydraulic conductivity of the bedrock controls storage processes (Hale et al. 2016; Pfister et al. 2017). Most importantly, the ratio of the hydraulic conductivity to recharge rates has been shown to be relevant for water table elevation (Gleeson and Manning 2008). Haitjema and Mitchell-Bruker (2005) propose a criterion based on the Dupuit-Forchheimer approximation combining this ratio with geometrical aquifer properties and topographical characteristics to determine whether the water table is controlled by the topography or the recharge. From the above review it can be seen that various studies have used spatially distributed, synthetic groundwater models to identify and explore how topography, recharge and/or bedrock permeability influence groundwater fluxes and flow patterns (e.g., Gleeson and Manning 2008; Welch et al. 2012; Welch and Allen 2012; Welch and Allen 2014).

These studies highlight the complex interplay of topography and hydrogeology on groundwater flow. They, however, mainly focus on the geology of the bedrock, no studies mentioned the important role of tectonic structure on the groundwater flow. Thus, based on this study in the Otindag Desert, we proposed a simple conceptual model of multiprocesses that constrain the mechanism of groundwater recharge in the desert, namely mountain water (M) – tectonic fault hydrology (T) – unconfined vadose zone with underlying buried fault (V) – groundwater formation and recharge (G), i.e. the MTVG mechanism. Although the model is still conceptual but not practical at present, it provides a new perspective into the origin and evolution of groundwater resources in the middle-latitude deserts of the arid Asia.

## **5. Conclusions**

In the middle-latitude desert zone of northern China, many deserts such as the Otindag and Badanjilin Deserts, are unexpectedly rich in groundwater resources, although they have no surface runoff and have been under an arid or hyper-arid climate for a long period of time. How groundwaters originated and recharged in these deserts are thus key questions that are still under debate. For some earth scientists, the direct recharge is thought to be very important for groundwaters in the wide desert lands of northern China, due to the lack of surface runoffs. However, groundwater availability is very much a function of the local- and regional-scale



geological and climatic settings. To achieve an integrated understanding of the groundwater recharge and its controlling mechanisms is of great significance. In this study, groundwater recharge was explored using multiple environmental tracers in the Otindag Desert of northern China, a region that is under the influence of the East Asian Summer Monsoon (EASM) climate. Compared to modern summer precipitation, the groundwaters, river waters and spring waters are depleted in  $\delta D$  and  $\delta^{18}O$ . All these waters shared a same Craig line, indicating a genetic relationship on their recharge sources. The stable isotopic signals of the groundwaters is more depleted than those of the modern summer precipitation and this suggests that the groundwaters studied could only be sourced from cold water different from the EASM precipitation. In general, the analyses revealed that the highland remote water resources from the Daxing'Anling and Yinshan Mountains were isotopically and geochemically traced to be a major source for the groundwater in the Otindag. It suggests that the modern indirect recharge mechanism, instead of the direct recharge and the palaeo-water recharge, is the most significant for groundwater recharge in the eastern Otindag. This study provides a new perspective into the origin and evolution of groundwater resources in the middle-latitude desert zone of northern China.

#### Acknowledgements

This study was financially supported by the National Natural Science Foundation of China (41771014), the National Key Research and Development Program of China (2016YFA0601900), and the National Natural Science Foundation of China (41602196). We thank the China Meteorological Data Sharing Service system for providing the weather data. Sincere thanks are also extended to Profs. Xiaoping Yang, Xunming Wang, Jule Xiao and other workmates, e.g., Ziting Liu, Hongwei Li, and DeguoZhang for their generous help in the research work.

#### References:

- Andermann, C., Longuevergne, L., Bonnet, S., Crave, A., Davy, P., and Gloaguen, R.: Impact of transient groundwater storage on the discharge of Himalayan rivers. *Nature Geoscience*, 5, 127-132, 2012.
- Bazuhair, A.S., and Wood, W.W.: Chloride mass-balance method for estimating ground water recharge in arid areas: examples from western Saudi Arabia. *Journal of Hydrology*, 186, 153-159, 1996.
- Bense, V.F., Gleeson, T., Loveless, S.E., Bour, O., and Scibek, J.: Fault zone hydrogeology. *Earth-Science Reviews*, 127, 171-192, 2013.
- Birkel, C., Soulsby, C., and Tetzlaff, D.: Developing a consistent process-based conceptualization of catchment functioning using measurements of internal state variables. *Water Resources Research*, 50, 3481-3501, 2014.
- Blasch, K.W., and Bryson, J.R.: Distinguishing sources of ground water recharge by using  $\delta^2H$  and  $\delta^{18}O$ . *Ground Water*, 45, 294-308, 2007.
- Boronina, A., Renard, P., Balderer, W., and Stichler, W.: Application of tritium in precipitation and in groundwater of the Kouris catchment (Cyprus) for description of the regional groundwater flow. *Applied Geochemistry*, 20, 1292-1308, 2005.
- Carlier, C., Wirth, S.B., Cochand, F., Hunkeler, D., and Brunner, P.: Geology controls

- streamflow dynamics. *Journal of Hydrology*, 566, 756–769, 2018.
- Chebotarev, I.I.: Metamorphism of natural waters in the crust of weathering. *Geochimica et Cosmochimica Acta*, 8, 22-32, 1955.
- Chen, F., Chen, J., Holmes, J., Boomer, I., Austin, P., Gates, J.B., Wang, N., Brooks, S.J., and Zhang, J.: Moisture changes over the last millennium in arid central Asia: a review, synthesis and comparison with monsoon region. *Quaternary Science Reviews*, 29, 1055-1068, 2010.
- Chen, J., Chen, X., and Wang, T.: Isotopes tracer research of wet sand layer water sources in Alxa Desert. *Advances in Water Science*, 25, 196-206 , 2014 (in Chinese).
- Chen, J., Li, L., Wang, J., Barry, D.A., Sheng, X., Gu, W., Zhao, X., and Chen, L.: Water resources: groundwater maintains dune landscape. *Nature*, 432, 459-460, 2004.
- Chen, J., Liu, X., Wang, C., Rao, W., Tan, H., Dong, H., Sun, X., Wang, Y., and Su, Z.: Isotopic constraints on the origin of groundwater in the Ordos Basin of northern China. *Environmental Earth Sciences*, 66, 505-517, 2012a.
- Chen, J., Sun, X., Gu, W., Tan, H., Rao, W., Dong, H., Liu, X., and Su, Z.: Isotopic and hydrochemical data to restrict the origin of the groundwater in the Badain Jaran Desert, Northern China. *Geochemistry International* 50, 455-465, 2012b.
- Chen, J.S., and Wang, C.Y.: Rising springs along the Silk Road. *Geology* 37, 243-246, 2009.
- Chen, J., Yang, Q., and Hao, G.: Using hydrochemical and environmental isotopical data to analyse groundwater recharge in the Hunshandake Sandy Land. *Inner Mongolia Science Technology & Economy*, 17, 9-12, 2008 (in Chinese).
- Clark, I.D.: *Groundwater Geochemistry and Isotopes*. CRC Press, Boca Raton, 2015.
- Craig, H.: Isotopic Variations in Meteoric Waters. *Science*, 133, 1702-1703, 1961.
- Dansgaard, W.: Stable isotopes in precipitation. *Tellus*, 16, 436-468, 1964.
- Dogramaci, S., Skrzypek, G., Dodson, W., and Grierson, P.F.: Stable isotope and hydrochemical evolution of groundwater in the semi-arid Hamersley Basin of subtropical northwest Australia. *Journal of hydrology*, 475, 281-293, 2012.
- Doll, P., and Fiedler, K.: Global-scale modeling of groundwater recharge. *Hydrology and Earth System Sciences*, 12, 863-885, 2008.
- Doll, P.: Vulnerability to the impact of climate change on renewable groundwater resources: a global-scale assessment. *Environmental Research Letters*, 4, 035006, doi:10.1088/1748-9326/4/3/035006, 2009.
- Drever, J.I.: Catchment mass balance. In: Saether, O.M., and de Caritat, P. (Eds.), *Geochemical Processes, Weathering and Groundwater Recharge in Catchments*. A.A, Balkema, Rotterdam, pp. 241-261, 1997.
- Edmunds, W.M., Ma, J., Aeschbach-Hertig, W., Kipfer, R., and Darbyshire, D.P.F.: Groundwater recharge history and hydrogeochemical evolution in the Minqin Basin, North West China. *Applied Geochemistry*, 21, 2148-2170, 2006.
- Eizenhöfer, P.R., Zhao, G., Zhang, J., and Sun, M.: Final closure of the Paleo-Asian Ocean along the Solonker Suture Zone: Constraints from geochronological and geochemical data of Permian volcanic and sedimentary rocks. *Tectonics*, 33, 441-463, 2014.
- Freeze, R.A., and Cherry, J.A.: *Groundwater*. Prentice-Hall, Inc, New Jersey, 1979.
- Gat, J.R.: Precipitation, groundwater and surface waters: control of climate parameters on their isotopic composition and their utilization as

750 palaeoclimatological tools. In: Palaeoclimates and palaeowaters: a collection of  
 751 environmental isotope studies. Proc. Adv. Gp. Meeting, Vienna, 25–28 Nov 1980,  
 752 pp 3–12, IAEA, Vienna, 1983.

753 Gat, J.R., and Issar, A.: Desert isotope hydrology: water sources of the Sinai Desert.  
 754 *Geochimica et Cosmochimica Acta*, 38, 1117-1131, 1974.

755 Gates, J., Edmunds, W.M., Ma, J., and Scanlon, B.: Estimating groundwater recharge  
 756 in a cold desert environment in northern China using chloride. *Hydrogeology*  
 757 *Journal*, 16, 893-910, 2008.

758 Giordano, M.: Global groundwater? Issues and solutions. *Annual Review of*  
 759 *Environment and Resources*, 34, 153-178, 2009.

760 Gleeson, T., and Manning, A.H.: Regional groundwater flow in mountainous terrain:  
 761 Three-dimensional simulations of topographic and hydrogeologic controls.  
 762 *Water Resources Research*, 44, 1-16, 2008.

763 Guendouz, A., Moulla, A.S., Edmunds, W.M., Zouari, K., Shand, P., and Mamou, A.:  
 764 Hydrogeochemical and isotopic evolution of water in the Complexe Terminal  
 765 aquifer in the Algerian Sahara. *Hydrogeology Journal*, 11, 483-495, 2003.

766 Haitjema, H.M., and Mitchell-Bruker, S.: Are water tables a subdued replica of the  
 767 topography? *Ground Water*, 43, 781-786, 2005.

768 Hale, V.C., McDonnell, J.J., Stewart, M.K., Solomon, D.K., Doolittle, J., Ice, G.G., and  
 769 Pack, R.T.: Effect of bedrock permeability on stream base flow mean transit time  
 770 scaling relationships: 2. Process study of storage and release. *Water Resources*  
 771 *Research*, 52, 1375-1397, 2016.

772 Healy, R.W.: Estimating groundwater recharge. Cambridge University Press, New York,  
 773 2010.

774 Herczeg, A.L., and Leaney, F.: Review: environmental tracers in arid-zone hydrology.  
 775 *Hydrogeology Journal*, 19, 17-29, 2011.

776 Jahn, B.M.: The Central Asian Orogenic Belt and growth of the continental crust in  
 777 the Phanerozoic. *Geological Society London Special Publications*, 226, 73-100,  
 778 2004.

779 Jian, P., Liu, D., Kroner, A., Windley, B.F., Shi, Y., Zhang, W., Zhang, F., Miao, L., Zhang,  
 780 L., and Tomurhuu, D.: Evolution of a Permian intraoceanic arc-trench system in  
 781 the Solonker suture zone, Central Asian Orogenic Belt, China and Mongolia.  
 782 *Lithos*, 118, 169-190, 2010.

783 Jin, K., Rao, W., Tan, H., Song, Y., Yong, B., Zheng, Y., Chen, T., and Han, L.: H-O isotopic  
 784 and chemical characteristics of a precipitation-lake water-groundwater system  
 785 in a desert area. *Journal of Hydrology*, 559, 848-860, 2018.

786 Jobbágy, E., Noretto, M., Villagra, P., and Jackson, R.: Water subsidies from mountains  
 787 to deserts: their role in sustaining groundwater-fed oases in a sandy landscape.  
 788 *Ecological Applications*, 21, 678-694, 2011.

789 Kaser, D., and Hunkeler, D.: Contribution of alluvial groundwater to the outflow of  
 790 mountainous catchments. *Water Resources Research*, 52, 680-697, 2016.

791 Kazemi, G.A., Lehr, J.H., and Perrochet, P.: Groundwater age. John Wiley & Sons,  
 792 Hoboken, 2006.

793 Li, J.: Permian geodynamic settings of Northeast China and adjacent regions: closure  
 794 of the Paleo-Asian Ocean and subduction of the Paleo-Pacific Plate. *Journal of*  
 795 *Asian Earth Sciences*, 26, 207-224.

796 Li, S., Sun, W., Li, X., and Zhang, B.: Sedimentary characteristics and environmental

797 evolution of Otindag sandy land in Holocene. *Journal of Desert Research*, 15,  
798 323-331, 1995 (in Chinese).

799 Liu, Z., and Yang, X.: Geochemical-geomorphological evidence for the provenance of  
800 aeolian sands and sedimentary environments in the Hunshandake Sandy Land,  
801 eastern Inner Mongolia, China. *Acta Geologica Sinica (English Edition)*, 87,  
802 871-884, 2013.

803 Love, A.J., Herczeg, A.L., Leaney, F.W., Stadter, M.H., Dighton, J.C., and Armstrong, D.:  
804 Groundwater residence time and palaeohydrology in the Otway Basin, South  
805 Australia. *Journal of Hydrology*, 153, 157–187, 1994.

806 Love, A.J., Herczeg, A.L., Sampson, L., Cresswell, R.G., and Fifield, L.K.: Sources of  
807 chloride and implications for <sup>36</sup>Cl dating of old groundwater, south-western  
808 Great Artesian basin, Australia. *Water Resources Research*, 36(6), 1561-1574,  
809 2000.

810 Ma, J., Ding, Z., Gates, J.B., and Su, Y.: Chloride and the environmental isotopes as the  
811 indicators of the groundwater recharge in the Gobi Desert, northwest China.  
812 *Environmental Geology*, 55, 1407-1419, 2008.

813 Ma, J., and Edmunds, W.M.: Groundwater and lake evolution in the BadainJaran  
814 Desert ecosystem, Inner Mongolia. *Hydrogeology Journal*, 14, 1231-1243, 2006.

815 Ma, J., Pan, F., Chen, L., Edmunds, W.M., Ding, Z., He, J., Zhou, K., and Huang, T.:  
816 Isotopic and geochemical evidence of recharge sources and water quality in the  
817 Quaternary aquifer beneath Jinchang city, NW China. *Applied Geochemistry*, 25,  
818 996-1007, 2010.

819 Merlivat, L., and Jouzel, J.: Global climatic interpretation of the deuterium-oxygen 18  
820 relationship for precipitation. *Journal of Geophysical Research*, 84, 5029-5033,  
821 1979.

822 Meybeck, M.: Global occurrence of major elements in rivers. In: Drever, J.I. (Ed.),  
823 *Surface and Ground Water, Weathering, and Soils*. Holland, H.D., and Turekian,  
824 K.K. (Exec.Eds), *Treatise on Geochemistry*, vol. 5. Elsevier-Pergamon, Oxford, pp.  
825 207-223, 2004.

826 Naef, F., Margreth, M., and Floriancic, M.: Festlegung von Restwassermengen: Q347,  
827 eine entscheidende, aber schwer zu fassende Größe. *Wasser Energie Luft*, Heft  
828 4(107. Jahrgang), 277–284, 2015.

829 Petrides, B., Cartwright, I., and Weaver, T.R.: The evolution of groundwater in the  
830 Tyrrell catchment, south-central Murray Basin, Victoria, Australia. *Hydrogeology*  
831 *Journal*, 14, 1522-1543, 2006.

832 Pfister, L., Martinez-Carreras, N., Hissler, C., Klaus, J., Carrer, G.E., Stewart, M.K., and  
833 McDonnell, J.J.: Bedrock geology controls on catchment storage, mixing, and  
834 release: A comparative analysis of 16 nested catchments. *Hydrological Processes*,  
835 31, 1828-1845, 2017.

836 Rizk, Z.S., and El-Etr, H.A.: Hydrogeology and hydrogeochemistry of some springs in  
837 the United Arab Emirates. *Arabian Journal for Science and Engineering*, 22,  
838 95-111, 1997.

839 Scanlon, B.R., Keese, K.E., Flint, A.L., Flint, L.E., Gaye, C.B., Edmunds, W.M., and  
840 Simmers, I.: Global synthesis of groundwater recharge in semiarid and arid  
841 regions. *Hydrological Processes*, 20, 3335-3370, 2006.

842 Seiler, K.P., and Gat, J.R.: *Groundwater Recharge From Run-Off, Infiltration and*  
843 *Percolation*. Springer, The Netherlands, 2007.

844 Stolp, B.J., Solomon, D.K., Suckow, A., Vitvar, T., Rank, D., Aggarwal, P.K., and Han, L.F.:  
 845 Age dating base flow at springs and gaining streams using helium-3 and tritium:  
 846 Fische-Dagnitz system, southern Vienna Basin, Austria. *Water Resources*  
 847 *Research*, 46, W07503, doi:10.1029/2009WR008006, 2010.

848 Sultan, M., Sturchio, N., Gheith, H., Hady, Y.A., and Anbeawy, M.: Chemical and  
 849 Isotopic Constraints on the Origin of Wadi Elitarfa Ground Water, Eastern Desert,  
 850 Egypt. *Ground Water*, 38, 743-751, 2000.

851 Sun, D., Wu, F., Zhang, Y., and Gao, S.: The final closing time of the west Lamulun  
 852 River-Changchun-Yanji plate suture zone-Evidence from the Dayushan granitic  
 853 pluton, Jilin Province. *Journal of Jilin University (Earth Science Edition)*, 34,  
 854 174-181, 2004 (in Chinese).

855 Sun, J., Ye, J., Wu, W., Ni, X., Bi, S., Zhang, Z., Liu, W., and Meng, J.: Late  
 856 Oligocene-Miocene mid-latitude aridification and wind patterns in the Asian  
 857 interior. *Geology*, 38, 515-518, 2010.

858 Tague, C., and Grant G.E.: A geological framework for interpreting the low-flow  
 859 regimes of Cascade streams, Willamette River basin, Oregon. *Water Resources*  
 860 *Research*, 40(4), 1-9, 2004.

861 Tian, F., Wang, Y., Liu, J., Tang, W., and Jiang, N.: Late Holocene climate change  
 862 inferred from a lacustrine sedimentary sequence in southern Inner Mongolia,  
 863 China. *Quaternary International*, 452, 22-32, 2017.

864 Uchida, T., Miyata, S., and Asano Y.: Effects of the lateral and vertical expansion of the  
 865 water flowpath in bedrock on temporal changes in hillslope discharge.  
 866 *Geophysical Research Letters*, 35, 2-6, 2008.

867 Wang, P., Yu, J., Zhang, Y., and Liu, C.: Groundwater recharge and hydrogeochemical  
 868 evolution in the Ejina Basin, northwest China. *Journal of Hydrology*, 476, 72-86,  
 869 2013.

870 Wang, Q., and Liu, X.Y.: Paleoplate tectonics between Cathaysia and Angaraland in  
 871 Inner Mongolia of China. *Tectonics*, 5, 1073-1088, 1986.

872 Wang, W., and Feng, Z.D.: Holocene moisture evolution across the Mongolian Plateau  
 873 and its surrounding areas: a synthesis of climatic records. *Earth-Science Reviews*,  
 874 122, 38-57, 2013.

875 Welch, L.A., and Allen, D.M.: Consistency of groundwater flow patterns in  
 876 mountainous topography: Implications for valley bottom water replenishment  
 877 and for defining groundwater flow boundaries. *Water Resources Research*, 48,  
 878 1-17, 2012.

879 Welch, L.A.A., Allen, D.M.M., and van Meerveld, H.J.: Topographic controls on deep  
 880 groundwater contributions to mountain headwater streams and sensitivity to  
 881 available recharge. *Canadian Water Resources Journal*, 37, 349-371, 2012.

882 Welch, L.A., and Allen, D.M.: Hydraulic conductivity characteristics in mountains and  
 883 implications for conceptualizing bedrock groundwater flow. *Hydrogeology*  
 884 *Journal*, 22, 1003-1026, 2014.

885 Wu, J., An, N., Ji, Y., and Wei, X.: Analysis on Characteristics of Precipitation and  
 886 Runoff in Silas MuLun River Basin. *Meteorology Journal of Inner Mongolia*,  
 887 23-25, 2014 (in Chinese).

888 Xiao, J., Si, B., Zhai, D., Itoh, S., and Lomtadze, Z.: Hydrology of Dali Lake in  
 889 central-eastern Inner Mongolia and Holocene East Asian monsoon variability.  
 890 *Journal of Paleolimnology*, 40, 519-528, 2008.

- Yang, X., Li, H., and Conacher, A.: Large-scale controls on the development of sand seas in northern China. *Quaternary International*, 250, 74-83, 2012.
- Yang, X., Ma, N., Dong, J., Zhu, B., Xu, B., Ma, Z., and Liu, J.: Recharge to the inter-dune lakes and Holocene climatic changes in the BadainJaran Desert, western China. *Quaternary Research*, 73, 10-19, 2010.
- Yang, X., Scuderi, L.A., Wang, X., Scuderi, L.J., Zhang, D., Li, H., Forman, S., Xu, Q., Wang, R., Huang, W., and Yang, S.: Groundwater sapping as the cause of irreversible desertification of Hunshandake Sandy Lands, Inner Mongolia, northern China. *PNAS*, 112, 702-706, 2015.
- Yang, X., Wang, X., Liu, Z., Li, H., Ren, X., Zhang, D., Ma, Z., Rioual, P., Jin, X., and Scuderi, L.: Initiation and variation of the dune fields in semi-arid China – with a special reference to the Hunshandake Sandy Land, Inner Mongolia. *Quaternary Science Reviews*, 78, 369-380, 2013.
- Yang, X., and Williams, M.A.J.: The ion chemistry of lakes and late Holocene desiccation in the BadainJaran Desert, Inner Mongolia, China. *Catena*, 51, 45-60, 2003.
- Yang, X., Zhu, B., Wang, X., Li, C., Zhou, Z., Chen, J., Yin, J., and Lu, Y.: Late Quaternary environmental changes and organic carbon density in the Hunshandake Sandy Land, eastern Inner Mongolia, China. *Global and Planetary Change*, 61, 70-78, 2008.
- Yao, S., Zhu, Z., Zhang, S., Zhang, S., and Li, Y.: Using SWAT model to simulate the discharge of the river Shandianhe in Inner Mongolia. *Journal of Arid Land Resources and Environment*, 27, 175-180, 2013 (in Chinese).
- Zhang, Z., Li, K., Li, J., Tang, W., Chen, Y., and Luo, Z.: Geochronology and geochemistry of the Eastern Erenhot ophiolitic complex: implications for the tectonic evolution of the Inner Mongolia-Daxinganling Orogenic Belt. *Journal of Asian Earth Sciences*, 97, 279-293, 2015.
- Zhao, J., Ma, Y., Luo, X., Yue, D., Shao, T., and Dong, Z.: The discovery of surface runoff in the megadunes of BadainJaran Desert, China, and its significance. *Science China Earth Sciences*, 60, 707-719, 2017.
- Zhao, L., Xiao, H., Dong, Z., Xiao, S., Zhou, M., Cheng, G., Yin, L., and Yin, Z.: Origins of groundwater inferred from isotopic patterns of the Badain Jaran Desert, Northwestern China. *Ground Water*, 50, 715-725, 2012.
- Zhen, Z., Li, C., Li, W., Hu, Q., Liu, X., Liu, Z., and Yu, R.: Characteristics of environmental isotopes of surface water and groundwater and their recharge relationships in Lake Dali basin. *Journal of Lake Sciences*, 26, 916-922, 2014 (in Chinese).
- Zhu, B.Q., Yu, J.J., Rioual, P., Gao, Y., Zhang, Y.C., and Xiong, H.G.: Climate effects on recharge and evolution of natural water resources in middle-latitude watersheds under arid climate. In: Ramkumar, M. U., Kumaraswamy, K, and Mohanraj, R. (Eds.), *Environmental Management of River Basin Ecosystems*. Springer Earth System Sciences, Springer-Verlag, Heidelberg, pp. 91-109, 2015.
- Zhu, B.Q., Wang, X.M., and Rioual, P.: Multivariate indications between environment and ground water recharge in a sedimentary drainage basin in northwestern China. *Journal of Hydrology*, 2017, 549, 92-113, 2017.
- Zhu, G.F., Li, Z.Z., Su, Y.H., Ma, J.Z., and Zhang, Y.Y.: Hydrogeochemical and isotope evidence of groundwater evolution and recharge in Minqin Basin, Northwest

938 China. Journal of Hydrology, 333, 239-251, 2007.  
939 Zhu, G.F., Su, Y.H., and Feng, Q.: The hydrochemical characteristics and evolution of  
940 groundwater and surface water in the Heihe River Basin, northwest China.  
941 Hydrogeology Journal, 16, 167-182, 2008.  
942 Zhu, Z., Wu, Z., Liu, S., and Di, X.: An Outline of Chinese Deserts. Science Press,  
943 Beijing, 1980 (in Chinese).  
944  
945

**Figure Captions:**

**Fig. 1.** The Geographical location of the Otindag Desert in northern China. (a) The study area shown at a large scale, and (b) the study area shown at a smaller scale, with detailed information about the boundary and tectonic settings of the desert land. 1, the palaeo lake area of the megalake Dali; 2, the boundary of the Otindag; 3, the modern lake area; 4, the boundary of Fig. 2; 5, the boundary between the westerlies and the East Asian Summer Monsoon (EASM) climate systems. ①, the Xilamulun River. ②, the Gonggeer River. ③, the Shepi River. ④, the Tuligen River. The boundary between the westerlies and the EASMin (a) and (b) is modified from Chen et al. (2010). The palaeo lake area of the megalake Dali and the palaeo channel in (b) is modified from Yang et al. (2015). The location of the Xar Moron Fault is referenced from Eizenhöfer et al. (2014). Section S1 is an elevation section starting from the upstream of the Dali Lake and ending with a spring sample (s2) in the riverhead of Xilamulun River.



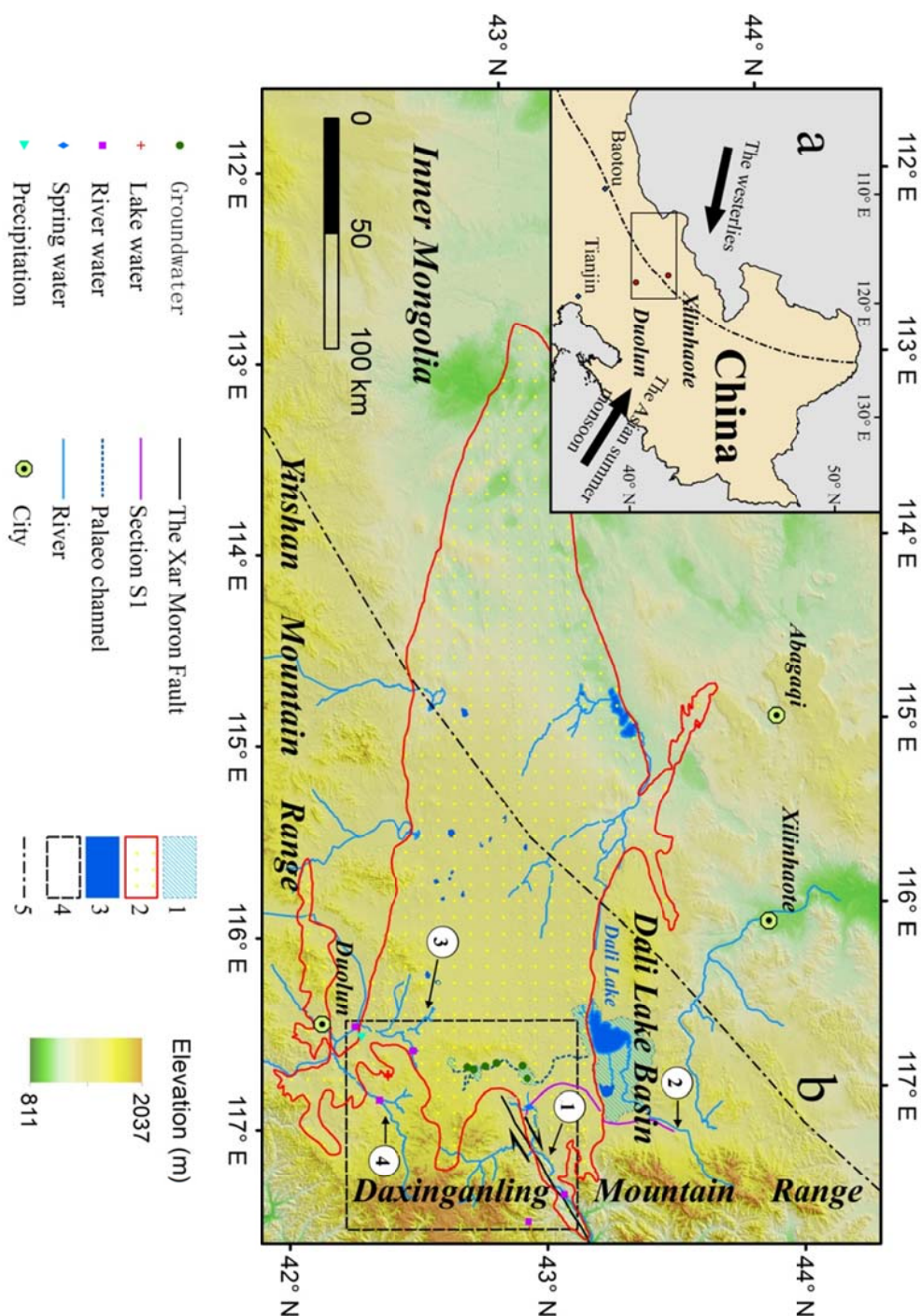


**Fig. 2.** (a) Tectonic framework of the north China-Mongolian segment of the Central Asian Orogenic Belt (modified after Jahn, 2004). (b) Geological sketch map of the northern China-Mongolia tract (modified after Jian et al., 2010). The Solonker suture zone represents the tectonic boundary between the northern (Hutag Uul Block-Northern orogen) and the southern (southern orogen-Northern margin of North China craton) continental blocks. Note that the red line marks the early Permian paleobiogeographical boundary (Wang and Liu, 1986; Li, 2006), which coincides with the northern boundary of the suture zone.

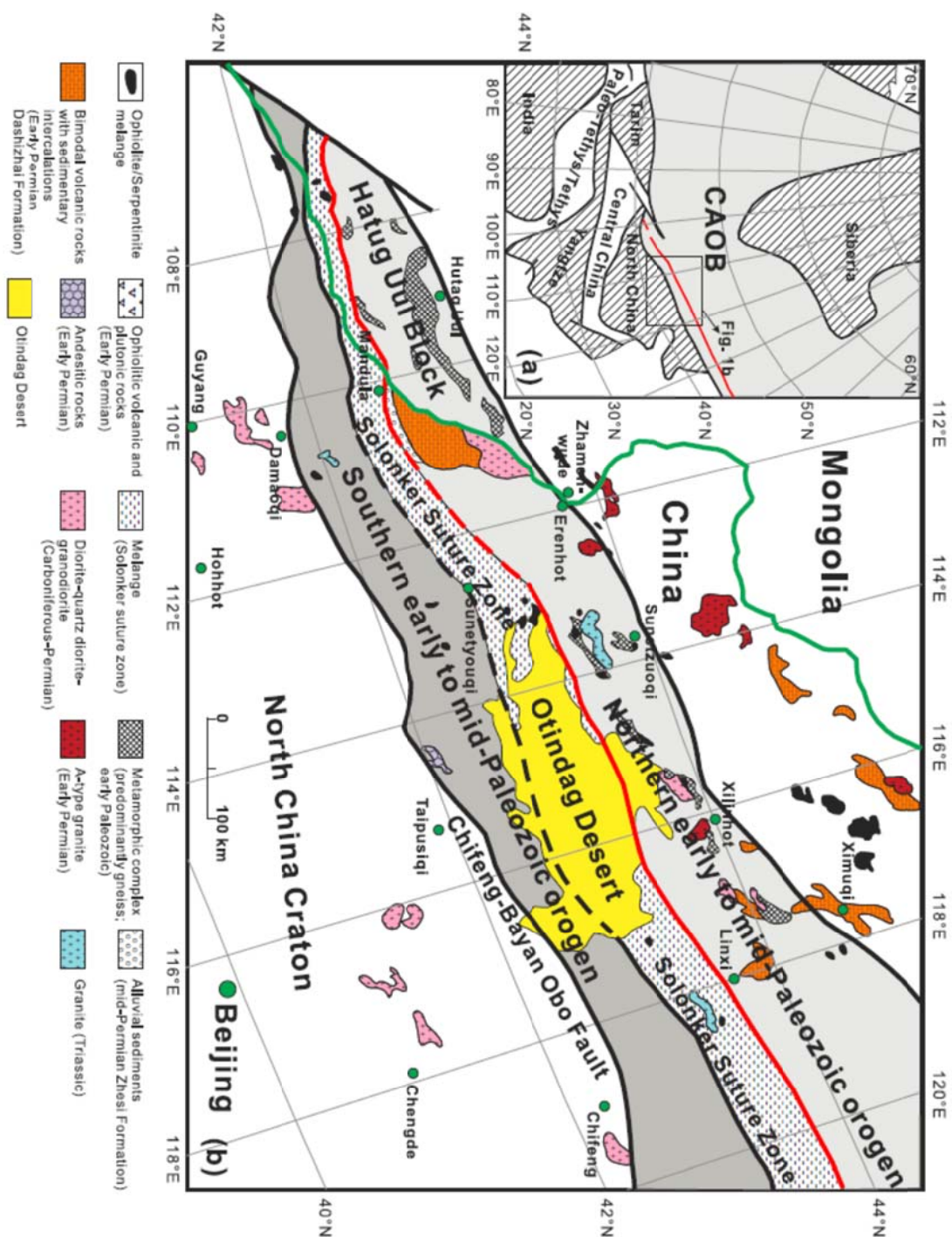


**Fig. 3.** The hydrogeological division map of the Otindag Desert.



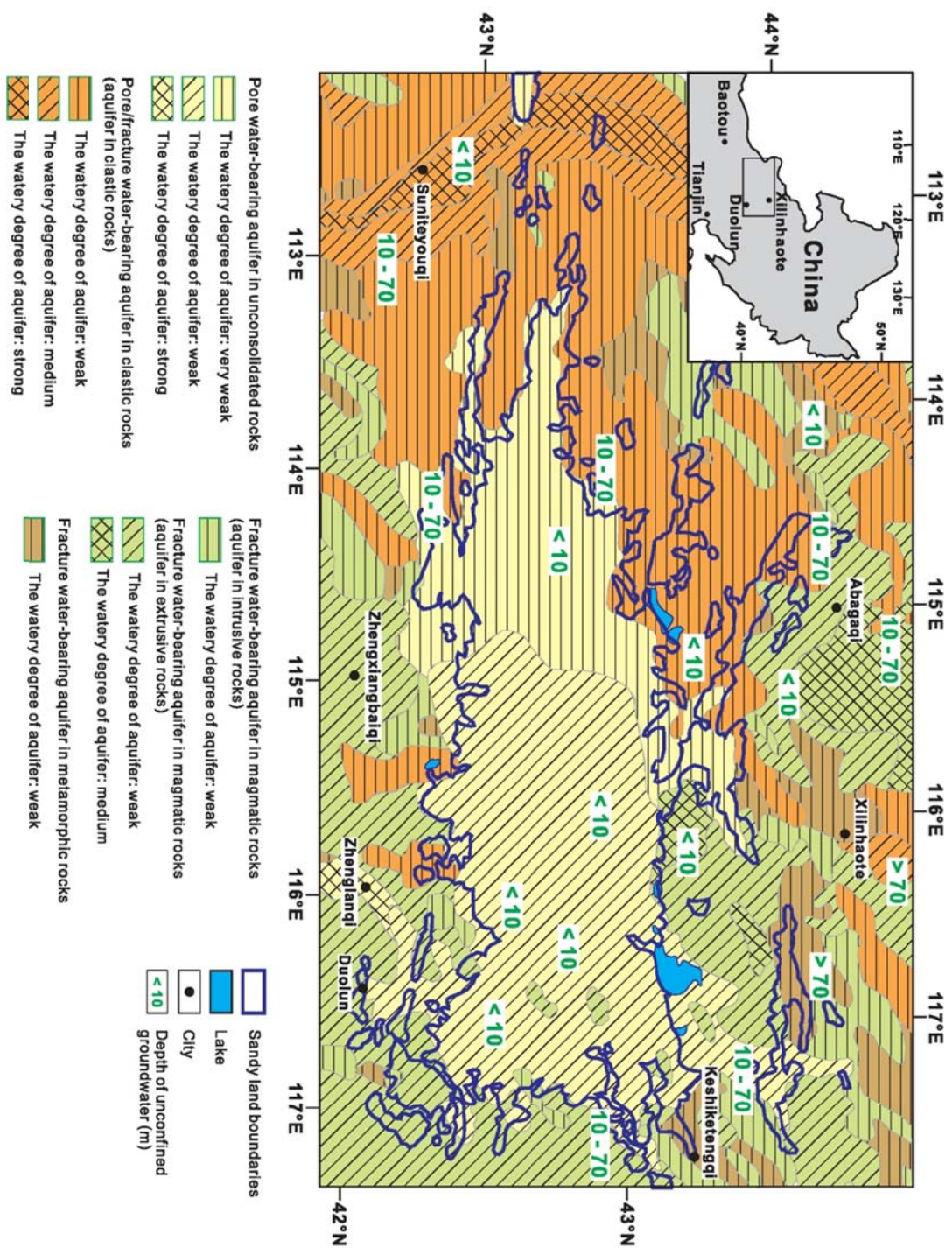
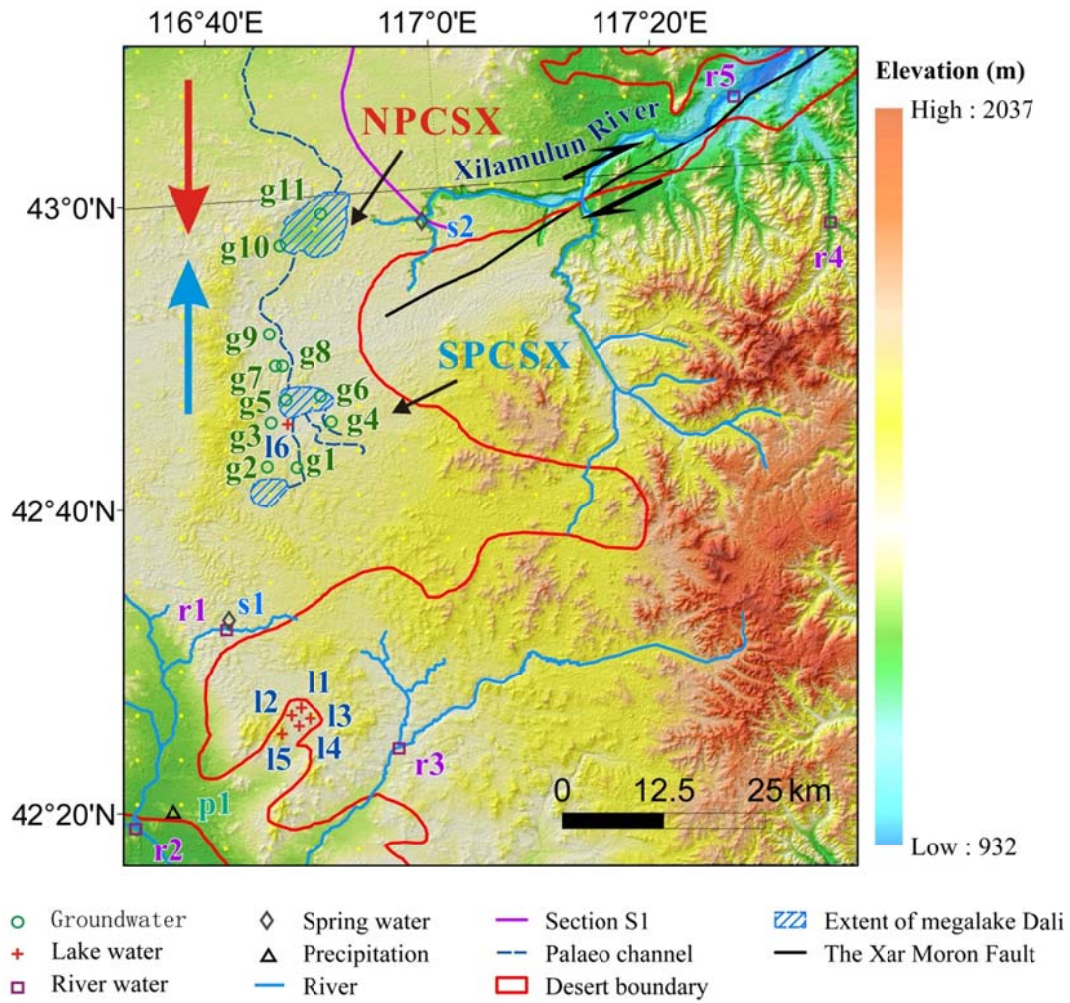


**Fig. 4.** The locations of the water sampling sites in this study.



1011  
1012  
1013  
1014  
1015  
1016  
1017  
1018

1019 **Fig. 5.** The fingerprint diagram showing the variations of multiple ions'  
1020 concentrations in the studied water samples in an equivalent unit. The  $\text{HCO}_3+\text{CO}_3$   
1021 concentration in the sample p1 was not shown, due to its value being lower than the  
1022 detection limit.

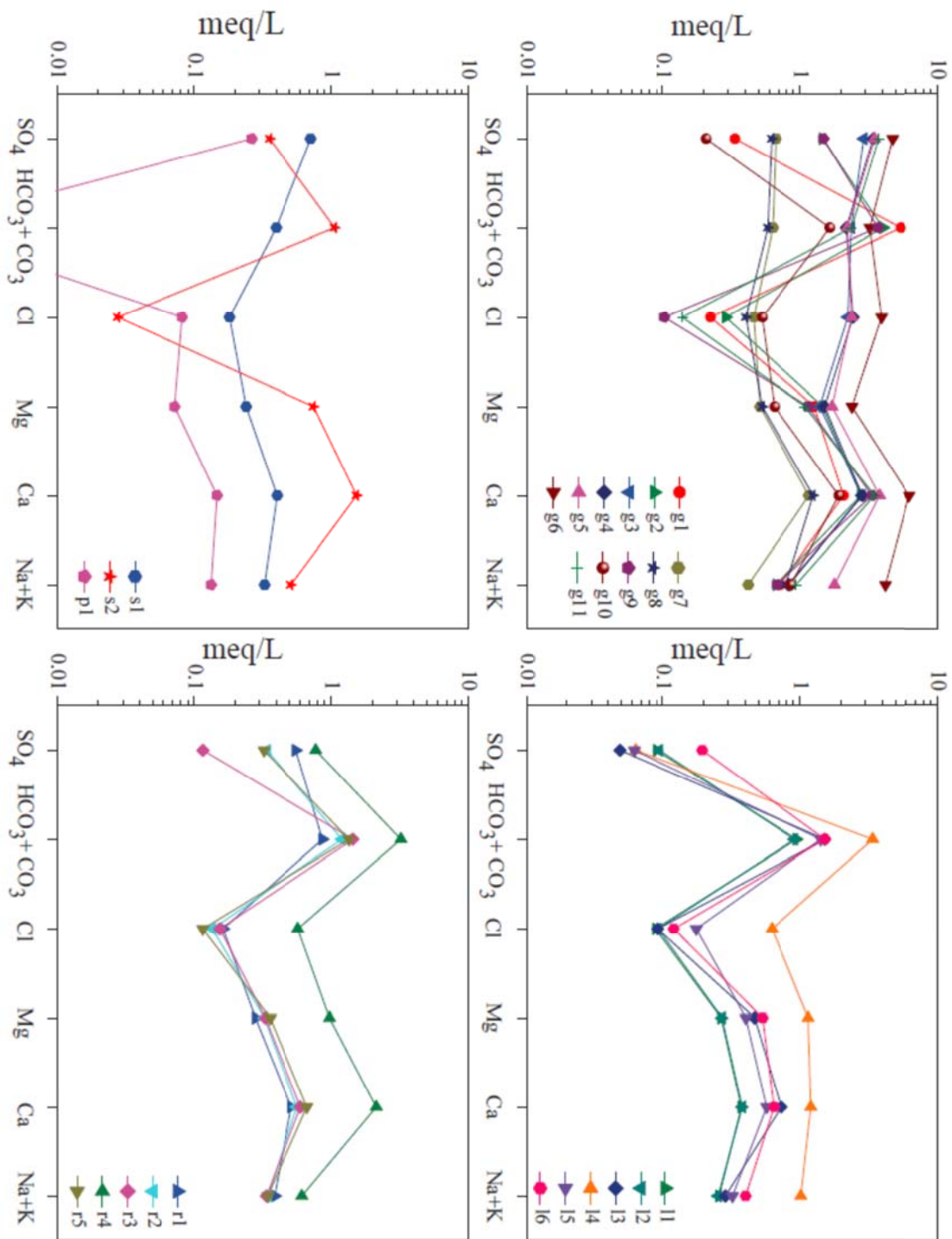




**Fig. 6.** The Piper diagram showing the relative abundances of major cations and anions in the studied water samples. Major water types are also shown in this diagram.

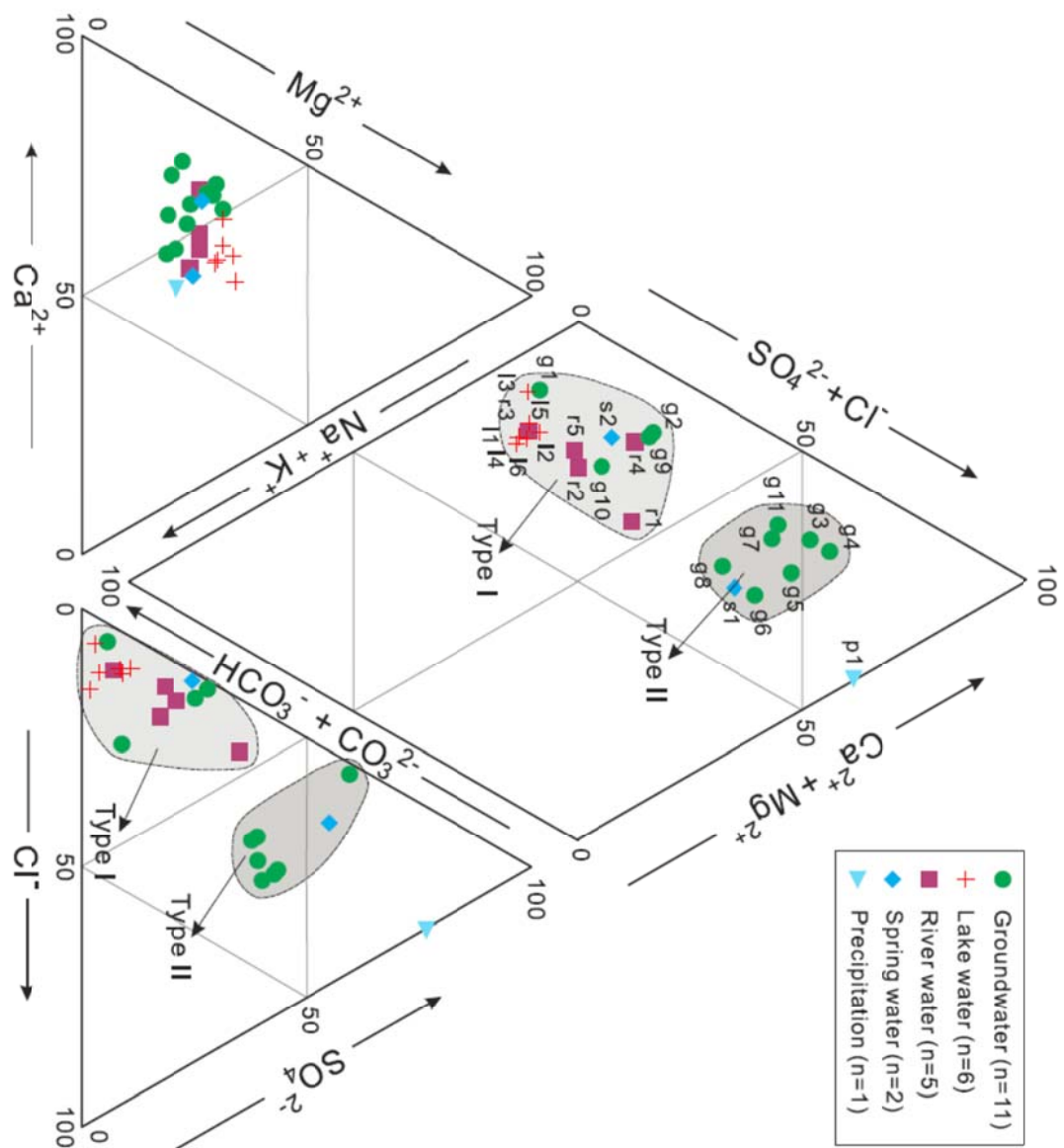


**Fig. 7.** The bivariate diagram of  $\delta D$  and  $\delta^{18}O$ , i.e. the Craig diagram, for the natural water samples in this study. Different relationships between the groundwaters, lake waters, river waters, spring waters and the precipitation waters are illustrated. AWMB, the annual weighted mean value at the Baotou station; AWMT, the annual weighted mean value at the Tianjin station; LWMB, the long-term weighted means at the Baotou station; LWMT, the long-term weighted means at the Tianjin station; GMWL, the Global Meteoric Water Line; LMWL-B, the local meteoric water line calculated based on the data from the Baotou station; LMWL-T, the local meteoric water line calculated based on the data from the Tianjin station; EL1, the evaporation line calculated based on the data of water samples collected in this study.

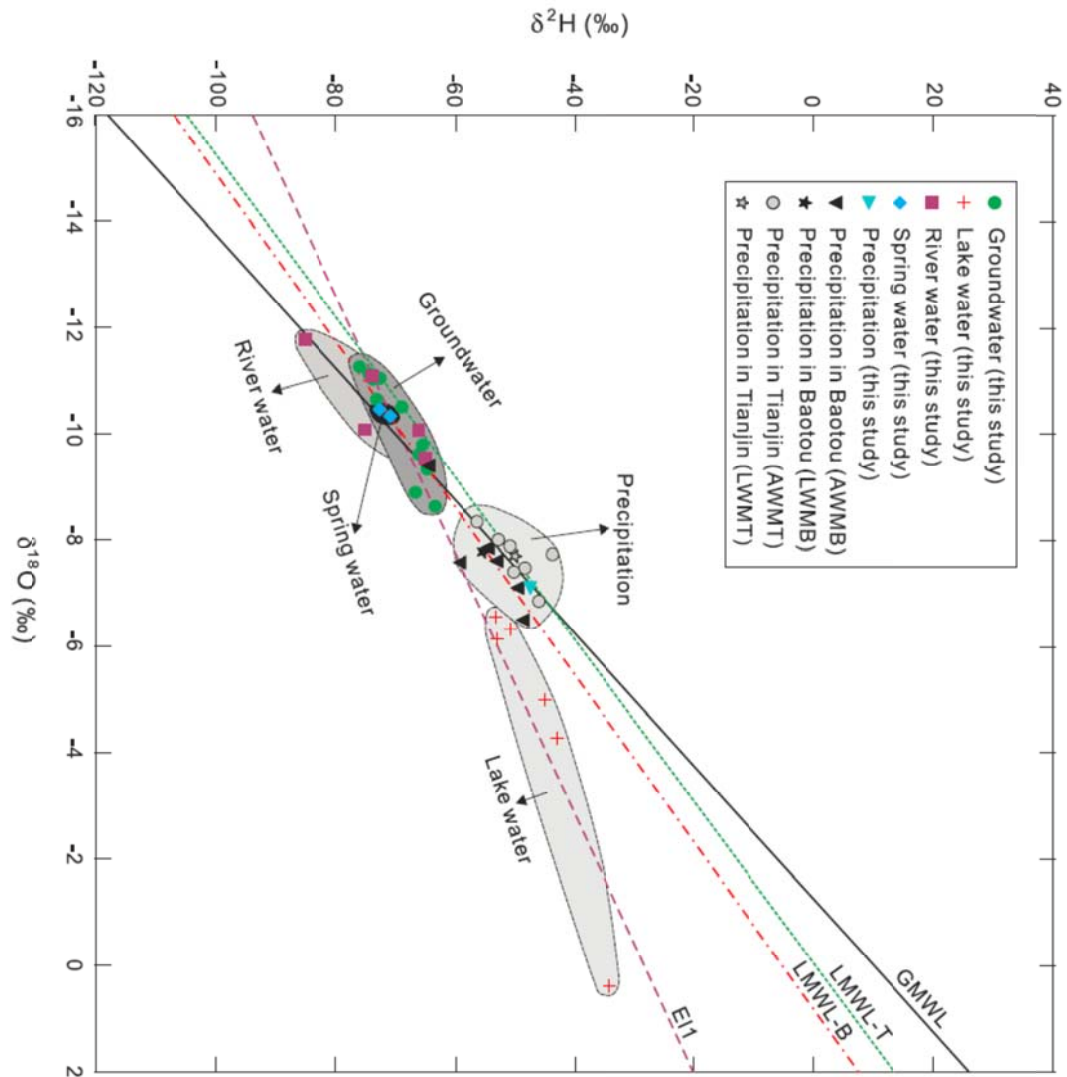




**Fig. 8.** The seasonal mean distributions of (a) precipitation, (b) surface air temperature and (c) water vapor pressure from the Baotou and Tianjin weather stations (station sites seen in **Fig. 1a**) in the surrounding areas of the Otindag for the period 1981-2010. The seasonal mean distributions of (d)  $\delta^{18}\text{O}$  and (e)  $\delta\text{D}$  values in precipitation from the Baotou and Tianjin weather stations in the surrounding areas of the Otindag for the period 1986-2001.

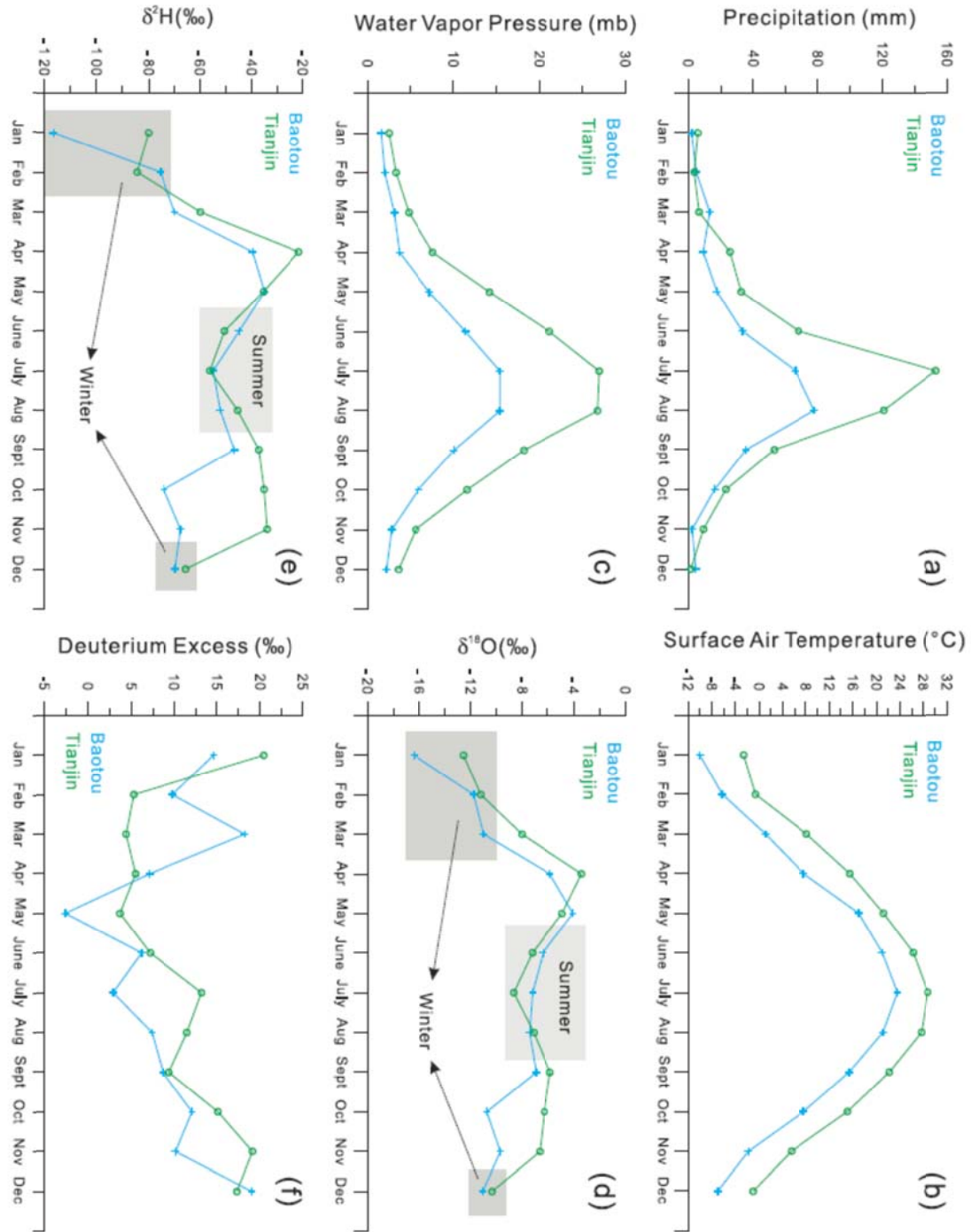


**Fig. 9.** The bivariate diagram of  $\delta\text{D}$  and  $\delta^{18}\text{O}$ , i.e. the Craig diagram, for the natural water samples collected in the Otindag (this study) and the Dali Basin. Different

relationships between the groundwaters, lake waters, river waters, spring waters and the precipitation waters are clearly illustrated. AWMB, AWMT, LWMB, LWMT, GMWL, LMWL-B, LWML-T, and EL1 are the same as in Fig. 7. EL2, the evaporation line calculated based on the data from the groundwater, lake water, river water and spring water samples collected from the Otindag and Dali Basin. The data for the Dali were taken from Chen et al. (2008) and Zhen et al. (2014).

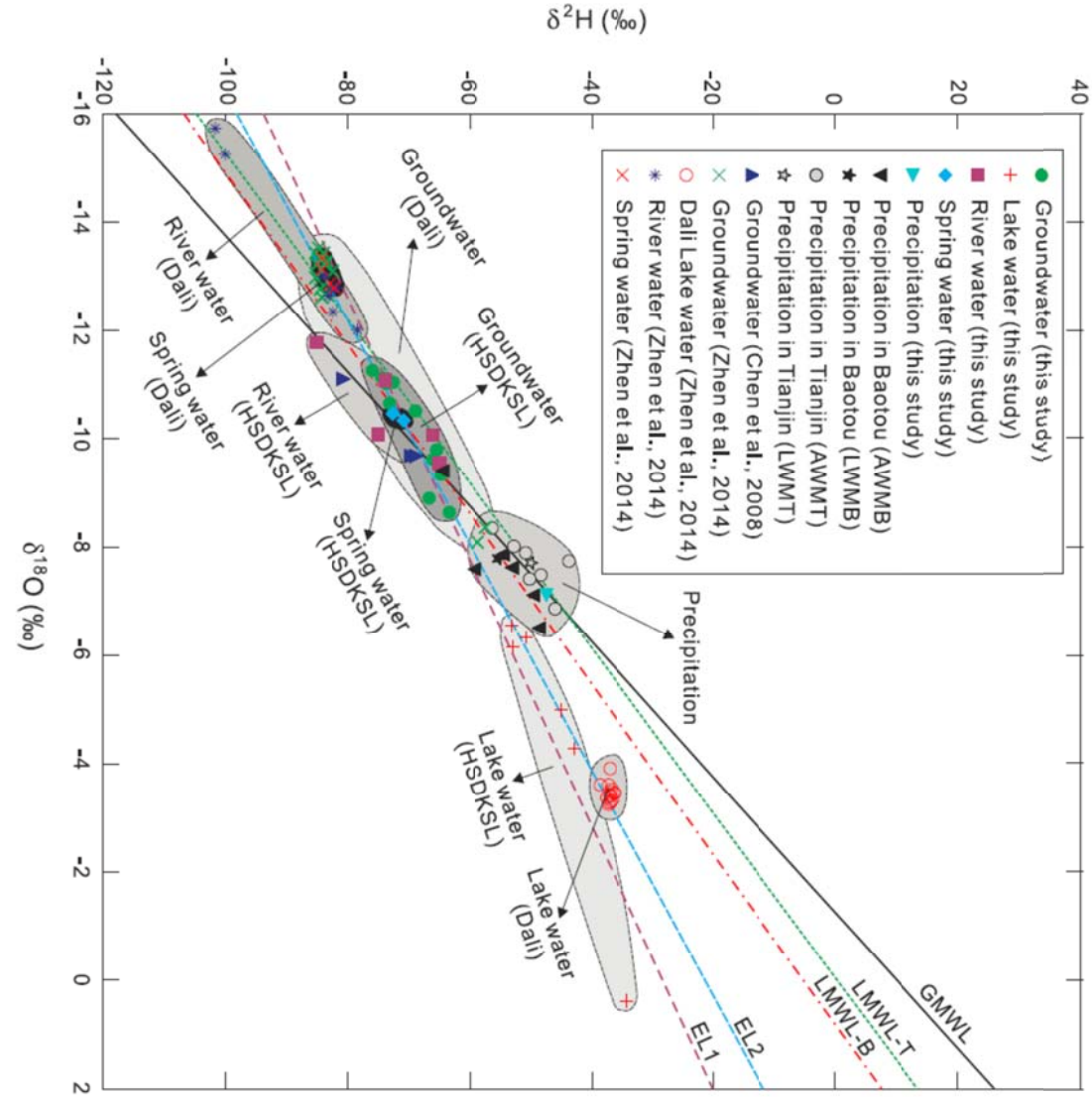


**Fig. 10.** (a) Sketch map showing the relationship between the groundwaters in the NPCSX and SPCSX areas, based on variations of (a) the chloride concentrations, (b) the TDS concentrations, (c) the  $\delta^{18}\text{O}$  values and (d) the  $\delta\text{D}$  values of these water samples versus their distances away from the water sample g1 along the palaeo river channel (PCSX) from south to north. The dashed line in (c) and (d) represents the corresponding values of the spring water sample s2, and divides samples into the NPCSX and SPCSX parts. (e) Variations of tritium contents vs. deuterium excess for the groundwater samples in the study area. The sample g6 was omitted due to its potential contamination.

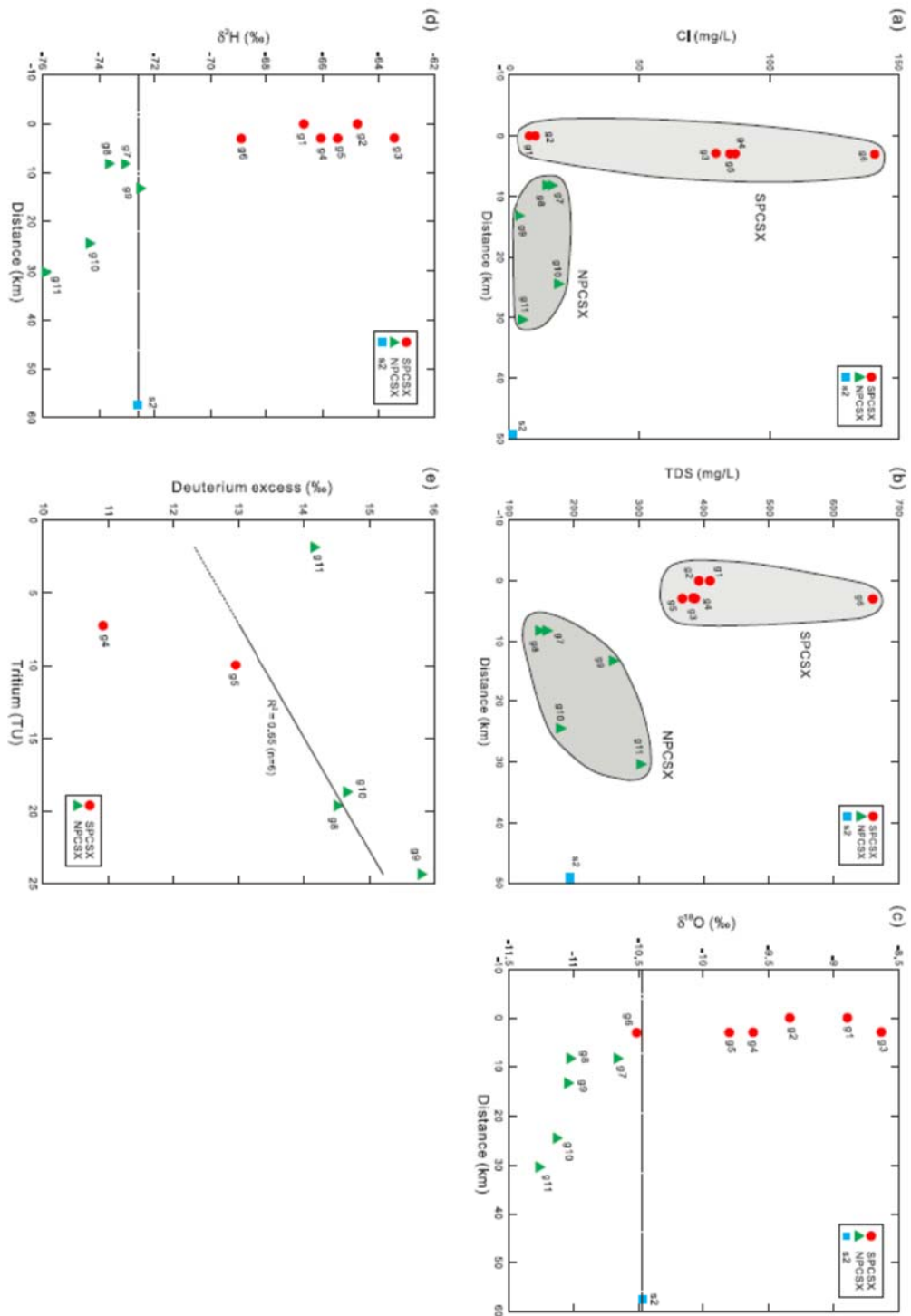
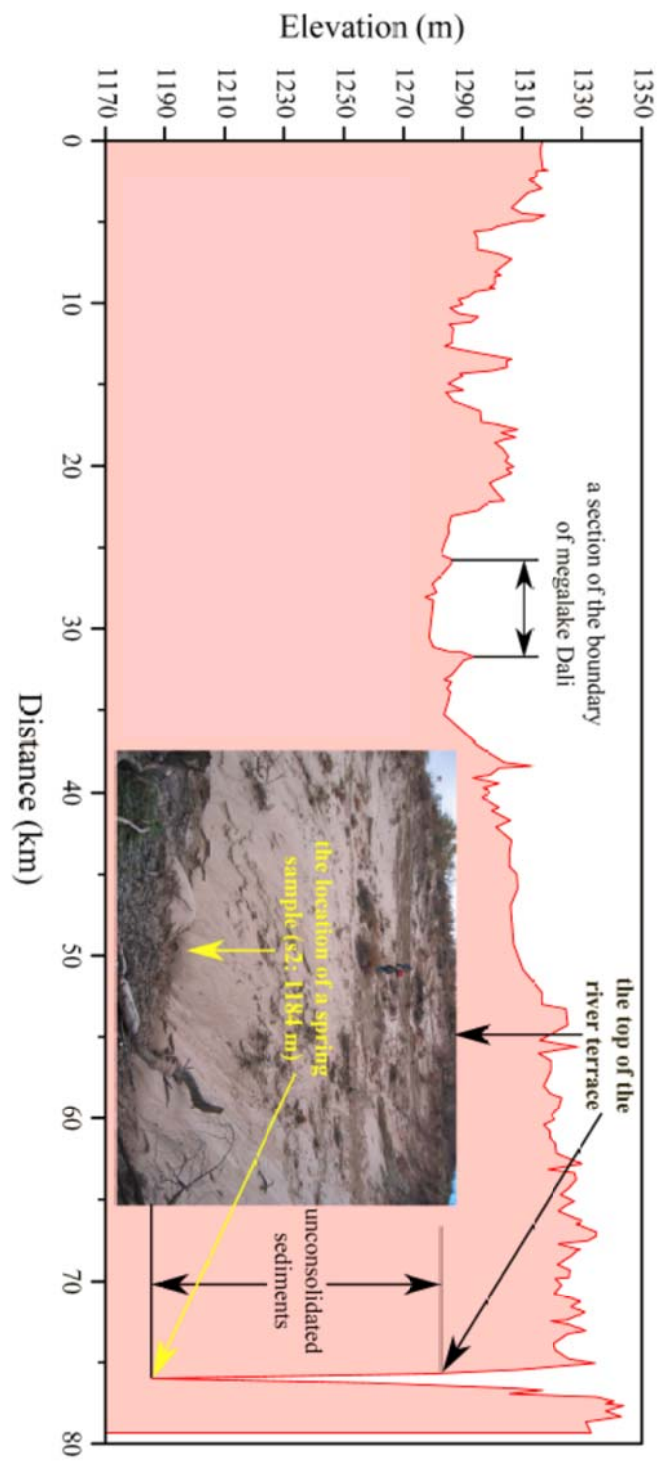


**Fig. 11.** Variation of the topographical elevation along the section S1 (see Fig. 1b) from the upstream of the Dali Lake to the location site of the spring water sample (s2) in the riverhead of the Xilamulun River. Note that no river water samples are shown in this figure.



1144

**Table Captions:**

1145

**Table 1.** The physical parameters measured for the natural water samples in the study area.

Sample ID	Water type	Latitude (N, degree)	Longitude (E, degree)	Elevation (m a.s.l)	Depth (m)	Temperature (°C)	pH	Eh (mV)	EC (µS/cm)	TDS (mg/L)	Salinity (%)	Alkalinity (meq/L)	Hardness (°dH)
g1	Groundwater	42.736306	116.747333	1396	12	5.8	6.72	3	769	410	0.6	5.47	9.42
g2	Groundwater	42.736306	116.747333	1396	26	6.0	6.91	-10	736	393	0.5	4.07	12.0
g3	Groundwater	42.760194	116.760139	1355	32	7.7	6.88	-6	725	384	0.5	2.39	11.9
g4	Groundwater	42.759694	116.760417	1360	7	10.0	6.74	1	725	387	0.5	2.20	12.3
g5	Groundwater	42.759556	116.760556	1362	27	7.6	6.46	16	691	368	0.5	2.23	15.6
g6	Groundwater	42.760111	116.760250	1365	7	10.3	6.26	22	1240	660	0.8	3.25	24.5
g7	Groundwater	42.806361	116.747806	1352	20	6.8	6.71	2	297	158	0.2	0.63	4.70
g8	Groundwater	42.806361	116.747806	1352	16	6.5	6.92	-8	276	147	0.2	0.58	5.00
g9	Groundwater	42.850333	116.735722	1347	30	7.2	6.74	-1	487	260	0.4	3.73	12.7
g10	Groundwater	42.949861	116.759194	1321	37	9.9	6.75	-2	337	179	0.2	1.66	7.23
g11	Groundwater	42.967111	116.827528	1317	60	8.6	6.99	-14	571	302	0.4	2.40	12.9
l1	Lake water	42.424611	116.769194	1368	/	16.9	9.44	-151	126	67	0.1	0.95	1.79
l2	Lake water	42.424611	116.769194	1368	/	19.6	9.18	-137	132	70	0.1	0.92	1.82
l3	Lake water	42.424611	116.757806	1365	/	20.2	7.38	-36	196	105	0.1	1.53	3.36
l4	Lake water	42.427083	116.757639	1366	/	20.5	7.87	-64	448	238	0.2	3.42	6.61
l5	Lake water	42.421806	116.756917	1360	/	20.1	8.23	-83	173	92	0.1	1.43	2.73
l6	Lake water	42.736389	116.747222	1374	/	10.7	8.35	-89	194	103	0.1	1.53	3.30
r1	River water	42.530917	116.641250	1355	/	20.6	7.31	-33	180	96	0.1	0.88	2.23
r2	River water	42.310883	116.494817	1231	/	14.9	7.67	-52	178	95	0.1	1.21	2.50
r3	River water	42.385778	116.886194	1362	/	9.5	7.62	-48	177	94	0.1	1.45	2.62
r4	River water	42.931417	117.585306	1217	/	10.5	7.97	-69	474	252	0.3	3.22	8.73
r5	River water	43.079083	117.457389	1006	/	12.9	7.87	-62	191	101	0.1	1.37	2.88
s1	Spring water	42.530917	116.641250	1359	/	20.9	6.63	5	165	88	0.1	0.40	1.81
s2	Spring water	42.965417	116.975361	1184	/	19.0	7.47	-46	371	195	0.2	1.07	6.40
p1	Precipitation	42.330750	116.551694	1260	/	20.2	4.61	109	78	42	0.0	/	0.61

1146

1147

**Table 2.** The concentrations of major cations and anions measured for the water samples in the study area.

Sample	F <sup>-</sup> (mg/L)	Cl <sup>-</sup> (mg/L)	NO <sub>2</sub> <sup>-</sup> (mg/L)	NO <sub>3</sub> <sup>-</sup> (mg/L)	SO <sub>4</sub> <sup>2-</sup> (mg/L)	CO <sub>3</sub> <sup>2-</sup> (mg/L)	HCO <sub>3</sub> <sup>-</sup> (mg/L)	Li <sup>+</sup> (mg/L)	Na <sup>+</sup> (mg/L)	NH <sub>4</sub> <sup>+</sup> (mg/L)	K <sup>+</sup> (mg/L)	Mg <sup>2+</sup> (mg/L)	Ca <sup>2+</sup> (mg/L)
g1	0.13	7.90	2.32	0.48	16.1	0.00	335	0.02	13.8	10.5	4.59	15.5	41.8
g2	0.21	10.2	0.00	6.15	70.6	0.10	248	0.02	13.4	6.56	3.45	17.9	56.0
g3	0.11	79.6	0.00	0.00	141	0.00	145	0.01	17.9	2.28	1.76	17.1	57.3
g4	0.10	86.9	0.00	5.73	165	0.00	134	0.02	18.0	0.00	2.02	18.5	57.3
g5	0.07	84.8	0.00	0.76	169	0.00	136	0.00	39.7	1.02	2.72	20.9	76.9
g6	0.07	141	0.00	111	229	0.00	198	0.00	79.8	0.00	29.47	29.3	126.7
g7	0.37	16.3	0.00	306	32.0	0.00	38.7	0.06	7.83	0.00	3.09	6.21	23.4
g8	0.29	14.3	0.00	35.5	29.9	0.00	35.5	0.02	16.2	0.11	3.38	6.44	25.1
g9	0.10	3.66	0.15	1.19	71.6	0.00	227	0.06	12.9	0.55	4.50	14.1	67.5
g10	0.24	18.8	0.00	49.5	9.97	0.00	101	0.00	18.5	0.00	2.09	7.92	38.7
g11	0.28	4.94	0.00	0.00	182	0.00	146	0.05	20.4	2.59	2.06	13.3	70.6
l1	0.16	3.15	0.00	0.07	4.32	0.00	57.9	0.01	5.42	0.00	0.86	3.24	7.49
l2	0.16	3.30	0.00	1.66	4.57	0.00	55.8	0.00	5.33	0.00	0.84	3.29	7.61
l3	0.11	3.27	0.00	0.61	2.33	0.00	93.3	0.01	5.88	0.00	1.19	5.68	14.7
l4	0.17	22.1	0.00	0.39	3.04	0.10	208	0.00	9.21	0.70	24.2	14.1	24.2
l5	0.09	6.24	0.00	0.65	2.97	0.10	86.8	0.01	6.72	0.00	1.16	4.91	11.4
l6	0.18	4.29	0.00	0.80	9.34	0.10	93.0	0.01	8.41	0.00	1.36	6.47	13.0
r1	0.30	5.76	0.00	2.38	26.7	0.30	52.4	0.01	7.15	0.00	2.99	3.41	10.3
r2	0.19	4.82	0.00	0.65	16.4	0.10	73.1	0.01	6.82	0.00	1.92	3.96	11.4
r3	0.64	5.46	0.00	0.43	5.57	0.00	88.1	0.01	7.11	0.00	1.13	4.04	12.1
r4	1.08	20.4	0.00	19.3	37.3	0.50	195	0.01	13.0	0.00	1.96	11.9	42.8
r5	0.19	4.10	0.00	1.08	15.6	0.00	82.6	0.01	6.71	0.00	2.08	4.38	13.4
s1	0.16	6.44	0.00	1.95	34.3	0.00	24.3	0.02	6.56	0.00	1.62	2.92	8.10
s2	0.05	0.98	0.00	0.45	17.2	0.00	64.9	0.02	9.87	0.00	3.32	9.10	30.8
p1	0.61	2.90	0.00	9.46	12.7	0.00	0.00	0.00	2.09	2.07	1.64	0.88	2.95

1148  
1149  
1150  
1151

**Table 3.** The analytical data of stable and radioactive isotopes measured for the water samples in this study.



Sample ID	$\delta D$ (‰)	$\sigma$ ‰	$\delta^{18}O$ (‰)	$\sigma$ ‰	deuterium excess (d)	Tritium ( $^3H$ ) (TU)
g1	-66.7	0.199	-8.90	0.026	4.50	/
g2	-64.8	0.291	-9.34	0.039	9.93	/
g3	-63.4	0.269	-8.64	0.008	5.66	/
g4	-66.1	0.149	-9.62	0.062	10.9	7.25
g5	-65.5	0.111	-9.80	0.027	13.0	9.98
g6	-68.9	0.287	-10.5	0.039	15.2	22.9
g7	-73.1	0.298	-10.7	0.041	12.2	/
g8	-73.7	0.220	-11.0	0.037	14.5	19.6
g9	-72.5	0.181	-11.0	0.015	15.8	24.3
g10	-74.4	0.201	-11.1	0.026	14.7	18.7
g11	-75.9	0.340	-11.3	0.015	14.2	1.86
l1	-53.1	0.229	-6.55	0.002	-0.704	/
l2	-50.7	0.304	-6.32	0.026	-0.161	/
l3	-42.9	0.239	-4.29	0.034	-8.55	/
l4	-34.2	0.243	0.381	0.040	-37.2	/
l5	-45.1	0.206	-4.99	0.009	-5.16	/
l6	-52.9	0.187	-6.15	0.049	-3.67	/
r1	-66.2	0.118	-10.1	0.015	14.4	/
r2	-65.0	0.148	-9.55	0.012	11.4	/
r3	-73.8	0.315	-11.1	0.021	14.9	/
r4	-85.2	0.244	-11.8	0.005	9.09	/
r5	-75.0	0.195	-10.1	0.003	5.69	/
s1	-70.8	0.074	-10.3	0.007	11.9	/
s2	-72.6	0.281	-10.5	0.046	11.1	/
p1	-47.4	0.374	-7.14	0.017	9.69	/

1152  
1153  
1154  
1155

**Table 4.** The statistical frequency of rainfall events being >20 mm per year during the recent 30 years from 1985 to 2014. The data come from the China Meteorological Data

1156 Sharing Service System.

Station	One time/year	Two times/year	Three times/year	Four times/year	Five times/year	Six times/year	Seven times/year	Mean times/year
Duolun	2	8	8	4	4	3	1	3.4
Xilinhaote	8	5	2	6	3	2	0	2.5

1157  
1158 **Table 5.** The measured contents of tritium in the groundwater samples studied and the calculated ages of these samples.

Sample-ID	Tritium content (T.U.)	Possible ages (years)
g1	not measured	not clear
g2	not measured	not clear
g3	not measured	not clear
g4	7.25	20-40
g5	9.97	13-33
g6	22.9	0-20
g7	not measured	not clear
g8	19.6	0-20
g9	24.3	0-17
g10	18.7	0-22
g11	1.86	40-65

1159  
1160 **Table 6.** Mineral saturation Index (MSI) of the water samples studied.

Sample-ID	Mineral (Formula)	Anhydrite (CaSO <sub>4</sub> )	Aragonite (CaCO <sub>3</sub> )	Calcite (CaCO <sub>3</sub> )	Dolomite (CaMg(CO <sub>3</sub> ) <sub>2</sub> )	Fluorite (CaF <sub>2</sub> )	Gypsum (CaSO <sub>4</sub> ·2H <sub>2</sub> O)	Halite (NaCl)	CH <sub>4</sub> (g) (CH <sub>4</sub> )	CO <sub>2</sub> (g) (CO <sub>2</sub> )	H <sub>2</sub> (g) (H <sub>2</sub> )	H <sub>2</sub> O(g) (H <sub>2</sub> O)	NH <sub>3</sub> (g) (NH <sub>3</sub> )	O <sub>2</sub> (g) (O <sub>2</sub> )
g1	SI	-2.76	-1.21	-1.05	-2.5	-2.69	-2.5	-8.48	-58.68	-1.5	-21.44	-2.04	-8.5	-47.28
	Log IAP	-7.1	-9.45	-9.45	-19.11	-13.56	-7.1	-6.95	-61.37	-2.71	-24.5	0	-6.32	-50
	Log KT	-4.34	-8.24	-8.4	-16.61	-10.86	-4.6	1.54	-2.69	-1.2	-3.06	2.04	2.18	-2.72

g2	SI	-2.04	-0.99	-0.83	-2.12	-2.19	-1.79	-8.39	-60.49	-1.76	-21.82	-2.04	-8.51	-46.44
	Log IAP	-6.39	-9.23	-9.23	-18.74	-13.05	-6.39	-6.86	-63.18	-2.97	-24.88	0	-6.33	-49.16
	Log KT	-4.34	-8.24	-8.4	-16.62	-10.86	-4.6	1.54	-2.69	-1.21	-3.06	2.04	2.18	-2.73
g3	SI	-1.77	-1.25	-1.09	-2.62	-2.8	-1.51	-7.38	-60.71	-1.96	-21.76	-1.99	-8.9	-45.9
	Log IAP	-6.11	-9.49	-9.49	-19.29	-13.63	-6.11	-5.84	-63.41	-3.2	-24.83	0	-6.77	-48.65
	Log KT	-4.34	-8.25	-8.4	-16.66	-10.83	-4.6	1.54	-2.71	-1.23	-3.07	1.99	2.14	-2.74
g4	SI	-1.72	-1.43	-1.27	-2.92	-2.94	-1.47	-7.35	-59.85	-1.88	-21.48	-1.92		-45.59
	Log IAP	-6.06	-9.69	-9.69	-19.64	-13.73	-6.06	-5.8	-62.58	-3.15	-24.56	0		-48.35
	Log KT	-4.34	-8.26	-8.41	-16.72	-10.8	-4.59	1.55	-2.73	-1.27	-3.08	1.92		-2.77
g5	SI	-1.6	-1.74	-1.59	-3.66	-3.09	-1.35	-7.02	-57.1	-1.73	-20.92	-1.99	-9.68	-47.62
	Log IAP	-5.94	-9.99	-9.99	-20.32	-13.93	-5.94	-5.48	-59.81	-2.96	-23.99	0	-7.54	-50.36
	Log KT	-4.34	-8.25	-8.4	-16.66	-10.83	-4.6	1.54	-2.71	-1.23	-3.07	1.99	2.14	-2.74
g6	SI	-1.39	-1.67	-1.52	-3.54	-3.01	-1.13	-6.53	-55.63	-1.45	-20.52	-1.91		-47.4
	Log IAP	-5.73	-9.93	-9.93	-20.27	-13.8	-5.73	-4.98	-58.36	-2.73	-23.6	0		-50.16
	Log KT	-4.34	-8.26	-8.41	-16.73	-10.79	-4.59	1.55	-2.73	-1.27	-3.08	1.91		-2.77
g7	SI	-2.79	-2.45	-2.29	-5.1	-2.12	-2.54	-8.44	-59.68	-2.43	-21.42	-2.01		-46.93
	Log IAP	-7.13	-10.69	-10.69	-21.74	-12.97	-7.13	-6.91	-62.38	-3.65	-24.49	0		-49.66
	Log KT	-4.34	-8.24	-8.4	-16.64	-10.85	-4.6	1.54	-2.7	-1.22	-3.07	2.01		-2.73
g8	SI	-2.65	-2.11	-1.95	-4.43	-2.19	-2.4	-8.15	-61.48	-2.6	-21.84	-2.02	-10.23	-46.21
	Log IAP	-6.99	-10.35	-10.35	-21.06	-13.04	-6.99	-6.61	-64.18	-3.82	-24.9	0	-8.07	-48.94
	Log KT	-4.34	-8.24	-8.4	-16.63	-10.85	-4.6	1.54	-2.7	-1.22	-3.06	2.02	2.17	-2.73
g9	SI	-1.96	-1.14	-0.98	-2.58	-2.77	-1.7	-8.85	-59.22	-1.67	-21.48	-2	-9.68	-46.66
	Log IAP	-6.3	-9.38	-9.38	-19.23	-13.6	-6.3	-7.31	-61.92	-2.9	-24.55	0	-7.53	-49.39
	Log KT	-4.34	-8.24	-8.4	-16.65	-10.84	-4.6	1.54	-2.7	-1.23	-3.07	2	2.15	-2.74
g10	SI	-2.99	-1.63	-1.47	-3.51	-2.24	-2.73	-7.98	-60.04	-2	-21.5	-1.92		-45.59
	Log IAP	-7.32	-9.88	-9.88	-20.23	-13.04	-7.32	-6.44	-62.77	-3.27	-24.58	0		-48.35
	Log KT	-4.34	-8.25	-8.41	-16.72	-10.8	-4.59	1.55	-2.73	-1.27	-3.08	1.92		-2.76
g11	SI	-1.59	-1.01	-0.86	-2.34	-1.92	-1.33	-8.54	-61.8	-2.04	-21.98	-1.96	-8.69	-45.12
	Log IAP	-5.92	-9.26	-9.26	-19.02	-12.74	-5.92	-6.99	-64.51	-3.29	-25.05	0	-6.57	-47.87
	Log KT	-4.34	-8.25	-8.41	-16.69	-10.82	-4.59	1.54	-2.72	-1.25	-3.07	1.96	2.12	-2.75
l1	SI	-3.95	0.37	0.52	0.92	-5.34	-3.7	-9.28	-85.36	-4.77	-26.88	-1.73		-32.25
	Log IAP	-8.29	-7.92	-7.92	-15.97	-16.04	-8.29	-7.72	-88.15	-6.14	-29.99	0		-35.08

	Log KT	-4.34	-8.29	-8.44	-16.9	-10.7	-4.58	1.56	-2.79	-1.37	-3.11	1.73	-2.83	
l2	SI	-3.9	0.18	0.33	0.58	-3.36	-3.66	-9.27	-83.39	-4.49	-26.36	-1.65	-32.33	
	Log IAP	-8.24	-8.12	-8.12	-16.38	-14.02	-8.24	-7.7	-86.2	-5.89	-29.49	0	-35.18	
	Log KT	-4.34	-8.3	-8.45	-16.96	-10.66	-4.58	1.57	-2.81	-1.4	-3.13	1.65	-2.85	
l3	SI	-3.92	-1.1	-0.95	-2.03	-3.4	-3.69	-9.24	-67.05	-2.47	-22.76	-1.64	-39.32	
	Log IAP	-8.27	-9.4	-9.4	-19	-14.06	-8.27	-7.67	-69.87	-3.88	-25.89	0	-42.18	
	Log KT	-4.34	-8.31	-8.45	-16.98	-10.66	-4.58	1.57	-2.82	-1.41	-3.13	1.64	-2.86	
l4	SI	-3.7	-0.07	0.07	0.2	-2.9	-3.46	-8.24	-71.14	-2.6	-23.74	-1.63	-7.72	-37.26
	Log IAP	-8.04	-8.38	-8.38	-16.78	-13.55	-8.04	-6.67	-73.96	-4.01	-26.87	0	-5.86	-40.11
	Log KT	-4.35	-8.31	-8.46	-16.98	-10.65	-4.58	1.57	-2.82	-1.41	-3.13	1.63	1.86	-2.86
l5	SI	-3.92	-0.36	-0.21	-0.51	-3.69	-3.68	-8.9	-74.69	-3.32	-24.46	-1.64	-35.96	
	Log IAP	-8.26	-8.67	-8.67	-17.48	-14.34	-8.26	-7.33	-77.51	-4.73	-27.59	0	-38.81	
	Log KT	-4.34	-8.31	-8.45	-16.97	-10.66	-4.58	1.57	-2.82	-1.41	-3.13	1.64	-2.86	
l6	SI	-3.39	-0.32	-0.16	-0.49	-2.91	-3.13	-8.95	-74.42	-3.47	-24.7	-1.9	-38.88	
	Log IAP	-7.72	-8.58	-8.58	-17.23	-13.7	-7.72	-7.4	-77.16	-4.74	-27.79	0	-41.66	
	Log KT	-4.34	-8.26	-8.41	-16.74	-10.79	-4.59	1.55	-2.74	-1.28	-3.09	1.9	-2.77	
r1	SI	-3.01	-1.57	-1.43	-3.05	-2.69	-2.77	-8.91	-66.73	-2.65	-22.62	-1.63	-39.46	
	Log IAP	-7.36	-9.88	-9.88	-20.03	-13.35	-7.36	-7.34	-69.55	-4.06	-25.75	0	-42.32	
	Log KT	-4.35	-8.31	-8.46	-16.99	-10.65	-4.58	1.57	-2.82	-1.41	-3.13	1.63	-2.86	
r2	SI	-3.18	-1.09	-0.94	-2.14	-2.97	-2.94	-9	-69.01	-2.88	-23.34	-1.78	-40.05	
	Log IAP	-7.52	-9.37	-9.37	-18.98	-13.7	-7.52	-7.44	-71.79	-4.22	-26.44	0	-42.86	
	Log KT	-4.34	-8.28	-8.43	-16.85	-10.73	-4.58	1.56	-2.77	-1.34	-3.1	1.78	-2.81	
r3	SI	-3.62	-1.12	-0.97	-2.3	-1.8	-3.36	-8.91	-67.72	-2.78	-23.24	-1.93	-42.26	
	Log IAP	-7.95	-9.38	-9.38	-19.01	-12.61	-7.95	-7.36	-70.44	-4.04	-26.32	0	-45.02	
	Log KT	-4.34	-8.25	-8.41	-16.71	-10.8	-4.59	1.55	-2.72	-1.26	-3.08	1.93	-2.76	
r4	SI	-2.41	0.06	0.21	0	-0.93	-2.15	-8.11	-70.67	-2.78	-23.94	-1.9	-40.48	
	Log IAP	-6.74	-8.2	-8.2	-16.73	-11.72	-6.75	-6.56	-73.4	-4.06	-27.02	0	-43.25	
	Log KT	-4.34	-8.26	-8.41	-16.74	-10.79	-4.59	1.55	-2.73	-1.28	-3.08	1.9	-2.77	
r5	SI	-3.15	-0.8	-0.65	-1.61	-2.88	-2.89	-9.07	-70.47	-3.03	-23.74	-1.84	-39.99	
	Log IAP	-7.48	-9.07	-9.07	-18.4	-13.63	-7.48	-7.52	-73.23	-4.34	-26.84	0	-42.78	
	Log KT	-4.33	-8.27	-8.42	-16.8	-10.75	-4.59	1.55	-2.76	-1.31	-3.1	1.84	-2.79	
s1	SI	-2.99	-2.83	-2.68	-5.51	-3.34	-2.76	-8.9	-61.12	-2.44	-21.26	-1.62	-42.08	

1161  
1162

	Log IAP	-7.34	-11.14	-11.14	-22.5	-13.99	-7.34	-7.33	-63.95	-3.86	-24.39	0	-44.94	
	Log KT	-4.35	-8.31	-8.46	-16.99	-10.65	-4.58	1.57	-2.83	-1.42	-3.13	1.62	-2.86	
s2	SI	-2.8	-0.89	-0.74	-1.73	-3.79	-2.56	-9.55	-67.85	-2.72	-22.94	-1.67	-39.38	
	Log IAP	-7.14	-9.19	-9.19	-18.68	-14.46	-7.14	-7.98	-70.66	-4.12	-26.06	0	-42.23	
	Log KT	-4.34	-8.3	-8.45	-16.95	-10.67	-4.58	1.57	-2.81	-1.39	-3.12	1.67	-2.85	
p1	SI	-3.81				-2.59	-3.57	-9.73			-17.22	-1.64	-10.5	-50.4
	Log IAP	-8.15				-13.25	-8.15	-8.16			-20.35	0	-8.63	-53.26
	Log KT	-4.34				-10.66	-4.58	1.57			-3.13	1.64	1.87	-2.86